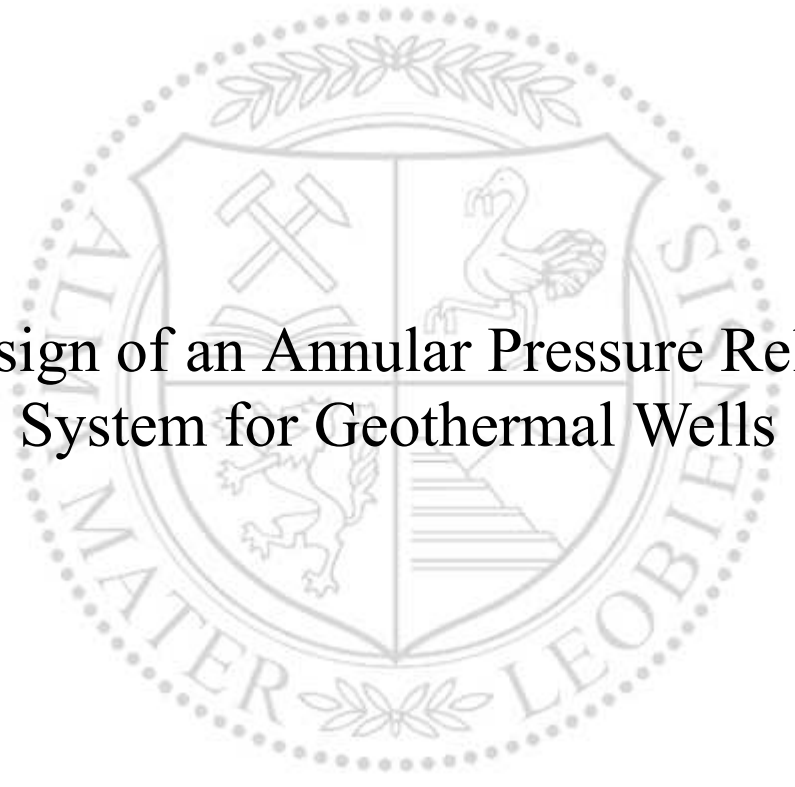




Chair of Petroleum and Geothermal Energy Recovery

Master's Thesis



Design of an Annular Pressure Relief  
System for Geothermal Wells

Matthias Sturm, BSc

May 2019



## EIDESSTÄTTLICHE ERKLÄRUNG

Ich erkläre an Eides statt, dass ich diese Arbeit selbständig verfasst, andere als die angegebenen Quellen und Hilfsmittel nicht benutzt, und mich auch sonst keiner unerlaubten Hilfsmittel bedient habe.

Ich erkläre, dass ich die Richtlinien des Senats der Montanuniversität Leoben zu "Gute wissenschaftliche Praxis" gelesen, verstanden und befolgt habe.

Weiters erkläre ich, dass die elektronische und gedruckte Version der eingereichten wissenschaftlichen Abschlussarbeit formal und inhaltlich identisch sind.

Datum 11.05.2019

---

Unterschrift Verfasser/in  
Matthias, Sturm  
Matrikelnummer: 01031596



## Acknowledgement

This work was developed with the support of many people. I am grateful for their help. In particular I would like to thank:

- Dipl.-Ing. David Lentsch from ERDWERK GmbH for the primary idea which induced this thesis and especially for his patience during our frequent discussions on most of the topics covered by this thesis and his outstanding knowledge about geothermal wells which I was able to benefit from.
- Dipl.-Ing. Patrick Eisner for supervision of this thesis and his constructive advice and problem oriented solutions whenever needed.
- Dipl.-Ing. Dipl.-Ing. Dr. mont. Clemens Langbauer for his supervision during the beginning phase of this thesis.
- Dr. Achim Schubert from ERDWERK GmbH for the possibility to write this thesis in his company and his continuous support throughout this thesis.
- Alexander, Thorsten, Martin and Hans for their effort during writing this thesis. You helped me to find a solution when I thought I was already stuck.
- Albert, Alois, Johann and Michael for their support throughout the entire time of my study and especially during writing this thesis.
- My family (especially Chiara) for giving me the confidence and strength to finish my studies and for their constant support.

## Kurzfassung

Die Inbetriebnahme eines (geothermischen) Bohrlochs hat einen Temperaturanstieg im Ringraum zufolge. Diese steigende Temperatur führt aufgrund des beschränkten Volumens zu einem Druckanstieg, da Flüssigkeit (sogenanntes Ringraum Fluid) im Ringraum eingeschlossen ist. Dieses Phänomen ist als Annular Pressure Build-Up (APB) oder als Trapped Annular Pressure (TAP) bekannt.

APB ist häufig die Ursache für Schäden an der Verrohrung im Bohrloch. Da das Fluid im Ringraum eingeschlossen ist, kann es entweder zu einer Verformung oder Beschädigung der inneren oder der äußeren Verrohrung kommen. Im schlimmsten Fall kann APB zu einem Verlust der Integrität des Bohrlochs führen.

Die vorliegende Arbeit ist eine Studie zur Konzeption eines Bauteils, welches APB verhindern bzw. verringern soll. Das als Annular Pressure Relief System (APRS) bezeichnete Bauteil soll an der Verrohrung befestigt werden und eine Beschädigung dieser durch APB verhindern. Aufgrund des geringen Raumangebots zwischen den Verrohrungen ist das optimale Verhältnis zwischen einem möglichst klein konzipierten Bauteil und einer großen Volumskapazität maßgebend. Eine große Herausforderung für die Bauteilkonstruktion stellen auch die hohen Drücke und Temperaturen dar. Zudem muss das Bauteil an unterschiedliche Bohrlochkonstruktionen (verschiedene Drücke, Temperaturen und Bohrlochdimensionen) angepasst werden. Das Montagekonzept gewährleistet, dass das Bauteil installiert werden kann, ohne das Bohrloch zu beschädigen oder den Zementationsprozess negativ zu beeinflussen.

Unterschiedliche Konzepte wurden konstruktiv ausgearbeitet, die Funktionsweisen sowie technischen Details beschrieben, bewertet und gegenübergestellt. Zudem werden die Vor- und Nachteile dieser Bauteile mit bereits vorhandenen Methoden, um APB zu verhindern, ebenso aufgezeigt.

Die Arbeit gibt zudem einen Überblick über die aktuell verfügbaren Methoden für den Umgang mit bzw. der Vermeidung von APB. Die Notwendigkeit einer neuen Methode, die Entwicklung eines neuen Bauteils etwa, wird dadurch erkennbar. Die notwendigen Berechnungsschritte für die Konstruktion des Bauteils werden zur Definition der Randbedingungen beschrieben sowie eine Grafik dargestellt, mit der das benötigte Volumen durch Kenntnis der Druck- und Temperaturbedingungen im Bohrloch abgeschätzt werden kann.

## Abstract

In a geothermal well, annular pressure is generated during production, when trapped annular fluids are heated up between casing strings. Due to the encapsulated fluid, an expansion of the fluid is not possible and thus, the pressure increases. This phenomenon is known as Annular Pressure Build up (APB) or Trapped Annular Pressure (TAP).

It has been identified, that APB is an important cause, when casing collapse occurs. The fluid trapped in the annulus can cause a deformation of either the inner or the outer casing string, which can lead to a loss of the integrity of the well.

This thesis is a conceptual study of downhole tools, which act against APB. The tool, named Annular Pressure Relieve System (APRS), should be fixed on the casing string and therefore, prevents the well from getting damaged by APB. Due to the small amount of available space between the casing strings, an important point of the tool is to find the balance between a small constructed space and a high-volume capacity. Further the high pressure and temperature conditions are a big challenge for the tool design. Another challenge is that the tool must be customized for different well designs (varying pressure and temperature conditions). Therefore, a mounting concept is designed to be able to adapt the APRS to different diameters. Furthermore, the mounting concept ensures that the tool can be installed without damaging the well or hindering the cement job.

The thesis deals with the development of different concepts and describes the functional operation and technical details of them. Moreover, all concepts are evaluated and compared to each other. The upsides and downsides of the tool concepts are compared to existing methods.

The thesis includes an overview of the current, available methods how to handle or avoid APB and the necessity of developing a new method (tool) is demonstrated. The thesis describes the necessary calculation steps to define the boundary conditions for the design of the tool. A graph is presented, which can be used to estimate the needed volume to compensate the pressure increase by knowing the pressure and temperature conditions.

Finally, the two most suitable concepts are discussed and an outlook for the detailed design process is given.

## Table of Content

	<b>Page</b>
<b>1 INTRODUCTION.....</b>	<b>1</b>
<b>2 LITERATURE REVIEW .....</b>	<b>3</b>
2.1 Theory of APB.....	3
2.2 Existing Methods to Handle or Avoid APB .....	6
2.3 The Motivation for Developing a New Tool .....	10
<b>3 DESCRIPTION OF A REPRESENTATIVE WELL.....</b>	<b>11</b>
3.1 Problem Definition.....	12
3.2 Boundary Conditions.....	13
3.3 Fluid Properties.....	16
3.4 Properties of Water .....	18
<b>4 APB VOLUME AND PRESSURE CALCULATION .....</b>	<b>20</b>
4.1 Volume Expansion due to APB .....	21
4.2 Expansion Volume due to APB.....	28
4.3 Pressure increase due to APB.....	29
<b>5 THEORY OF OPERATION .....</b>	<b>31</b>
<b>6 FUNCTIONAL OPERATION.....</b>	<b>33</b>
6.1 Option 1: Volume Consideration .....	34
6.2 Option 2: Pressure and Volume Consideration .....	35
6.3 Option 3: Pressurized Pressure Chamber .....	37
6.4 Concerning Design Options .....	39
<b>7 DESIGN CHALLENGES.....</b>	<b>40</b>
7.1 Static Strength .....	40
7.2 Material Selection .....	49
7.3 Wall Thickness.....	54
7.4 Feasibility Study.....	57
<b>8 CONCEPT DESCRIPTION .....</b>	<b>58</b>
8.1 Concepts for Fixation of the Pressure Chamber .....	58
8.2 Concept A – “Small Pipe”.....	62
8.3 Concept B – “Big Pipe” .....	64

---

8.4	Concept C – “Single Pipe” .....	66
8.5	Concept D – “Ring Pipe” .....	71
8.6	Concept F – “Cross Pipe” .....	75
8.7	Concept G – “Membrane Pipe” .....	78
<b>9</b>	<b>CONCEPTS OVERVIEW .....</b>	<b>81</b>
<b>10</b>	<b>CONCLUSION AND OUTLOOK .....</b>	<b>83</b>
	<b>REFERENCES .....</b>	<b>90</b>
	<b>LIST OF TABLES .....</b>	<b>94</b>
	<b>LIST OF FIGURES .....</b>	<b>96</b>
	<b>ABBREVIATIONS .....</b>	<b>99</b>
	<b>NOMENCLATURE .....</b>	<b>100</b>
	<b>APPENDICES .....</b>	<b>102</b>
	Appendix A.....	102
	Appendix B.....	104
	Appendix C.....	105
	Appendix D.....	106
	Appendix E.....	108
	Appendix F.....	109

# 1 Introduction

Deep geothermal energy in the Munich area is experiencing a success story over the past 20 years. Today, 33 geothermal projects generate over 295.9 MW thermal energy and 33 MW electrical energy [1]. Geothermal energy is not only very efficient but also remains ecologically sound in terms of space requirements and CO<sub>2</sub> emissions as a perfect solution [2].

Nonetheless, the use of deep geothermal energy places great demands on technology. The high production temperatures and production rates pose significant challenges, in particular, to the well design [3]. Due to the structure of the well, the cementation process can result in unavoidable encapsulation of fluids in the annulus [4].

At these high production temperatures, significant problems can arise when fluids are encapsulated in the annulus [3]. Because of the rise in temperature in the annulus at the start of production, the encapsulated fluid cannot expand. In turn, this spatial restriction leads to an increasing pressure in the annulus. This phenomenon is known as "Annular Pressure Build-Up" (APB) or "Trapped Annular Pressure" (TAP) [5,6].

If the casing is not sufficiently designed, in terms of collapse or burst resistance, the functionality of the wellbore is endangered. Further, a casing design which can withstand the high stresses occurring from APB, would not be economic or technically infeasible. In a worst-case scenario, the pressure increase can result in the collapse of the casing, and therefore in the loss of the integrity of the wellbore [4]. Figure 1 shows such a damaged casing downhole.

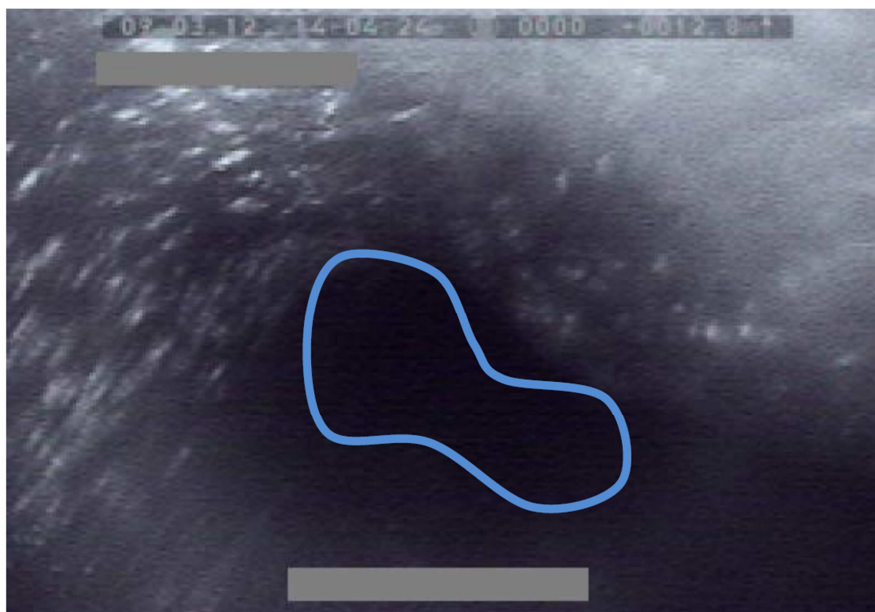


Figure 1: Camera Inspection of the Casing Collapse [7]

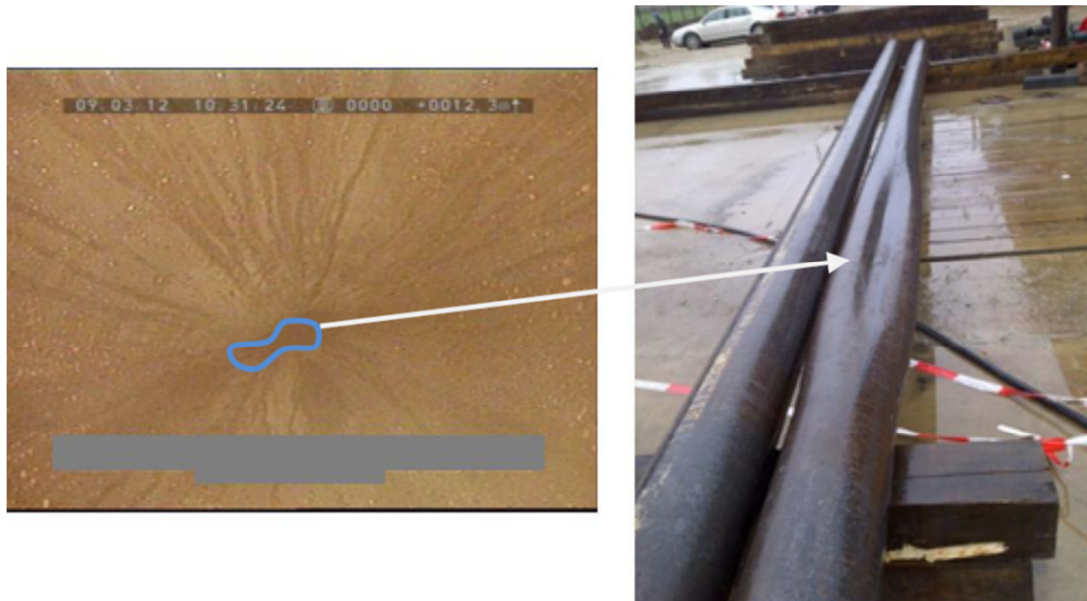


Figure 2: Picture from the Camera and Pulled Casing String [7]

Figure 2 displays the same casing on the surface. Due to this issue, a technical solution is desirable. This thesis deals with the development of potential concepts to avoid APB – an Annular Pressure Relief System (APRS).

### Tasks and Goals

The project aim is to develop a suitable tool which is attached to the casing or liner in order to prevent a pressure increase in the annulus.

The tasks are structured as follows:

- Acquisition and processing of the relevant data for the calculation and design of the tool
- Calculation of the pressure increase due to APB in a closed annulus and calculation of the necessary discharge volume to restore an uncritical pressure level. This pressure level is set within a range, avoiding a damage of the borehole and the installed components
- Conceptual planning of components for pressure relief considering the calculated values for the required discharge volume
- Design of the components according to the expected load scenarios (installation of the component, cementation of the pipe run, heating of the annulus, etc.)
- Evaluate concepts for feasibility, cost, risk, manufacturing time, compatibility, flexibility in use, manufacturing criteria, and other technical criteria
- Restriction to concepts with the best technical suitability and good economic viability

## 2 Literature Review

The literature review gives a quick overview of the principle APB theory and the basics to calculate it. Further, existing solutions are reviewed.

### 2.1 Theory of APB

The following chapter describes the underlying physical mechanism of APB and the necessary equations to calculate the pressure or volume increase created by APB.

When production starts, the hot production fluid heats the cold fluid located in the annulus due to heat exchange and the temperature of the annular fluid increases. Due to the temperature increase, the annular fluid wants to expand. Figure 3 shows a schematic sketch of a wellbores cross-section, including the most used phrases throughout the thesis and their location.

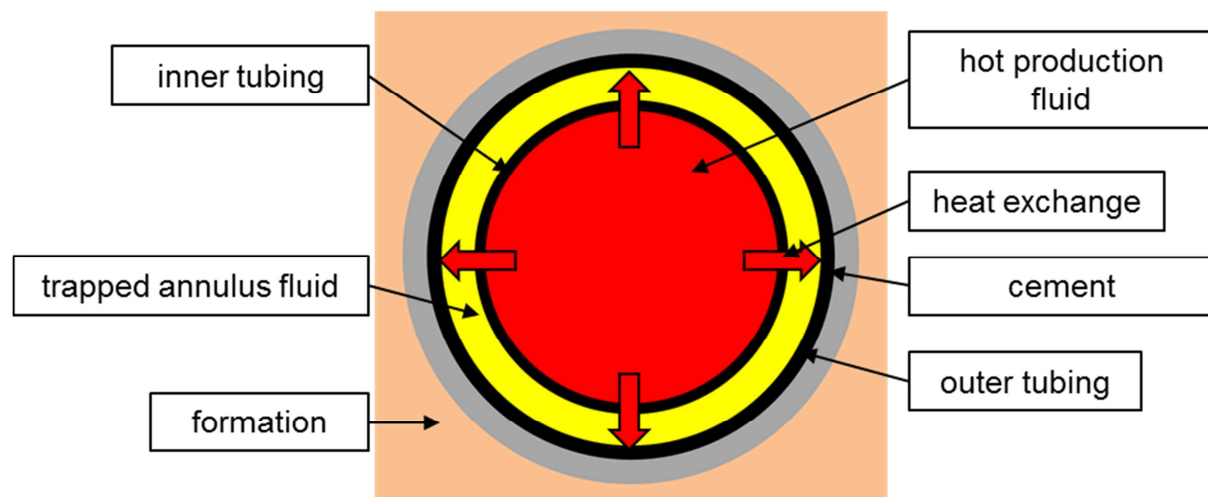


Figure 3: Cross-Section Annulus

### Physical Background

By keeping the mass of liquids, solids, and gases constant a change in temperature results in a change in volume and or pressure [8]. If the volume is kept constant during a change in temperature, the pressure will be altered and if the pressure is held constant, the volume must increase.

The mechanism of avoiding APB is therefore based on enabling thermal expansion of encapsulated fluids. The expression “encapsulated fluid” or “trapped fluid” can be understood as a defined amount of fluid with a constant mass and volume. For the mechanism of APB two requirements have to be met: first, a sealed annulus and second, increasing temperature in the annulus [6]. By fulfilling these conditions, the pressure in the annulus will increase.



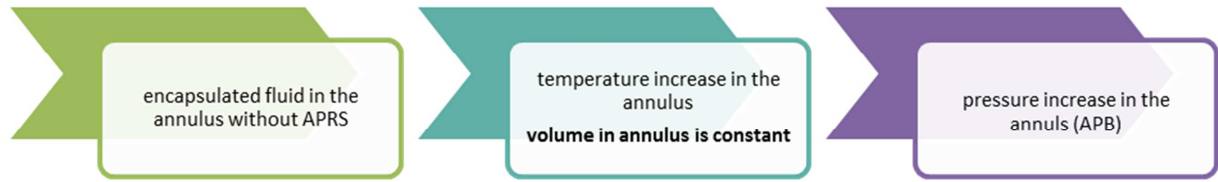


Figure 4: APB without APRS

Figure 4 shows that a temperature increase in the encapsulated annulus leads to a pressure increase. The two governing parameters which influence the amount of pressure increase are: first, the magnitude of the change in temperature and second, the thermodynamic properties of the encapsulated fluid. The physical relation can be described by Eq. 1 [8]:

$$\Delta p = \int_{T_i}^{T_f} \frac{\gamma(T)}{\kappa(T)} dT, \quad (\text{Eq. 1})$$

where  $\Delta p$  is the pressure change due to temperature change (MPa),  $T_i$  is the initial temperature of the fluid ( $^{\circ}\text{C}$ ),  $T_f$  is the final, or end temperature of the fluid ( $^{\circ}\text{C}$ ),  $\gamma$  is the thermal expansion coefficient ( $\text{K}^{-1}$ ) and  $\kappa$  is the isothermal compressibility of the annular fluid ( $\text{Pa}^{-1}$ ).

Figure 5 explains the physical relation with the installed APRS. This system allows expansion of the trapped fluid in the annulus, with the effect that no significant pressure increase occurs.

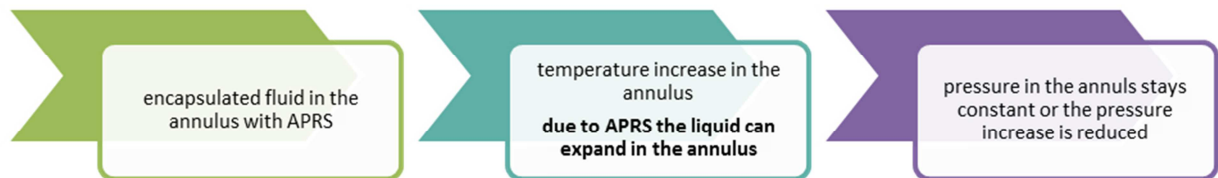


Figure 5: APB with APRS

If the pressure is constant, the physical relation can be described by Eq. 2 [9]:

$$\gamma = \frac{1}{V_i} \left( \frac{dV}{dT} \right)_p, \quad (\text{Eq. 2})$$

where  $V_i$  is the initial volume of the encapsulated annulus liquid ( $\text{m}^3$ ),  $dV$  is the volume change due to temperature change ( $\text{m}^3$ ), and  $dT$  is the temperature change in the annulus ( $^{\circ}\text{C}$ ).

For Eq. 1 and Eq. 2 the following assumptions are considered:

- The fluid in the annulus has a constant mass
- The change in volume of the casing due to temperature change is negligible
- Casing is considered as a rigid body

## Equations

Thermal expansion is the tendency of matter to change in shape, area, and volume in response to a change in temperature [9]. This effect leads to a change in volume when the temperature varies.

For constant pressure conditions, Eq. 2 can be expressed as Eq. 3 [9].

$$\frac{\Delta V}{V_i} = \exp\left(\int_{T_i}^{T_f} \gamma(T) dT\right) - 1 \quad (\text{Eq. 3})$$

If the thermal expansion coefficient is constant, Eq. 3 can be simplified to Eq. 4:

$$\Delta V = \gamma(T_f - T_i)V_i \quad (\text{Eq. 4})$$

For non-linear behaviour Eq. 3 can also be expressed by Eq. 5, using the density and assuming a constant mass:

$$\rho(T) = \rho(T_i) \exp\left(\int_{T_i}^{T_f} -\gamma(T) dT\right), \quad (\text{Eq. 5})$$

where  $V$  is the volume of the fluid ( $\text{m}^3$ ).

Especially for high pressure (HP) and high temperature (HT) wells, APB is a well-known problem. Theoretical models are proposed therefore from many authors e.g., Oudeman and Kerem (2013), Klementich and Jellison (1986), Adams (1991), MacEachran and Adams (1991), Halal and Mitchell (1993).

Oudeman and Kerem (2013) concisely describe how APB can be modelled in HP/HT wells. The following expression, Eq. 6 is adapted from [10] and is used to determine the change in pressure in the annulus:

$$\Delta p = \int_{T_i}^{T_f} \frac{\gamma(T)}{\kappa(T)} dT - \frac{1}{\kappa} \frac{\Delta V_{ann}}{V_{ann}} + \frac{1}{\kappa} \frac{\Delta V_{leak}}{V_{ann}}, \quad (\text{Eq. 6})$$

where  $\Delta V_{leak}$  is the amount of fluid leaking off the annulus while temperature increase ( $\text{m}^3$ ),  $\Delta V_{ann}$  is the change in annular volume due to thermal expansion or ballooning of the surrounding casing or cement sheet ( $\text{m}^3$ ), and  $V_{ann}$  is the annular volume ( $\text{m}^3$ ).

The equation consists of three summands which add up to the resulting pressure increase. The first term represents the pressure increase during temperature change, assuming a constant volume. The second one reduces the pressure increase due to the volume changes of the casing, caused by thermal expansion of the casing. This expression includes also the effect of ballooning due to the pressure increase. The last term takes the pressure change

due to fluid leak-off into account, where  $\Delta V_{leak}$  becomes negative. For a fluid influx the term  $\Delta V_{leak}$  becomes positive.

## 2.2 Existing Methods to Handle or Avoid APB

Since the problem with APB is well known, there are many different ideas, concepts and techniques to control or avoid this phenomenon. The range of methods begins with changing the drilling fluid or adding gases to the cement and ends up with heavy and complicated collars. Existing methods to avoid or handle APB can be in principle split into the following groups [11]:

**Increase of the material grade and wall thickness of the casing, to withstand the pressure increase:** This method leads, due to increased wall thickness, into a reduced inner diameter (ID) of the casing. Thus, the bit diameter of the next section must be reduced. This result in “exotic” bit diameters and, further increased costs. Another option would be to change the whole well design, which ends up in a reduced production rate or higher friction losses, due to the necessary increased flow rate, to achieve the same production rate. Often the required wall thickness to achieve the necessary collapse rating is technically not feasible, and therefore this is not an option to handle APB. Further, an increased wall thickness will result in increasing production costs for the casing.

**Isolating the production tubing, to decrease the temperature increase and therefore to reduce the pressure increase:** This solution leads to increased costs in production for the tubing as well as in increased installation costs. Due to economic reasons, not all kinds of wells are using production tubings. For instance, geothermal wells often produce directly through the casing to achieve the necessary production rates [3].

**Installation of compressible foams or using compressible liquids in the annulus, which allow an expansion of the encapsulated fluid:** These methods are very cost-intensive and need exact calculations and research before they can be applied.

**Installation of mechanical tools, which allow an expansion of the encapsulated fluid:** This thesis deals with a tool which is located in this category. In comparison to other existing systems, the developed tool should be much simpler, more flexible and more robust.

**Establishing a connection between the inner and the outer annulus, to equalize a pressure increase in one of them:** This method is the simplest one to realize, but the significant disadvantage is the wilfully destruction of the casing when APB occurs.

**Establishing a connection between the annulus and the surface or seafloor:** This method is not very common. The possibility of establishing a connection to the surface or seafloor is strongly dependent on the well design. Thus, this method can only be used in wells where all casings are linked to the surface or seafloor.

## 2.2.1 Installing Rupture Disks

Since 2000 rupture disk technology is formally applied in the oil and gas industry to solve the annular pressure problem [11].

A certain number of disks are installed on the casing string according to the estimated fluid level. The rupture disks open a flow path from the annulus into the casing string before the burst or collapse pressure is reached. The flow path is opened through the collapse of the disk. Consequently, the rupture disks remain open if they are once activated and the flow path cannot be closed again.

Figure 6 shows the principal working concept of this system. The major disadvantage of this system is that it establishes a connection between the casing and the annulus which leads to a loss of one well integrity barrier. Therefore, this method prevents the well from getting damaged by APB, but the loss of the barrier can lead to a fundamental integrity problem.

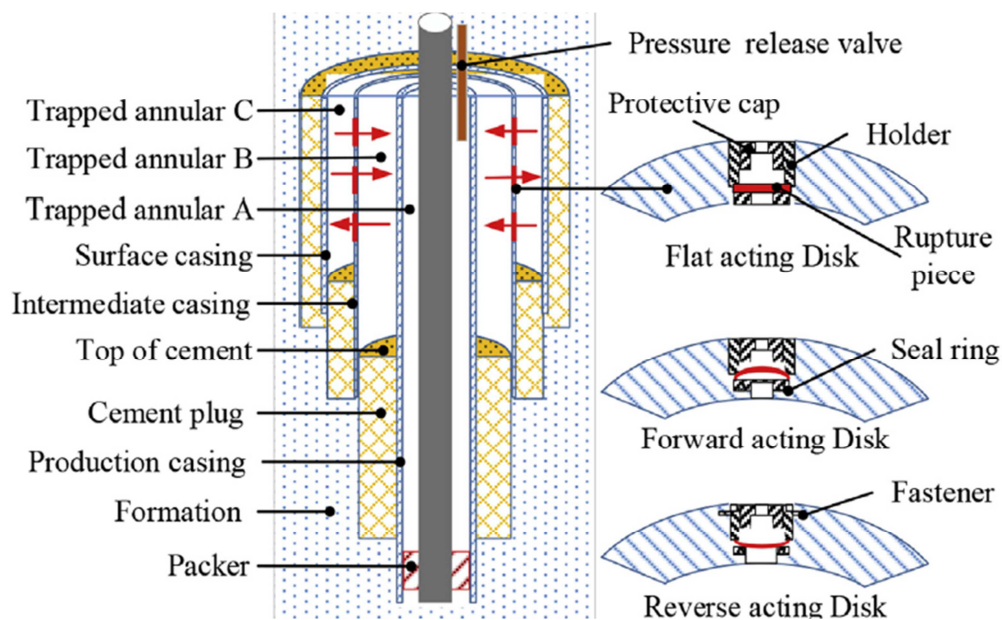


Figure 6: Schematic of Installed Rupture Disc [11]

Figure 7 shows the installed rupture disk at the well site.

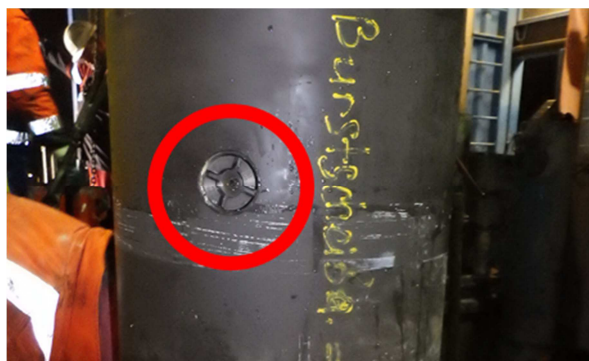


Figure 7: Rupture Disc at Well Side [12]

### 2.2.2 Annular Pressure Relief Collar

The annular pressure relief collar was designed and patented in 2004 to solve the problem of APB [13].

The main difference between this system and the previously mentioned rupture disk is that the annular pressure relief collar can close the connection between the casing strings if the pressure is released. This big advantage allows restoring the principle safety barrier of the casing string when the pressure is released. The tool is small and can be installed symmetrically [13]. However, due to the complexity of the installation and operation, the tool is not widely used [11]. The red arrows in Figure 8 indicate the fluid flow in case of APB.

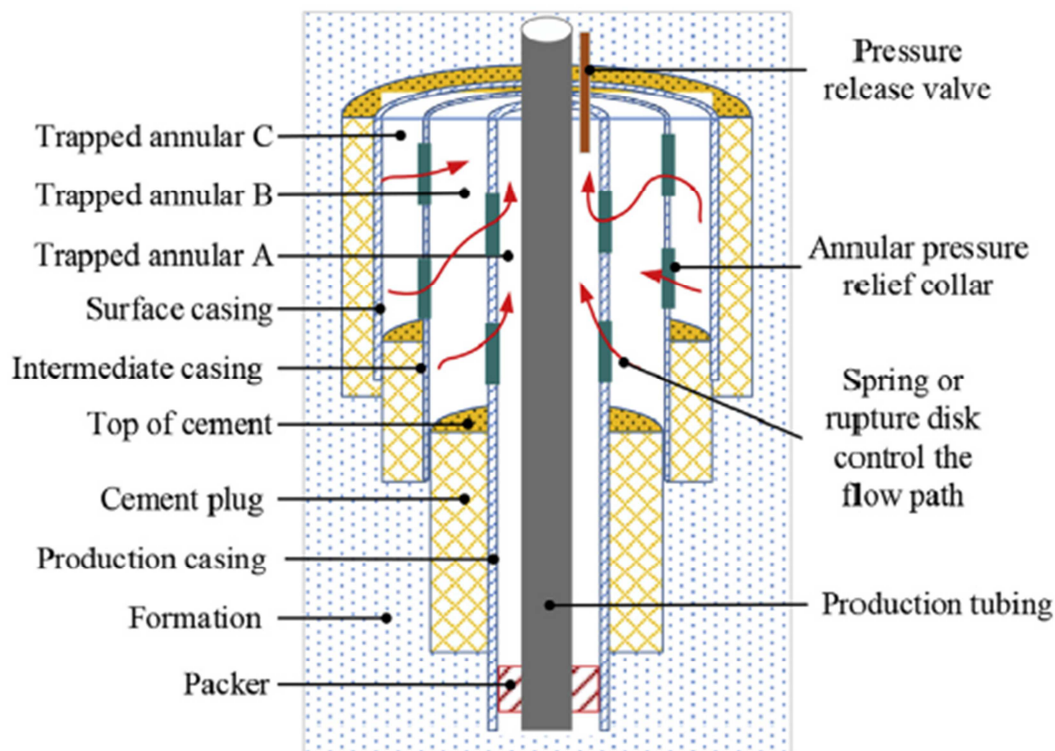


Figure 8: Schematic of Installed Annular Pressure Relief Collar [11]

### 2.2.3 Compound Compressible Foam

The foam technology was proposed in 1993 to control APB [14]. This method has the big advantage that it does not affect the integrity of the well. The basic principle is that the compression change of a compressible or crushable material balances the volume expansion of the heated fluid. Hence, the APB can be assumed to be zero. This is realized by installing compressible foams. When the pressure reaches a certain level, the foam starts to compress, and therefore the pressure will not increase anymore. This pressure is called the start-up pressure. The key of the technology is the selection of a suitable foam material and the exact determination of the start-up pressure. The foam material is strongly dependent on the temperature and pressure. The thickness of the foam depends on the size

of the annulus and ranges between 20 to 40 mm. The length should be 2 to 8 % of the annular depth [15]. Only 2 to 3 % of the foam volume can be compressed, thus a large volume of foam is needed to compensate the APB [11].

The green rectangles in Figure 9 represent the location of the foam. A practical example is shown in Figure 10.

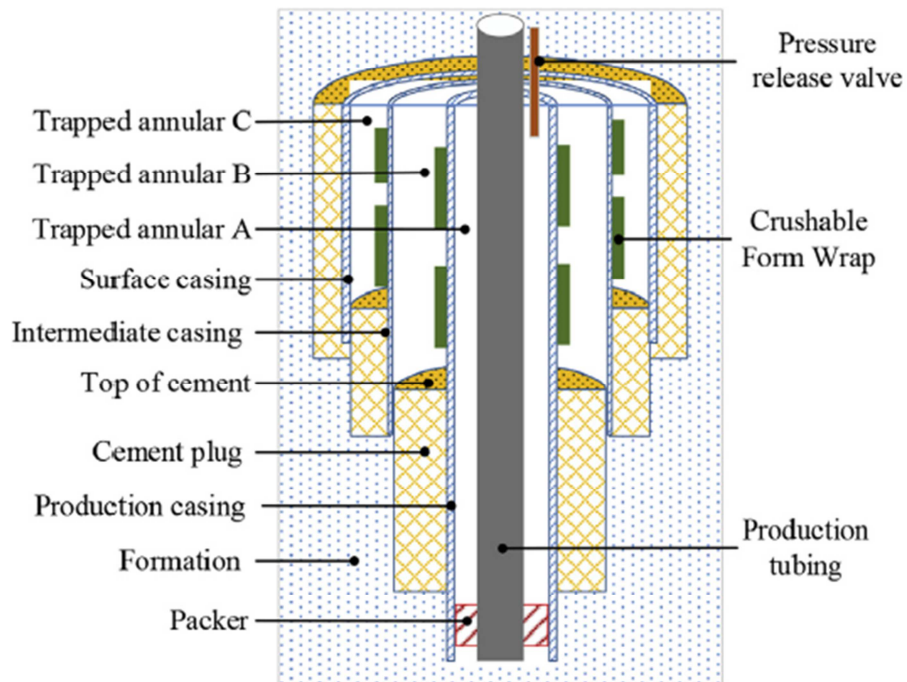


Figure 9: Schematic of Installed Foam [11]



Figure 10: Crushable Foam [16]



Successful applications of this technology are at oilfields such as Machar, MAD Dog, and Ram Powell in the North Sea and Gulf of Mexico. The disadvantage of this method is the huge space that the foam will occupy in the annulus and therefore is susceptible during cementing jobs or just during the installation of the casing. Further, the limited working pressure and temperature of the foams are often not suitable for geothermal wells [11].

### **2.3 The Motivation for Developing a New Tool**

Especially for deep-water oil and gas wells APB is a well-known problem in the industry [11]. Representative mentioned for casing collapse due to ABP, the following two wells are listed:

- A deep-water well in Marlin Oilfield was abandoned due to the collapse of the production casing, and trapped annular pressure was one of the main reasons [17].
- The casing of Well Pompano A-31 in Mexico Gulf was deformed by trapped annular pressure, causing a stuck drill pipe [18]. Besides, a pressure change in the wellbore could break well-sealing integrity, inducing sustained casing pressure [19].

Due to the disadvantages of the existing methods mentioned in the previous chapter, an alternative approach is desired. The novelty is to be seen in the development of a mechanically simple tool which can be used independently of drilling depth and temperature difference. For most currently available options, technically complex systems are necessary to install them. Therefore, the innovation of this project lies in the simple, robust and cost-effective application and installation of the tool as well as in saving time.

### 3 Description of a Representative Well

To get an idea of the necessary design criteria, a down-hole tool, the APRS, for a representative well was determined. Figure 11 describes the casing design of the well. The areas where APB can occur are marked with Position A and Position B1/B2. The difference between B1 and B2 is the usage of another casing diameter. Instead of a 20 in casing, a 18 5/8 in casing is used. Therefore, the annular volume is smaller, and hence the available space for the tool decreases.

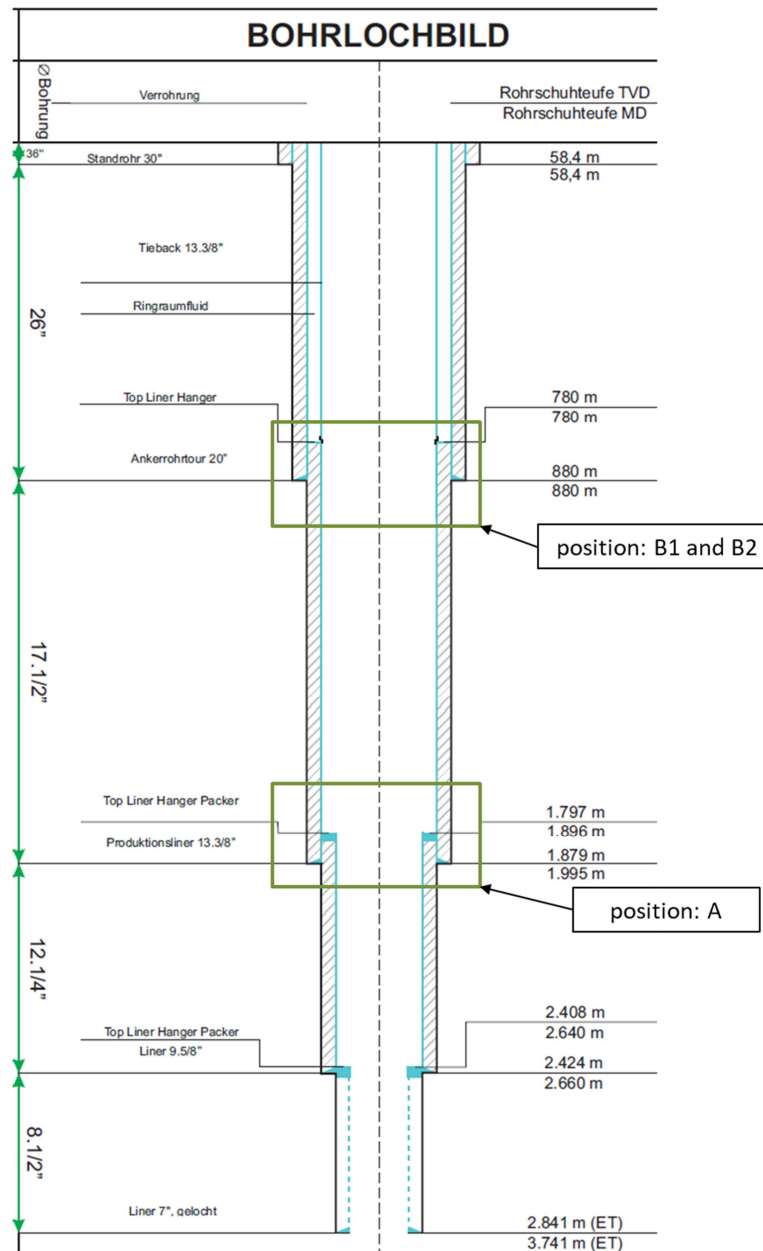


Figure 11: Well Schematic [12]

For the design, the worst-case scenario is used which means that for the volume the greatest value is chosen, and for the constructed space, the smallest value is designated.



### 3.1 Problem Definition

As mentioned before, APB occurs only in areas where barriers encapsulate the fluid. In Figure 12 different locations where APB can occur are shown, and the positions where the APRS can be installed are drawn schematically. The APRS is denoted as item 00.

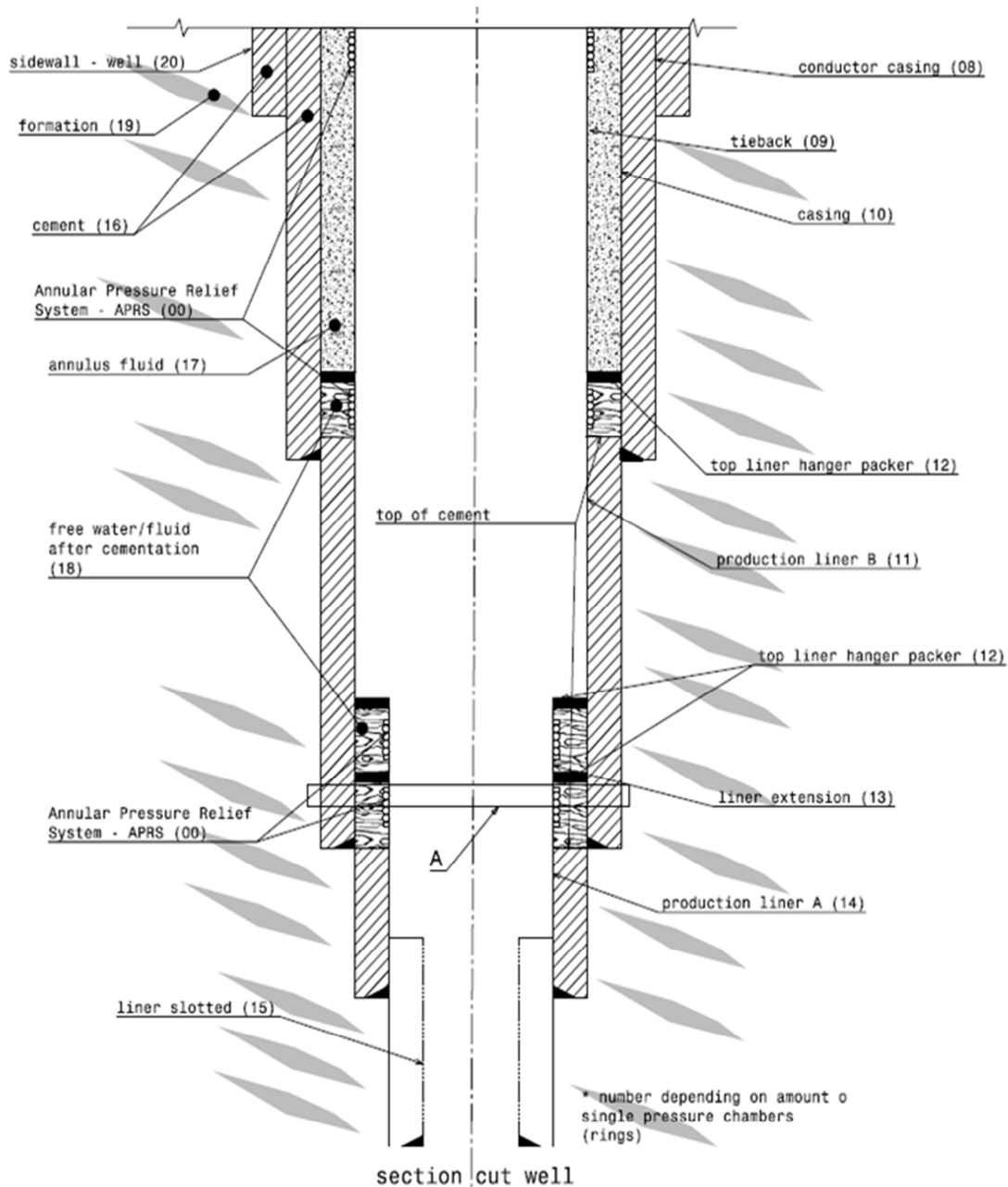


Figure 12: Installation Examples APRS

Some of the following locations might be required to avoid APB for this well:

**Location 1** could be necessary, if the annulus is sealed from above and below. This scenario can occur in subsea wells or due to technical reasons onshore. On top, the fluid is limited to expand, and on the bottom, the top liner hanger packer seals the annulus.

Consequently, the fluid can only expand by damaging the casing, denoted as item 10, or tieback, see item 09.

**Location 2** is a critical area for APB because the annulus is sealed on top with the top liner hanger packer and below with the cement of the production liner B, see item 11. Hence, APB will damage the production liner B or the casing, denoted as item 10.

**Location 3** is also an area where APB can occur because on top and bottom of the annulus a top liner hanger packer encapsulates the fluid in between, denoted as item 12. Thus, APB would destroy the liner extension, denoted as item 13, or the casing, see item 10.

**Location 4** is the deepest installation of the APRS. On top, the annulus is closed by the top liner hanger packer, and on bottom, the cement of the production liner A encapsulates the fluid in the annulus.

Hence, dependent on the installation and casing design, the installation depths and therefore the boundary conditions for the tool design can vary significantly.

## 3.2 Boundary Conditions

The boundary conditions and the primary load conditions are based on the representative well. The most important parameters like pressure and temperature are defined in a way that the tool can serve a very large operating range. The tool should withstand a maximum pressure difference of 600 bar, and the maximum expected production temperature is 170°C. Thus, the tool can operate in deep wells as well as in shallow wells without further design steps and the overall design goal to create a tool with a versatile operational area and load scenarios. Therefore, the pressure increase does not have to be determined for each scenario exactly.

These values are essential for the material selection and the stress calculation. The safety factor (SF) for the stress calculation is defined with 1.5, and the estimated volume will be increased by 20 % to account for unexpected behaviours.

For the initial start of the concept phase it was decided that the parameters for the APB calculation should be defined by the values of the exemplary well.

Table 1 illustrates the pressure and temperature with respect to the position A, B1, and B2.

Table 1: Boundary Conditions – Temperature and Pressure [12]

Position A	Value	Unit
initial temperature ( $T_i$ )	68	°C
final temperature ( $T_f$ )	120	°C
initial pressure ( $p_i$ )	202.649	bar

Position B1	Value	Unit
initial temperature ( $T_i$ )	37	°C
final temperature ( $T_f$ )	120	°C
initial pressure ( $p_i$ )	87.961	bar

Position B2	Value	Unit
initial temperature ( $T_i$ )	37	°C
final temperature ( $T_f$ )	120	°C
initial pressure ( $p_i$ )	87.961	bar

From these values, a worst-case scenario is defined, thus the values used for the initial design process of the tool are:

- $T_i = 68^\circ\text{C}$
- $T_f = 120^\circ\text{C}$
- $p_i = 88 \text{ bar}$

The background behind this choice is simply the fact that position A has less space for possible tools and therefore represents the worst-case scenario. The fact that the temperature difference at position B1 or B2 is bigger indicates an increased volume expansion or pressure increase. Compared to the larger annulus at position B1 the decision was made that this is easier to handle than a smaller annulus with a smaller temperature difference.

### Available Constructed Space

The amount of free space in the annulus is rare. The outer diameter (OD) of the inner liner and the inner diameter (ID) of the outer casing define the available space. Additionally, the required space for cementing and installation must be considered. The values for clearance are referenced to the dimensions of the top liner hanger packer, which is located near the possible downhole position of the tool and therefore has to satisfy similar requirements. The dimensions of the used casings are related to the data sheets provided by the manufacturer.

To ensure an excellent cementing job, the following definitions were set:

- If the tool will use the entire cross-section of the annulus, the clearance to the casing must have a gap of 5 mm to the API drift diameter. This value is related to the available clearance between the top liner hanger packer and the casing in the current well design.
- If the tool is only partly using the available space in the annulus, hence the cement is able to bypass the tool. The API drift diameter of the casing is the limiting factor.

Figure 13 shows the available free space for the tool. The open space between the casings or tubings or liners is represented by an “x”. The available clearance “x” is calculated according to the above-mentioned rules from the API drift diameter of the outer tubing minus the OD of the inner tubing.

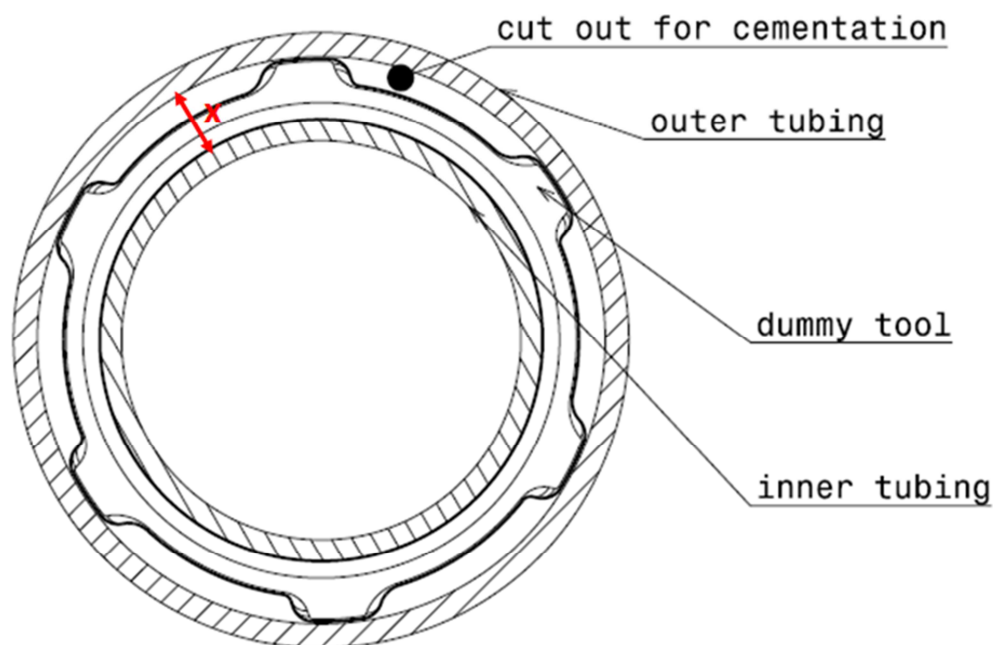


Figure 13: Clearance in Well

For the exemplary well the following constructed spaces are derived:

- Position A:
  - max distance (x): 27.76 mm (full cross-section)
  - max distance (x): 33.26 mm (partial cross-section)
- Position B1:
  - max distance (x): 55.13 mm (full cross-section)
  - max distance (x): 61.13 mm (partial cross-section)
- Position B2:
  - max distance (x): 46.01 mm (full cross-section)
  - max distance (x): 40.01 mm (partial cross-section)

### 3.3 Fluid Properties

The composition of the annular fluid varies with each well. However, major differences in fluid chemistry are due to different geological backgrounds in different hydrogeochemical provinces. To shed light on this issue, a few characteristic chemical compositions of the fluid from the Bavarian Molasse Basin [20] are selected.

The compositions are based on fluid analysis of existing wells in the provinces Rhine Graben [21] and the North German lowlands/plain [22]. The major difference affecting the fluid properties is the content of total dissolved solids and thus the interaction between electrolytes. Therefore, a prediction of the fluid properties is difficult.

To minimize the number of variables, a theoretical composition, see Table 2, and some known compositions, see Table 3, of actual producing wells are compared to pure water. The idea is to see if the composition, of the annular fluid, is essential for a rough estimation of volume expansion.

Table 2: Artificial System

Fluid Composition	
Na	100 mg/l
Cl	120 mg/l
Ca	10 mg/l

Table 3: Fluid Compositions

Well	Composition According to Citation (for details see appendix A)
Bruchsal	[21]
Groß Schönebeck	[22]
Pullach (Malm)	[20]

To evaluate the effect of fluid composition on fluid expansion due to temperature change, a calculation based on PHREEQC [23] was done. The main content of the written script can be found in appendix A: Eq. 29 [24] and Eq. 30 [24].

Figure 14 represents the output of the calculation.

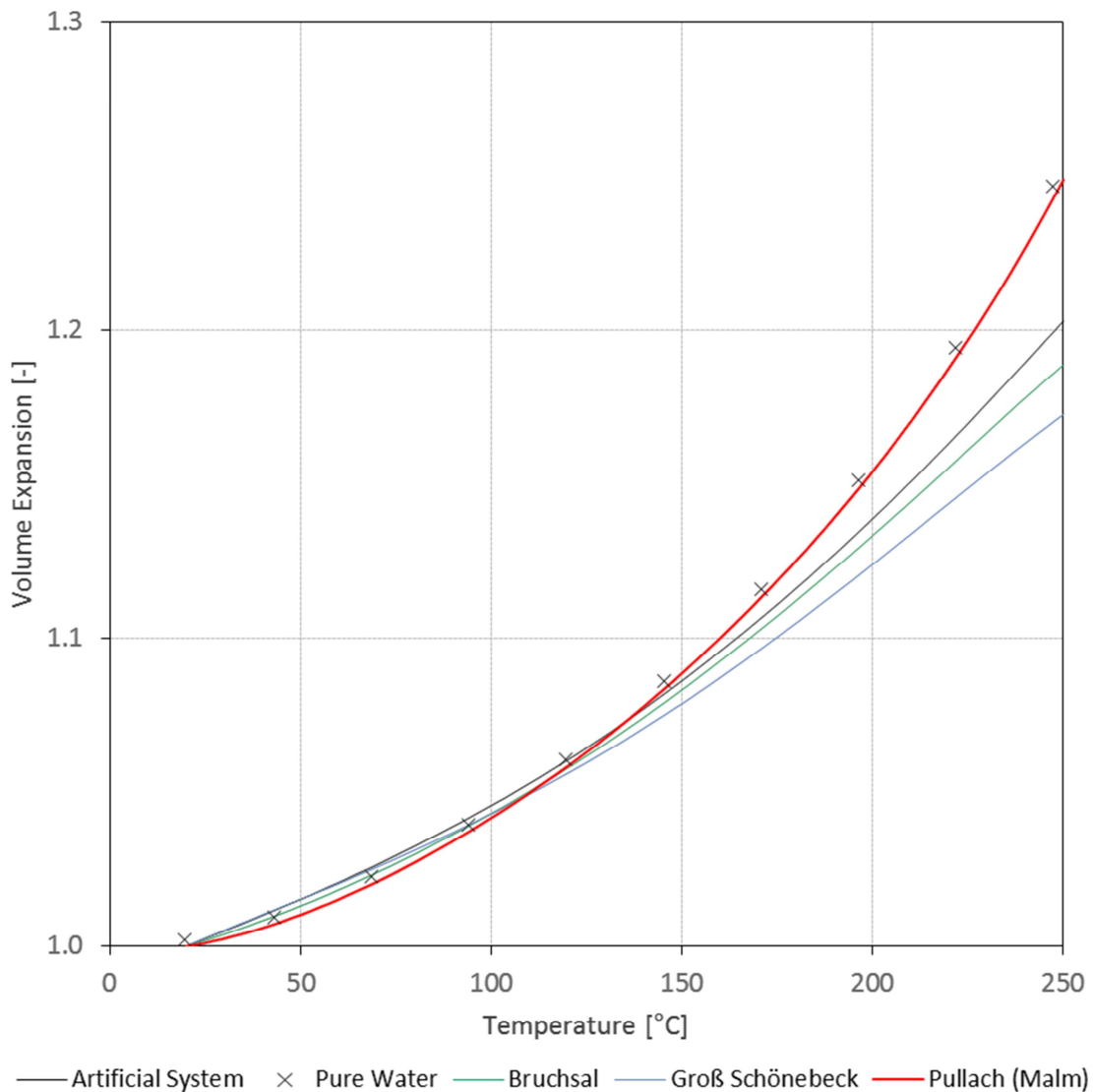


Figure 14: Volume Expansion Depending on the Composition of the Fluid

The plot of the fluid density for the mentioned compositions indicates the variety of the volume expansion. For example, the increase in volume for fluid “Bruchsal” is smaller compared to the expansion of pure water at the same boundary conditions, see Figure 14. Further, it was not surprising that the fluid “Pullach” has a similar behaviour as pure water, because the salinity of the fluid “Pullach” is very low. The general trend shows that pure water has the highest slope and therefore the largest volume expansion. Thus, the results can be simplified to the assumption that pure water has the most considerable effect on volume expansion. According to this, the worst case is the consideration of pure water, hence the calculations required for the design of the tool are based on the properties of pure water.

### 3.4 Properties of Water

The modified Spivey et al. correlations are used to calculate the density and the compressibility of water at a given temperature and pressure [25]. Additionally, the results are compared to literature values, to see if the calculation is accurate enough. The calculation was done in Microsoft Excel, and the used script can be found in the appendix B.

Spivey et al. use a rational function in temperature, of the form

$$a(T) = \frac{a_1 \left(\frac{T}{100}\right)^2 + a_2 \left(\frac{T}{100}\right) + a_3}{a_4 \left(\frac{T}{100}\right)^2 + a_5 \left(\frac{T}{100}\right) + 1} \quad (\text{Eq. 7})$$

as a general correlation for temperature-dependent parameters, see Eq. 7 [25,26]. Where  $a_i$  are the coefficients from Table 4,  $T$  is the temperature of interest ( $^{\circ}\text{C}$ ), and  $a(T)$  is a temperature depended factor for  $\rho_w(T, 70\text{MPa})$ ,  $E_w(T)$ , or  $F_w(T)$ .

Table 4: Coefficients for Equation of State [25]

$a_i$	$\rho_w(T, 70\text{MPa})$	$E_w(T)$	$F_w(T)$
$a_1$	-0.127213	4.221	-11.403
$a_2$	0.645486	-3.478	29.932
$a_3$	1.03265	6.221	27.952
$a_4$	-0.070291	0.5182	0.20684
$a_5$	0.639589	-0.4405	0.3768

With these parameters the density of pure water can be estimated by the following steps:

In **step one** the density of pure water is calculated,  $\rho_w(T, 70\text{MPa})$ , at a reference pressure of 70 MPa in  $\text{g/cm}^3$ , at a temperature of interest ( $T$ ) using Eq. 7 with the coefficients in Table 4. Next the values of the compressibility coefficients  $E_w(T)$  and  $F_w(T)$  are calculated by using the same equation but different coefficients.

**Step two** calculates the compressibility  $c_w(T,p)$  in  $\text{MPa}^{-1}$  of pure water at a temperature and pressure of interest from Eq. 8 [25,26].

$$c_w(T, p) = \frac{1}{70} \frac{1}{E_w(T) \left( \frac{p}{70} \right) + F_w(T)}, \quad (\text{Eq. 8})$$

where  $c_w(T,p)$  is the compressibility of pure water ( $\text{MPa}^{-1}$ ), and  $p$  is the pressure of interest (MPa).

In **step three** the density of pure water is calculated at a temperature ( $T$ ) and pressure ( $p$ ).

The values for  $I_w(T, 70 \text{MPa})$  and  $I_w(T, p)$  are calculated from Eq. 9 [25,26] and Eq. 10 [25,26].

$$I_w(T, 70 \text{MPa}) = \frac{1}{E_w(T)} \ln |E_w(T) + F_w(T)| \quad (\text{Eq. 9})$$

$$I_w(T, p) = \frac{1}{E_w(T)} \ln \left| E_w(T) \left( \frac{p}{70} \right) + F_w(T) \right| \quad (\text{Eq. 10})$$

Finally from Eq. 10 the temperature and pressure dependent density of pure water  $\rho_w(T,p)$  in  $\text{g/cm}^3$  is calculated, see Eq. 11 [25,26].

$$\rho_w(T, p) = \rho_w(T, 70 \text{MPa}) \text{EXP}[I_w(T, p) - I_w(T, 70 \text{MPa})] \quad (\text{Eq. 11})$$

The results for the temperature and pressure of interest are listed in Table 5.

Table 5: Density of Water  $\rho(p, T)$

Position	Temperature [°C]	Pressure [bar]	Density [ $\text{kg/m}^3$ ]
A	68	200	987.449
A	120	200	952.689
B1 and B2	37	88	997.128
B1 and B2	120	88	947.353



## 4 APB Volume and Pressure Calculation

The initial volume of trapped fluid  $V_i$  is calculated from the annular space. The annular space is defined by the inner diameter of the outer casing, liner or tubing  $d_{i,outer, csg}$  and the outer diameter of the inner casing, liner or tubing  $d_{o,inner,csg}$  in the section of interest. In this chapter, it should be mentioned that the word casing also stands for a liner, tubing or the other way around.

Figure 15 shows a schematic sketch of the annulus space, where the ID of the outer tubing is  $d_{i,outer, csg}$  and the OD of the inner tubing is  $d_{o,inner,csg}$ .

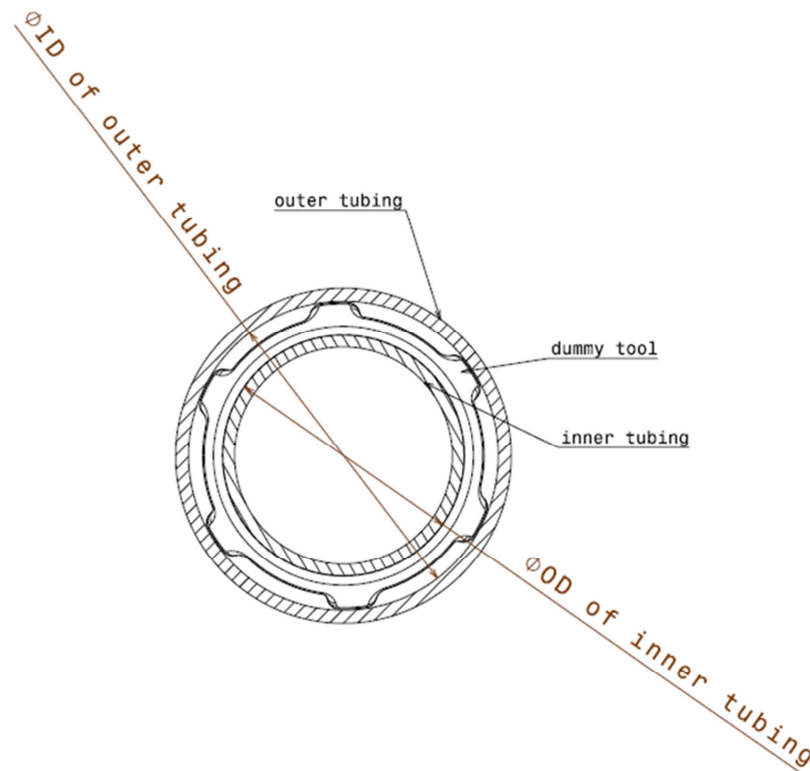


Figure 15: Cross Section of Annulus

To derive comparable values, the boundary conditions are determined as follows:

- Annulus height:  $h = 15 \text{ m}$
- Fluid level in annulus:  $100 \%$

By using Eq. 12 the total volume occupied by the fluid can be calculated as follows,

$$V_i = h \frac{(d_{i,outer,csg}^2 - d_{o,inner,csg}^2) \pi}{4}, \quad (\text{Eq. 12})$$

where  $h$  is the height of the fluid column in the annulus (mm),  $d_{i,outer, csg}$  is the ID of the outer casing (mm),  $d_{o,inner,csg}$  is the OD of the inner casing/liner (mm).

The results for the annular volume of each position are displayed in Table 6.

Table 6: Volume of Trapped Fluid

Position A	Value	Unit
$d_{i,outer, csg}$	313.61	mm
$d_{o,inner, csg}$	244.48	mm
$V_i$	0.455	m <sup>3</sup>
$V_i + 20\%$ (safety)	0.545	m <sup>3</sup>

Position B1	Value	Unit
$d_{i,outer, csg}$	466.75	mm
$d_{o,inner, csg}$	339.73	mm
$V_i$	1.207	m <sup>3</sup>
$V_i + 20\%$ (safety)	1.448	m <sup>3</sup>

Position B2	Value	Unit
$d_{i,outer, csg}$	436.5	mm
$d_{o,inner, csg}$	339.73	mm
$V_i$	0.885	m <sup>3</sup>
$V_i + 20\%$ (safety)	1.062	m <sup>3</sup>

The results heads to the first design challenge. Due to the vast differences between the volumes in position A, B1 and B2, it will be complicated to manage the APB with the same tool. To overcome the problem, the design of the tool should enable a quick adaption for the necessary volume.

## 4.1 Volume Expansion due to APB

Since common tables in literature for  $\gamma$  mostly assume a constant pressure of 1 bar, a constant pressure is used as boundary condition, if not otherwise denoted.

To minimize failures and to increase the accuracy of the obtained result, the volume expansion  $\Delta V$  due to APB, is calculated by five different methods. The results are then compared, and the most appropriate method selected. The selection is done by comparing the results of the method with values from literature. In the beginning it was necessary to estimate the expansion volume roughly to evaluate the potential concepts and narrow the

number of on-going concepts. Thus, a quick option to calculate the expansion volume was more important, than the accuracy of the result.

#### 4.1.1 Method 1

For a first estimation,  $\gamma$  is assumed to be constant. The value for  $\gamma$  is therefore calculated as an average between the final temperature and the initial temperature. Eq. 1 can be solved by applying the boundary values from Table 6 and Table 7.

For pure water, the expansion factors and the compressibility factors depending on temperature at constant pressure are shown in appendix B, see Table 27. Table 7 shows the mean values at a given temperature range for the calculation and is based on the properties given in Table 27.

Table 7: Mean values for  $\gamma$  and  $\kappa$

Position A	Value	Unit
$\gamma$	6.4E-04	K <sup>-1</sup>
$\kappa$	4.645E-10	Pa <sup>-1</sup>
Position B		
$\gamma$	5.41E-04	K <sup>-1</sup>
$\kappa$	4.595E-10	Pa <sup>-1</sup>

Figure 16 represents the thermal expansion coefficient ( $\gamma$ ) based on values available in the literature, see [27]. The curves of the plot represent the initial pressure of the fluid in steps of 100 bar, ranging from 1 to 1000 bar. The curves stop at the moment when water starts to vaporize, thus two phases exist, and the fluid expansion cannot be determined. Therefore,  $\gamma$  can be determined only for high pressures. The figure illustrates that pressure and temperature have a substantial impact on the magnitude of  $\gamma$  and therefore on the amount of fluid expansion. Hence, especially for high pressures and temperatures the influence is huge. Geothermal wells operate at high pressures and temperatures, hence the pressure dependency of  $\gamma$  cannot be neglected and a more accurate method is needed.

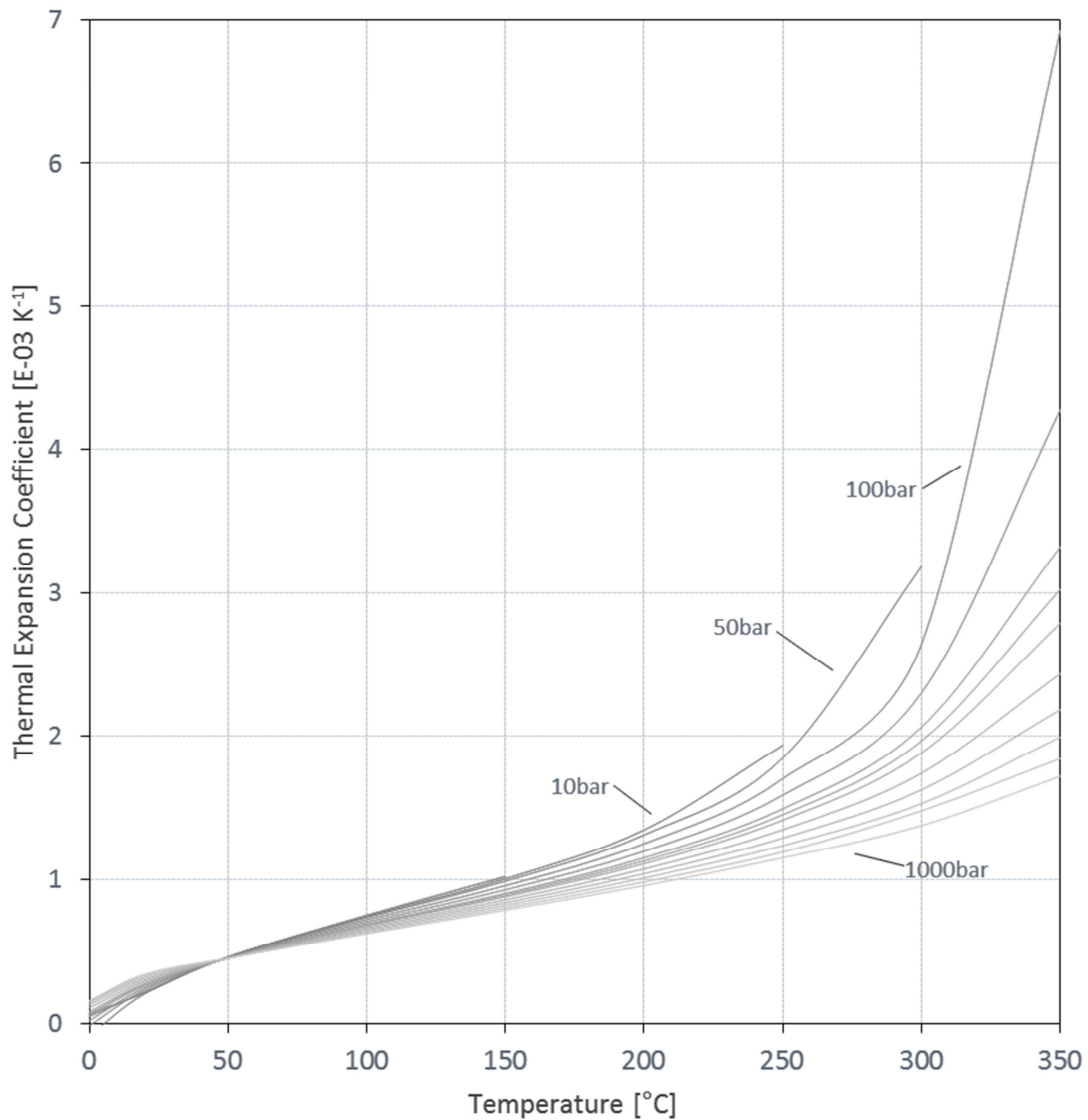
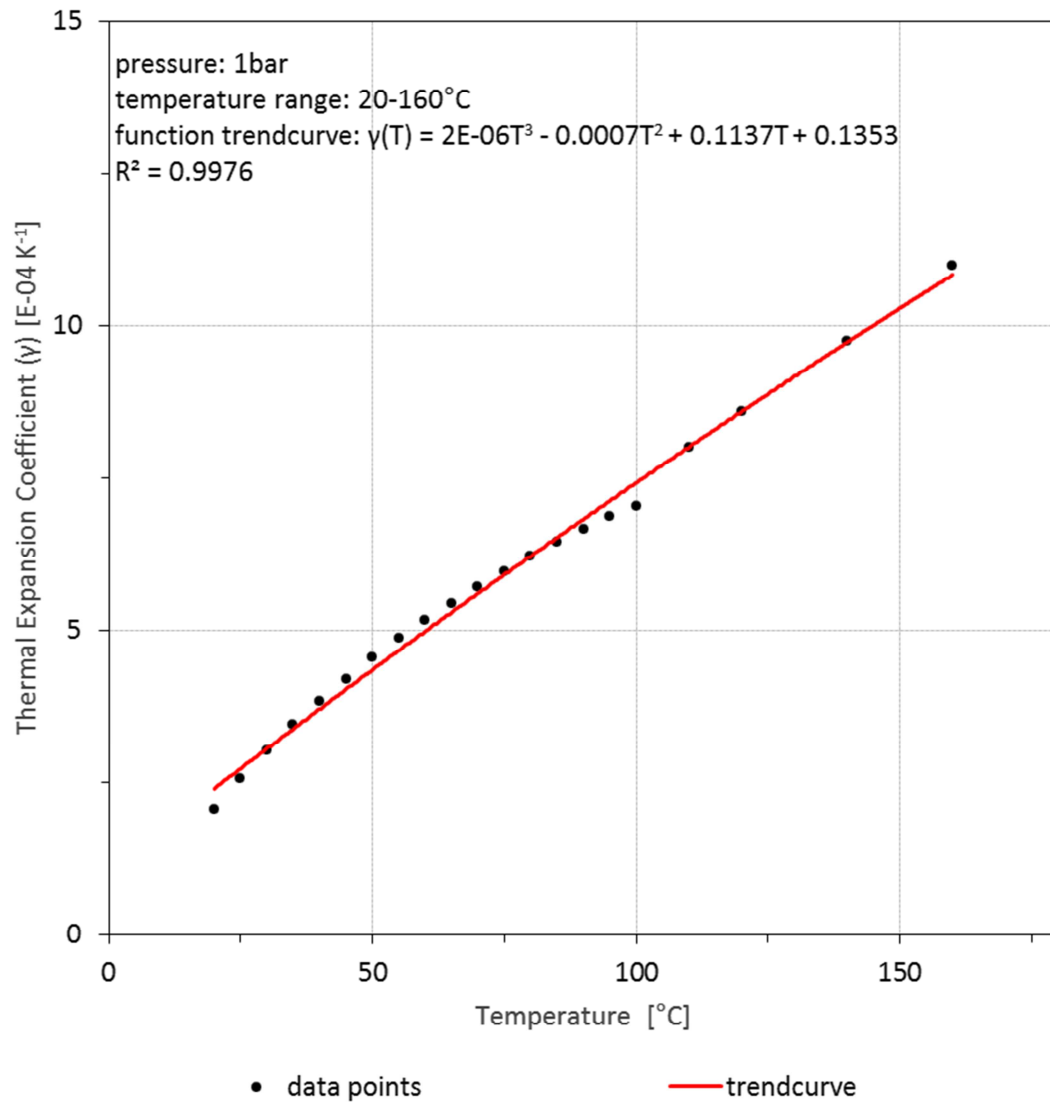


Figure 16: Thermal Expansion Coefficient of Pure Water

### 4.1.2 Method 2

Method 2 assumes that the coefficient,  $\gamma$ , is dependent on temperature by assuming still a constant pressure.

A trend curve is now constructed by applying data from various functions of  $\gamma(T)$ . To minimize failures and to increase the precision, many plots with varying data sources [27,27] and different types of trendlines, like linear, potential or exponential, are generated. A representative curve and the derived function for  $\gamma(T)$  is shown in Figure 17.

Figure 17:  $\gamma(T)$  - Trendcurve

For a first assumption the polynomial curve is accurate enough. Therefore, this curve is used for the APB calculations in the initial concept phase for a rough estimation of the volume and pressure increase due to APB. The trendcurve was then used in Eq. 3 to obtain the results for pressure or volume change in the annulus. The procedure to gain results is very complex, the risk of calculation errors and inaccuracy is high. Thus, this method is not very comfortable in practical applications and the pressure dependency is not accounted for.

### 4.1.3 Method 3

Method 3 accounts, contrary to method 2, for pressure dependency. This method was mainly used to improve the second method and to derive values which can be compared to method 4 and 5.

According to Figure 16 the thermal expansion coefficient is also dependent on pressure. To take this into account and to see if this influence is negligible, the volume expansion is calculated for different pressures. Similar to the previous method, different trendcurves are generated, to get the temperature dependent function of  $\gamma$ . The pressure range is set from 0 to 600 bar, and the temperature is set from 20 to 200°C.

The results are then compared to the reference calculation of 0 bar. Neglecting the pressure dependency will result in a total inaccuracy of approximately 2 to 14 %. Concluding from that we can say that for our initial concept phase the pressure dependency can be ignored

The main difference to the second method is that the available datasets for the thermal expansion coefficient are decreasing with increasing pressure. This means that the available data points to fit the trend curve are getting less at increased pressures. Thus, the derived function increases uncertainty with increasing pressure. It was also checked by evaluating the quality of the trendcurve if it's better to use a dataset with a large amount of values but only at a constant pressure of one bar, independent of the operating pressure. Further it was checked if the pressure dependency is more critical than the number of data points. Consequently, it turned out that in case of altering pressure, the curves for a further usage are not applicable.

#### 4.1.4 Method 4

Method 4 is based on the fact that the total mass continuity of the fluid. The density of water by varying of different pressures and temperature is calculated according to chapter 3.4. In Table 5 the corresponding density values for the exemplary well can be found. Using these results and rearranging the equations as follows, the expanded volume can be calculated. This method takes the pressure and temperature change into account.

$$m = \rho_o V_o = \rho_i V_i \quad (\text{Eq. 13})$$

and further

$$V_f = \frac{\rho(T_i, p_i)}{\rho(T_f, p_f)} V_i, \quad (\text{Eq. 14})$$

with

$$\Delta V = V_f - V_i \quad (\text{Eq. 15})$$

can be rearranged to:

$$\Delta V = V_i \left( \frac{\rho(T_i, p_i)}{\rho(T_f, p_f)} - 1 \right) \quad (\text{Eq. 16})$$

Where  $m$  is the mass of the fluid (kg),  $V_f$  is the final volume of fluid after expansion ( $m^3$ ). The corresponding script for the Microsoft Excel sheet can be found in appendix C.

#### 4.1.5 Method 5

This method uses the water formation volume factor,  $B_w$ , to derive the density of water for a given pressure and temperature. “The produced water formation volume factor (FVF),  $B_w$ , is defined as the volume at reservoir conditions occupied by 1 stock tank barrel (STB) of formation water plus its dissolved gas. It represents the change in volume of the formation water as it moves from reservoir conditions to surface conditions” [28].  $B_w$  considers the following three effects [28]:

- Liberation of gas from water as pressure is reduced
- Expansion of water as pressure is reduced
- Shrinkage of water as temperature is reduced

$B_w$  describes the volume change between the reservoir and the stock tank conditions, thus the volume change of the annular fluid can be calculated.

The initial volume at reservoir conditions,  $V_o$ , is known. Now the volume at surface conditions  $V_s$  is calculated.  $B_w$  is recalculated with increased downhole temperature ( $T_f$ ) and with the previously calculated volume  $V_s$  the final volume  $V_f$  can be estimated. Therefore, the pressure and temperature dependencies are included.

$B_w$  is calculated according to McCain [26] by using Eq. 17, Eq. 18 and Eq. 19.

$$B_w = (1 + \Delta V_{wp})(1 + \Delta V_{wT}) \quad (\text{Eq. 17})$$

where

$$\Delta V_{wp} = -1.0001 * 10^{-2} + 1.33391 * 10^{-4} * T + 5.50654 * 10^{-7} * T^2 \quad (\text{Eq. 18})$$

and

$$\Delta V_{wT} = -1.95301 * 10^{-9} * p * T - 1.72834 * 10^{-13} * p^2 * T - 3.58922 * 10^{-7} * p - 2.25341 * 10^{-10} * p^2, \quad (\text{Eq. 19})$$

where  $p$  is the pressure (psia),  $T$  is the temperature ( $^{\circ}\text{F}$ ).

### 4.1.6 Overview

The volume expansion due to APB is listed by different calculation methods in Table 8.

The input parameters for position A are:

initial temperature ( $T_i$ ) of 68°C, temperature of the production fluid ( $T_f$ ) 120°C, initial volume in the annulus 0.545 m<sup>3</sup> and initial pressure ( $p_i$ ) 203 bar.

The input parameters for position B1 are:

initial temperature ( $T_i$ ) of 37°C, temperature of the production fluid ( $T_f$ ) 120°C, initial volume in the annulus 1.448 m<sup>3</sup> and the initial pressure ( $p_i$ ) 88 bar.

The input parameters for position B2 are:

initial temperature ( $T_i$ ) of 37°C, temperature of the production fluid ( $T_f$ ) 120°C, initial volume in the annulus 1.062 m<sup>3</sup> and initial pressure ( $p_i$ ) 88 bar.

Table 8: Results of Expansion Volume Calculation

	Method Nr.	$\Delta V$ [m <sup>3</sup> ]	$\Delta V$ [l]	Comments
Position A	Method 1	0.0169	16.9	p=1bar
	Method 2	0.0204	20.4	p=1bar
	Method 3	0.0199	19.9	pressure dependency is considered
	<b>Method 4</b>	<b>0.0198</b>	<b>19.8</b>	
	Method 5	0.0173	17.3	
selected method: method 4				
	Method Nr.	$\Delta V$ [m <sup>3</sup> ]	$\Delta V$ [l]	Comments
Position B1	Method 1	0.0754	75.4	p=1bar
	Method 2	0.0785	78.5	p=1bar
	Method 3	0.0653	65.3	pressure dependency is considered
	<b>Method 4</b>	<b>0.0761</b>	<b>76.1</b>	
	Method 5	0.0689	68.9	
selected method: method 4				
	Method Nr.	$\Delta V$ [m <sup>3</sup> ]	$\Delta V$ [l]	Comments
Position B2	Method 1	0.0553	55.3	p=1bar
	Method 2	0.0575	57.5	p=1bar
	Method 3	0.0536	53.6	pressure dependency is considered
	<b>Method 4</b>	<b>0.0558</b>	<b>55.8</b>	
	Method 5	0.0505	50.5	
selected method: method 4				



As listed in Table 8 the results for  $\Delta V$  spread up to 9 %. Hence, for a proper tool design the pressure and temperature dependency should be taken into account. Consequently, for the following tool design, method 4 is defined as the most suitable one. The reason therefore is, that the pressure and temperature dependency of the density of water is easier to derive than the compressibility of water. Thus, the values can be calculated comparable easy contrary to the thermal expansion coefficient.

## 4.2 Expansion Volume due to APB

For further estimation of the expansion volume method 4 is used. To get an overview of the required volume for the tool design, a graphical representation of the necessary expansion volume was generated, see Figure 18. By knowing the initial temperature and the final temperature, the volume expansion can be determined graphically. This plot only represents the effect of APB at the following boundary conditions: corresponding to position A the annular volume is  $0.5 \text{ m}^3$  and the initial pressure is 200 bar.

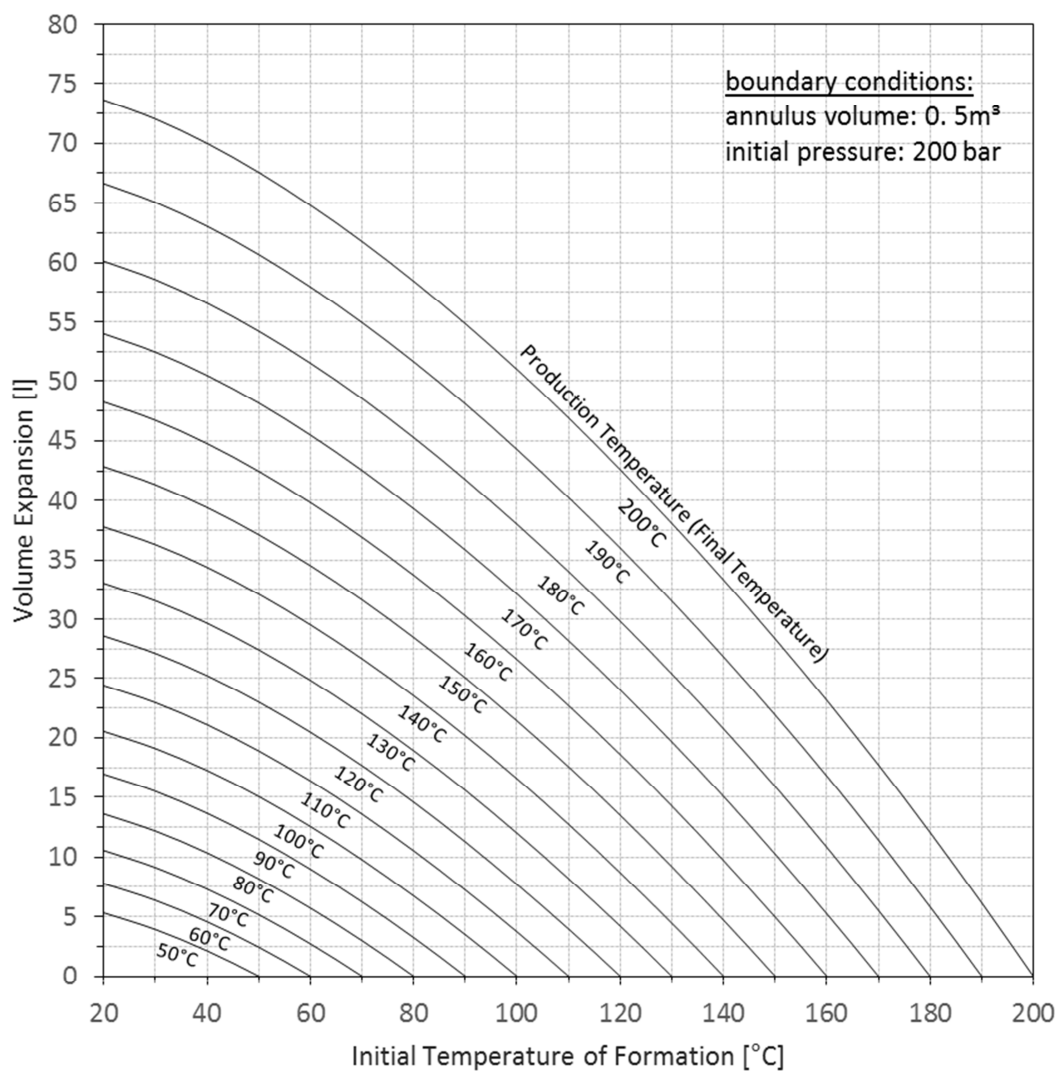


Figure 18: Volume Expansion at Position B

### 4.3 Pressure increase due to APB

The pressure increase is calculated to show the huge impact of fluid expansion and the potential risk out of this if APB is neglected.

Eq. 20 [10] is used to calculate the pressure increase. The equation shows the pressure increase as a function of the temperature increase assuming a constant volume.

$$\Delta p = \int_{T_i}^{T_f} \frac{\gamma(T)}{\kappa(T)} dT + \left( \frac{1}{\kappa} \frac{\Delta V_{ann}}{V_{ann}} \right) - \left( \frac{\frac{U}{W}}{\kappa} \frac{\Delta V_{leak}}{V_{ann}} \right) \quad (\text{Eq. 20})$$

In a first assumption the terms,  $W$  and  $U$  can be neglected. The reason behind this is simply as their contribution to the pressure variation is small compared to the first term of Eq. 20. Thus, for a rough estimation the first term is the most important one.

According to the previously mentioned reasons Eq. 20 can be reduced to Eq. 21.

$$\Delta p = \int_{T_i}^{T_f} \frac{\gamma(T)}{\kappa(T)} dT \quad (\text{Eq. 21})$$

The pressure increase for position A and B is calculated with Eq. 21. The results for the positions are:

- Position A: 793 bar
- Position B1: 1143 bar
- Position B2: 1143 bar

Compared to the initial pressure the obtained values are high, thus the pressure increase due to APB is massive.

Figure 19 displays the pressure increase due to APB related to the initial pressure,  $p_i$ . The final temperature is set corresponding to the production temperature of  $120^\circ\text{C}$ .

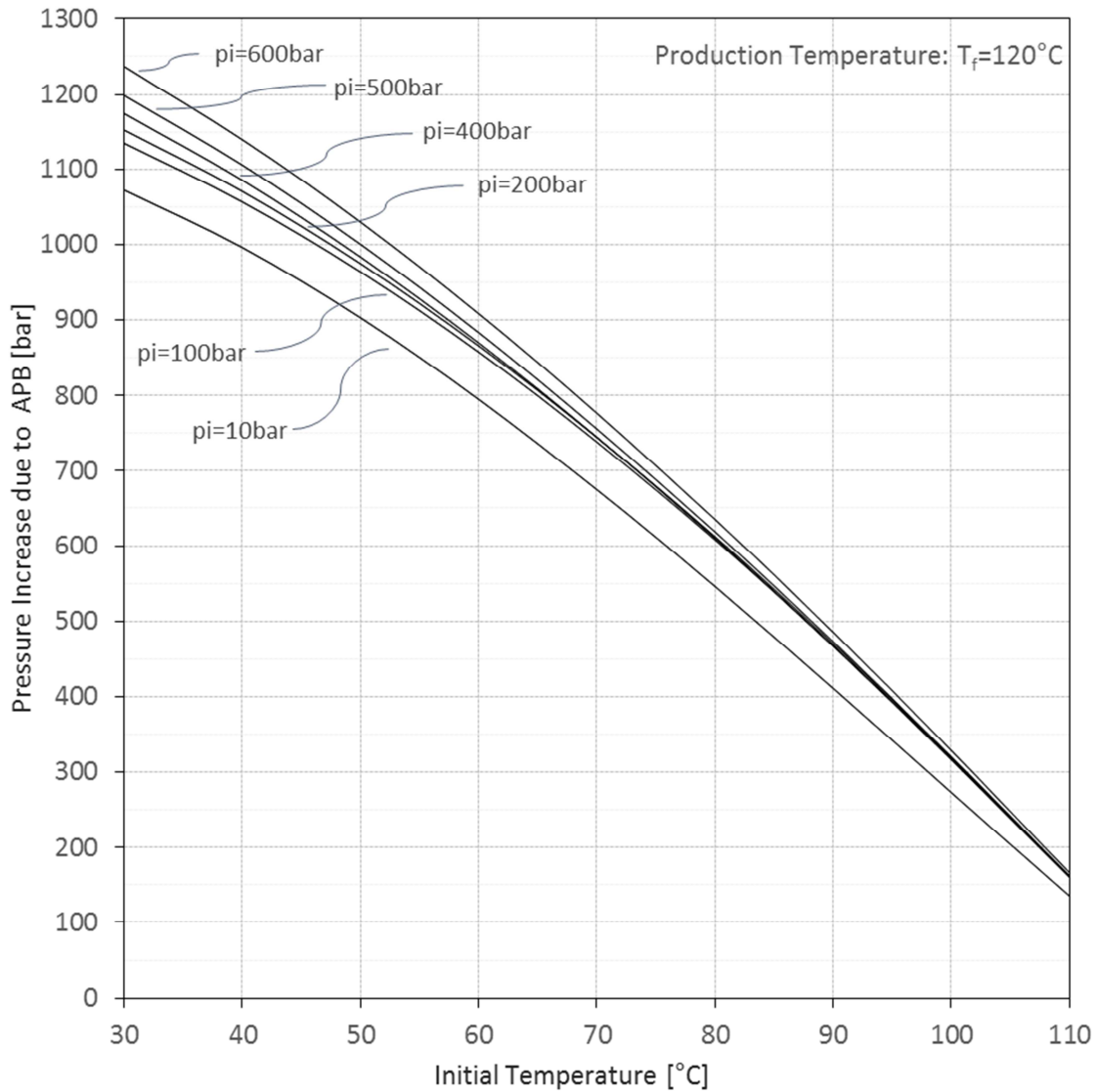


Figure 19: Pressure Increase Related to the Initial Downhole Temperature

The figure displays the effect of APB. With increasing depth, and therefore increasing initial pressure, the APB can reach up to 120 MPa.

## 5 Theory of Operation

This chapter gives an overview of the theory of operation of the APRS. All concepts assume that the pressure increase due to APB is avoided by allowing the trapped fluid to expand. This is achieved due to an additional chamber in the annulus, the so-called pressure chamber or pressure container. The chamber opens at a predefined pressure, and therefore the annular volume is raised by the volume of the pressure chamber. To avoid APB the volume of the chamber must be therefore equal to or bigger as the volume expansion due to a temperature change.

The theory of operation is illustrated in Figure 20 and Figure 21. Figure 20 represents the initial state: the pressure chamber is empty, and the fluid is trapped in the annulus.

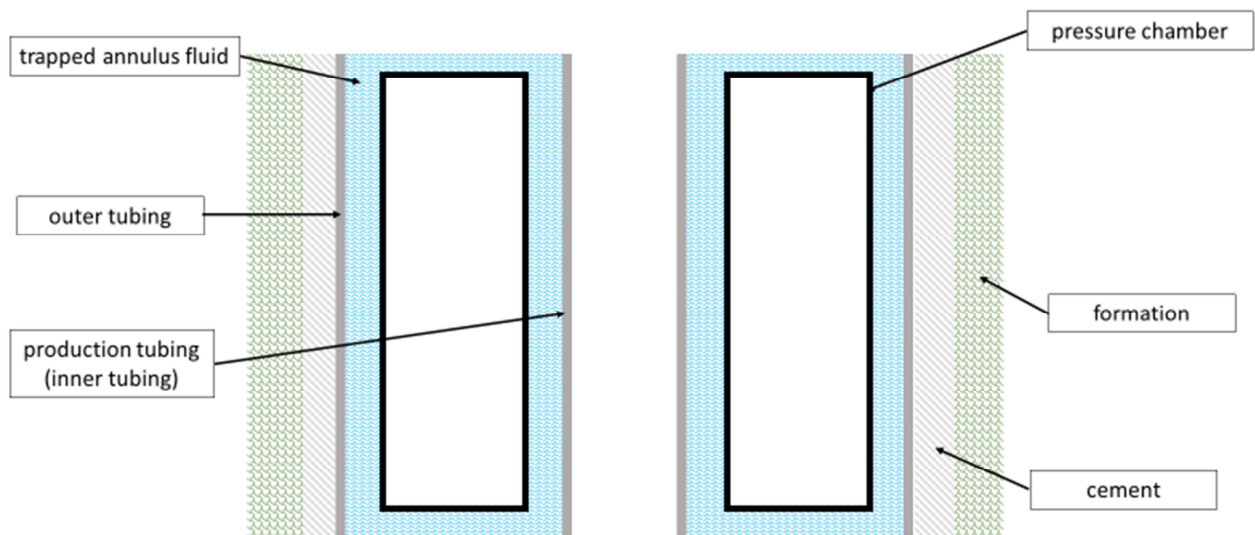


Figure 20: Function of APRS – Initial Stage

As soon as the well starts producing, the hot production fluid heats up the annulus and thus also the trapped fluid, see Figure 3 and Figure 21. The pressure increases to a certain level until the pressure chamber opens and compensates the thermal expansion of the annular fluid. Thus, the pressure is kept at constant level, predefined by the available volume of the chamber.

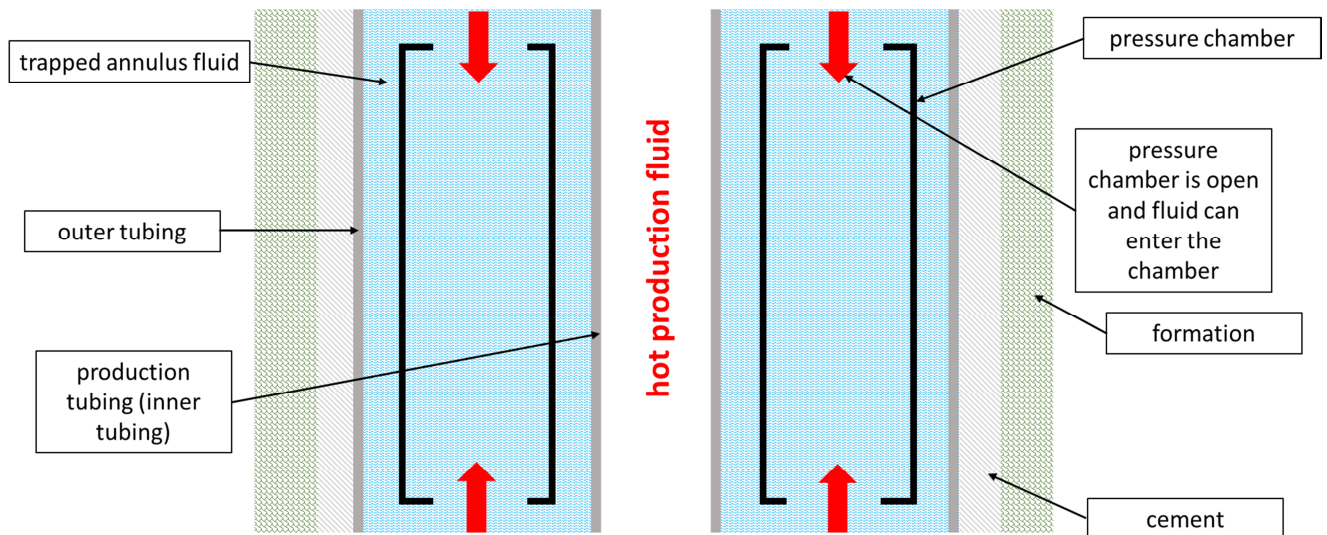


Figure 21: Function of APRS – Start of Production

The functional operation can be simplified to five steps:

1. The chamber is attached to the inner tubing in the annulus at the location where trapped fluid is assumed.
2. The temperature increases due to the start of production in the well
3. The pressure increases due to APB
4. At a predefined pressure, the pressure chamber is opened, and the fluid enters the chamber
5. The fluid can now expand, and consequently the pressure is kept constant

## 6 Functional Operation

This chapter describes the technical implementation of the theory of operation, see chapter 5.

As explained in chapter 5 the APRS requires the following parts:

- ✓ A pressure chamber
- ✓ A possibility to open the chamber
- ✓ A part which fixes the pressure chamber to the liner or casing and prevents the chamber from being damaged

The pressure chamber is initially filled with a compressible medium like air or nitrogen. The gas can also be pressurized up to several hundred bar if necessary.

### **Burst disc:**

For the concepts explained in this thesis, a burst disc acts as pull linkage in the pressure chamber. Burst discs, also called rupture discs, are designed to break at a predefined pressure. The pressure rating of the disc is equivalent to the magnitude of pressure which must be reached to break the disc.

For burst discs, the pressure rating is available in steps of a few bar. Thus, the pressure level can be exactly chosen. Further, such components are widely used in existing systems to avoid APB [11]. Since burst discs are available in all sizes and forms and are nearly similar in the main dimensions, it was decided to use only one design for the presented concepts. For an ongoing detailed design the manufacturer of the burst disc can be therefore easily changed and the concept adjusted to another burst disc model. Figure 22 displays the burst disc which is used in all concepts. The screw on the outside is used to fix the burst disc to the tool and allows a quick adjustment to different operating pressures by merely using another pressure rating of the burst disc.



Figure 22: Rupture or Burst disc [29]

## 6.1 Option 1: Volume Consideration

Based on the equations used in chapter 4.1.4 the volume expansion is calculated for the positions A, B1, and B2. Figure 23 represents the APB at position A.

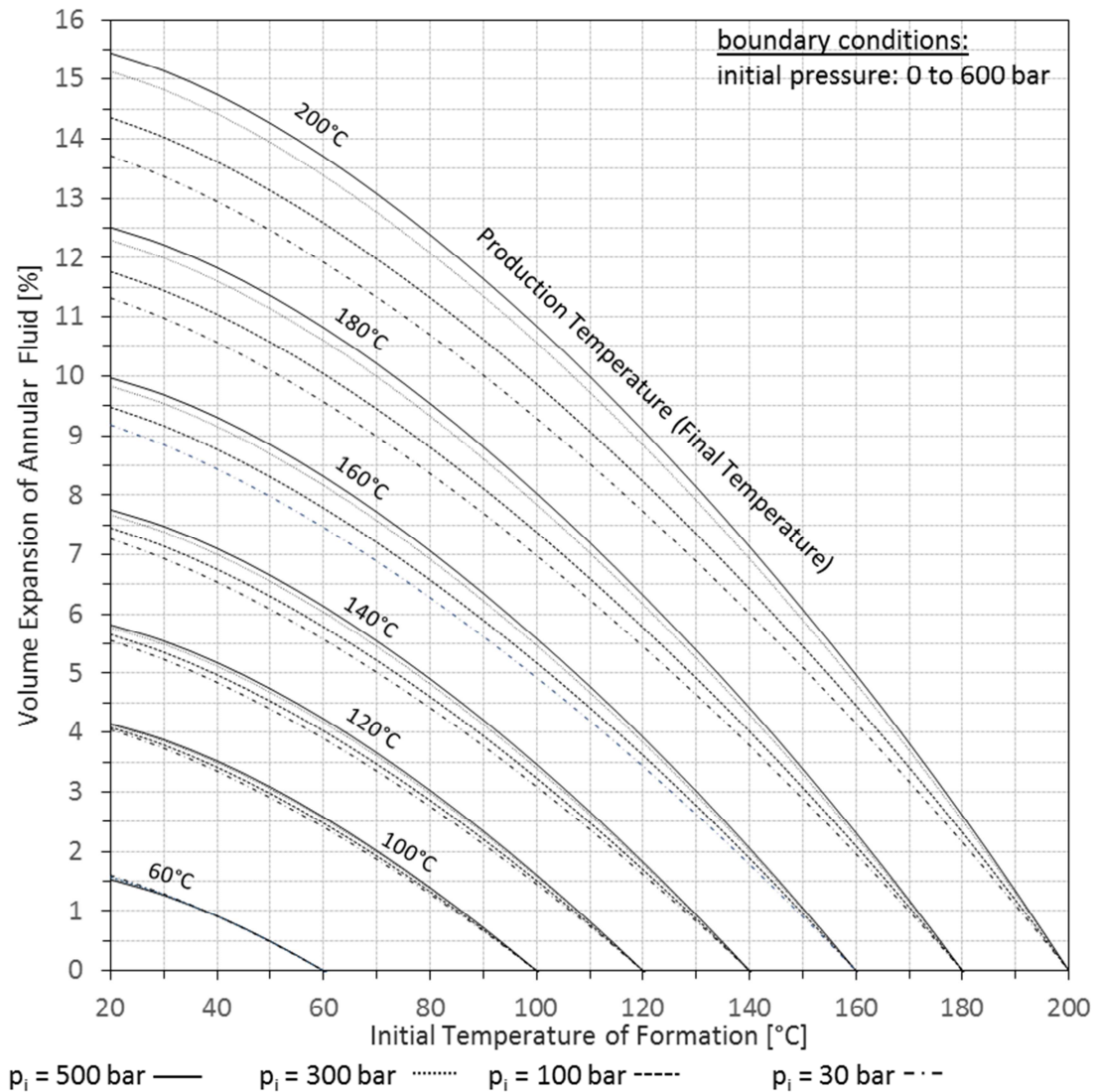


Figure 23: Volume Expansion at Constant Pressure

Related to the setting depth of the tool, the tool design is strongly influenced by the initial pressure. Therefore, the graph was generated to get a better understanding of the depth in the well, where the tool is located. Figure 23 shows the results. Similar to Figure 18 the volume expansion can be easily graphically determined from the plot.

## 6.2 Option 2: Pressure and Volume Consideration

Option 1 assumes that the pressure is nearly constant. Another possibility would be to allow a defined pressure increase by keeping the volume constant before the fluid is allowed to expand at a constant pressure. The significant advantage of this option would be the reduction of the needed expansion volume and therefore a smaller pressure chamber. This means that the tool can be slighter and is therefore easier to handle and to design. The idea is to allow a pressure increase up to a value below the collapse pressure of the casing, depending on the required SF. When this pressure is reached the pressure chamber opens and the fluid can expand. Therefore, the pressure will increase up to a certain level and then the pressure is kept constant due to an increased volume in the annulus.

### Evaluation of the required expansion volume:

From the allowable pressure increase,  $\Delta p$ , the finale temperature,  $T_f$ , can be calculated by rearranging Eq. 21:

$$\Delta p = \int_{T_i}^{T_f} \frac{\gamma(T)}{\kappa(T)} dT \rightarrow \text{solve for } T_f \text{ with } \Delta p = \text{allowable pressure increase} \quad (\text{Eq. 22})$$

Then  $T_f$  is used and set as an initial temperature. The volume change is now calculated by Eq. 3. The functions of the thermal expansion coefficient and isothermal compressibility are derived as described in chapter 4.1.

Table 9 shows the effect of the needed expansion volume at position A. The additional allowable pressure increase is derived for three different scenarios. All scenarios do not include any safety factor.

The casing parameters, such as burst pressure and collapse pressure, of the used casing are based on the data sheets provided by the manufacturer [30].

Table 9: Reduction of Expansion Volume due to an Allowed Pressure Increase ( $\Delta p$ )

Scenario	$\Delta p$ [MPa]	$\Delta V$ (Pressure is Assumed Constant)	$\Delta V$ (Pressure Increase Allowed)	Reduction
A	26		+2.45%	-32%
B	12.86	3.6%	+3.05%	-15%
C	50		+1.4%	-61%

**Scenario A:** The value is calculated from the minimum burst pressure of the outer casing, in this case a 13 3/8 in casing, and the minimum collapse pressure of the inner 9 5/8 in liner.

➤ Allowable pressure increase: 26 MPa



**Scenario B:** Based on the assumption that the fluid is trapped on the top of the section, the allowable pressure increase, with respect to the collapse or burst pressure of the outer and inner casing, is calculated on top of the casing. The theory behind this scenario is based on the idea that the casing or liner can theoretically withstand on top an additional pressure increase to the designed value. Higher loads are assumed at the bottom of the casing string.

- Allowable pressure increase: 12.86 MPa

**Scenario C:** To see the effect on a larger scale a random number is chosen

- Allowable pressure increase: 50 MPa

Figure 24 displays the required volume of the pressure chamber dependent on the allowable pressure increase before the pressure chamber opens. 100% represents the amount of expansion volume of the pressure chamber when no pressure increase is allowed.

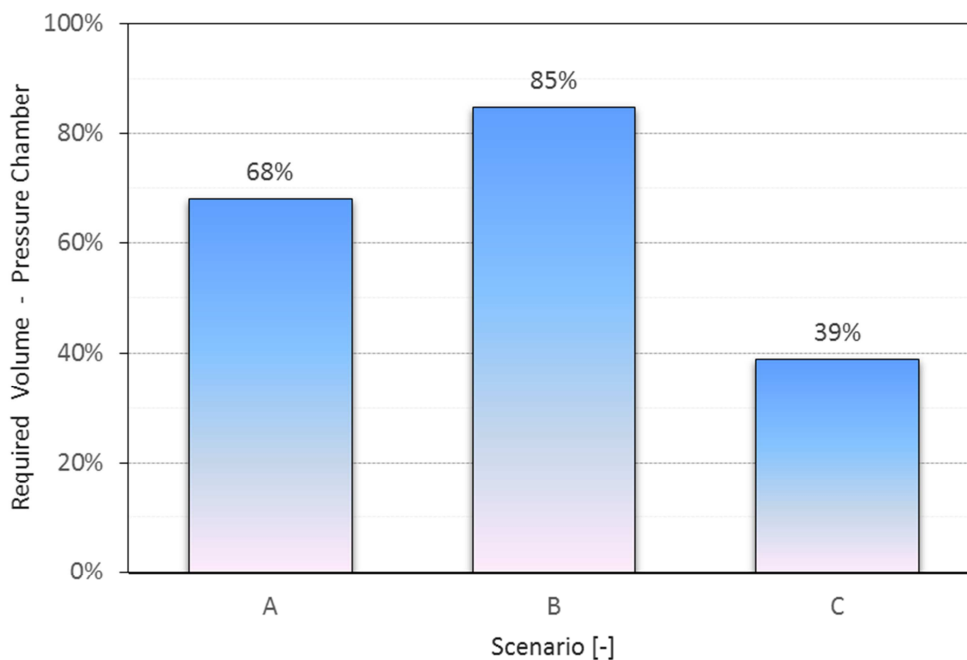


Figure 24: Reduction of Needed Volume due to the Additional Pressure Increase

A realistic scenario could be scenario B. In this case, the casing does not have to withstand higher pressures than it is initially designed for. The possible reduction of the pressure chamber would be up to 15 % allowing for a pressure increase of 128 bar. Furthermore, the value of the allowable pressure increase is strongly depended on the length of the casing section and therefore it makes little sense to design a concept which would work only in one special well design.

Allowing a pressure increase of maximum 60 bar would result in a further reduction of the expansion volume by 7 %. However, it turned out, that a 25 % reduction in expansion volume

would be required to be efficient in space reduction. But this would result in an allowable pressure increase of 150 bar which is economically not feasible.

However, this option shall still be kept in mind for further considerations.

### 6.3 Option 3: Pressurized Pressure Chamber

The idea is to increase the volume of the pressure chamber by decreasing the wall thickness. If the pressure chamber is pressurized, the differential pressure is smaller, and the wall thickness can be reduced. This leads to a higher possible volume of the pressure chamber and thus to a smaller tool by keeping the expansion volume constant.

The repercussions of the wall thickness on the available volume are strong. Figure 25 shows the substantial impact of the wall thickness on the volume. How this figure was derived is shown in chapter 6.1 and 6.3. If the pressure chamber is pressurized to 200 bar, the pressure difference between the inside of the chamber and the annulus reduces from 600°bar to 400°bar. Thus, the wall thickness can be decreased and the available volume in the chamber is increased to 0.41 l. Compared to a non-pressurized chamber with 0.32 l, the pressurized chamber enables more volume for compensating the thermal expansion of the annular fluid. Compared to the non-pressurized chamber, the expansion volume can be increased to 22 %.

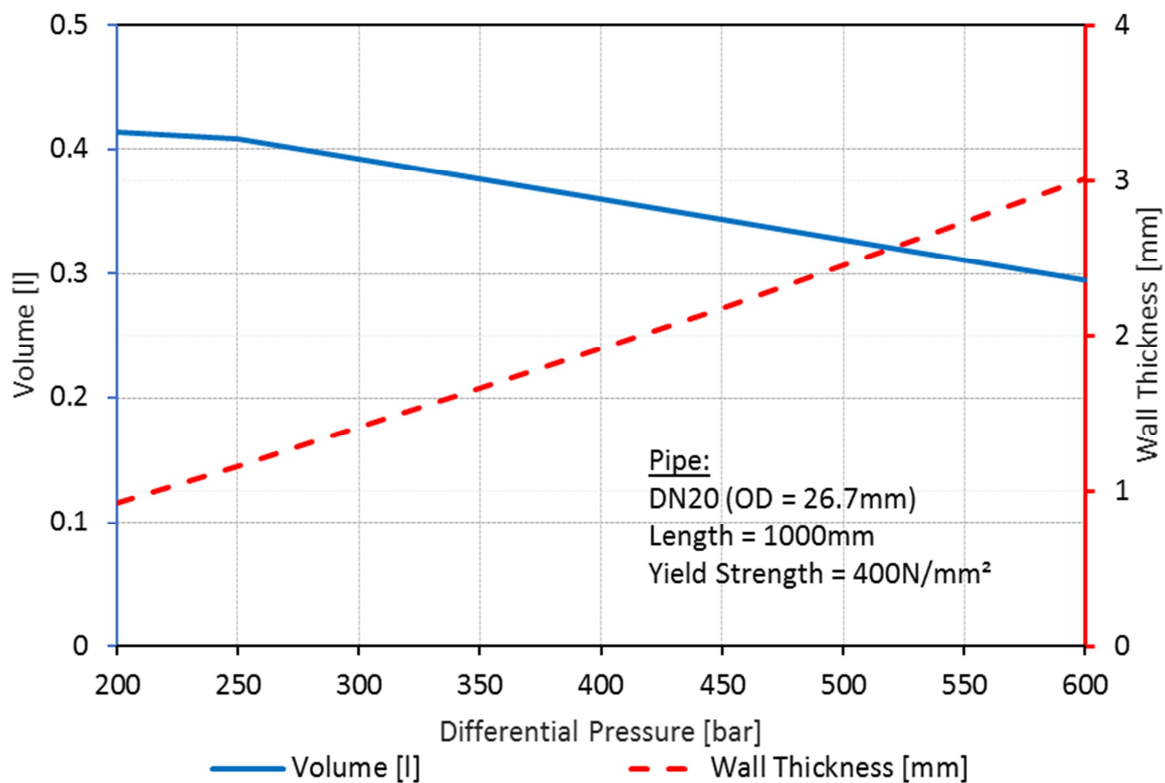


Figure 25: Influence of the Differential Pressure and Wall Thickness

However, the gas in the chamber also occupies space. Therefore, the next step is the calculation of the filled volume in the pressure chamber. The calculation is based the ideal gas law, also called the general ideal gas equation. It is the equation of state of an ideal gas and a good approximation of the behaviour of gases [31]. Therefore, it is accurate enough for the use of the concept design phase.

By using Eq. 23 [31] , the volume of the compressed gas,  $V_2$ , in the pressure chamber can be calculated by assuming a constant mass:

$$V_2 = \frac{p_1 T_2}{p_2 T_1} V_1, \quad (\text{Eq. 23})$$

where index one represents the initial state and index two represents the finale state. Thus,  $T_1$  is 68°C;  $p_1$  is 202 bar,  $V_1$  is 0.41 l,  $T_2$  is 120°C and  $p_2$  is 400 bar.

This volume has to be subtracted from the volume of the pressure chamber to get the available volume for the expansion of the fluid. The results are given in Table 10.

Table 10: Compressed Volume in Pressure Chamber

Parameter	Value	Unit
R	8.311459	J/(mol K)
$p_1$	2.00E+07	Pa
$V_1$	0.41	l
$T_1$	68	°C
n	3.1024	mol
$p_2$	4.00E+07	Pa
$T_2$	120	°C
$V_2$	0.253	l

The result shows quite well that the loss of 0.253 l (57 %) compensation volume is large and therefore cannot be neglected. Therefore, this design is not a good alternative if the gas goes not into solution with the fluid. But due to the high pressure it can be assumed that the gas will go into solution [32]. Thus, the gas volume can be neglected and if the load condition demands a very high wall thickness, this option would be a possibility.

## 6.4 Concerning Design Options

Based on these results of the three options, a pressure and volume increase is not sufficient enough and should not be considered. The operating pressure of the burst disc should be set below the collapse or burst pressure of the casings at the desired depth of the tool. Increased operating pressure is not very effective, and it is better to keep the magnitude of potential volume decrease as a safety option and not as a design criterion. The third option is also not making a huge improvement to optimize the volume of the pressure chamber, but it should be kept in mind in case the boundary conditions of the well, like a small annulus or high initial pressure, do not allow high volumes of the pressure chamber. According to the mentioned arguments for further design of the tool, the first option is used.

## 7 Design Challenges

This chapter describes the most important design challenges and requirements of the APRS.

The principal challenges to meet the requirements are:

- maximize the volume of the pressure chamber
- minimize the stress according to a maximum differential pressure of 600 bar and a SF of 1.5 to achieve the most robust design with a broad operating range
- maximize the available space between the tool and the ID of the casing for the cement job
- easy adjustment of the tool to different casing diameters
- installation of the tool without any modifications of the casing string
- flexibility of the tool for different pressure regimes
- minimize risks and problems during installation
- minimize the complexity of the tool: reduce failure occurrence
- minimize costs of
  - mounting or fixing parts
  - pressure chamber
- minimize the complexity of the concept related to
  - manufacturing of mounting parts
  - manufacturing of pressure chamber

The key design challenge is the limited space in the annulus in relation to the high pressure difference the pressure chamber has to withstand. Therefore, the objective was to design the chamber with the smallest possible wall thickness, to find a geometry which includes a large inner volume. Further, the tool must be able to withstand the load conditions during run in hole and further down hole.

To evaluate and compare the concepts and ideas a 3D-model of the tool was drawn by using CATIA. In order to check the feasibility of the concepts drawings of each component were made.

### 7.1 Static Strength

To guarantee that the tool can handle high pressure and temperature as well as the different load scenarios during installation, it was decided to calculate the static strength for each concept. Fulfilling this requirement is superior to all other load conditions, see chapter 3.2, because, the high stresses, which occur by applying a pressure difference of 600 bar require a very robust design. Therefore it was assumed that the load scenarios during installation results in a lower stress level and can be neglected. Thus, the pressure difference is the limiting factor, in this early phase of tool design.

Supplementary to that, a definition of possible load scenarios and the corresponding calculations are out of the scope of this thesis and are therefore not considered.

For a first assumption and to rate the concepts in an early stage of the design process, manual calculations are done to check the load scenarios. At a later stage the static strength of the tool is determined by using FEM simulations. In order to validate the simulation results also the manual calculation is used. All calculations include a safety factor of 1.5.

### 7.1.1 Manual Calculation

For first estimations of the design, manual calculations were performed as much less time is required compared to full FEM simulations. In addition, time consuming CAD modeling and grid meshing can be avoided. The manual scripts were implemented in Microsoft Excel. The manual calculation was simplified by the assumption that the load scenario displayed in Figure 26 is sufficient to estimate the wall thickness of the pressure chamber.

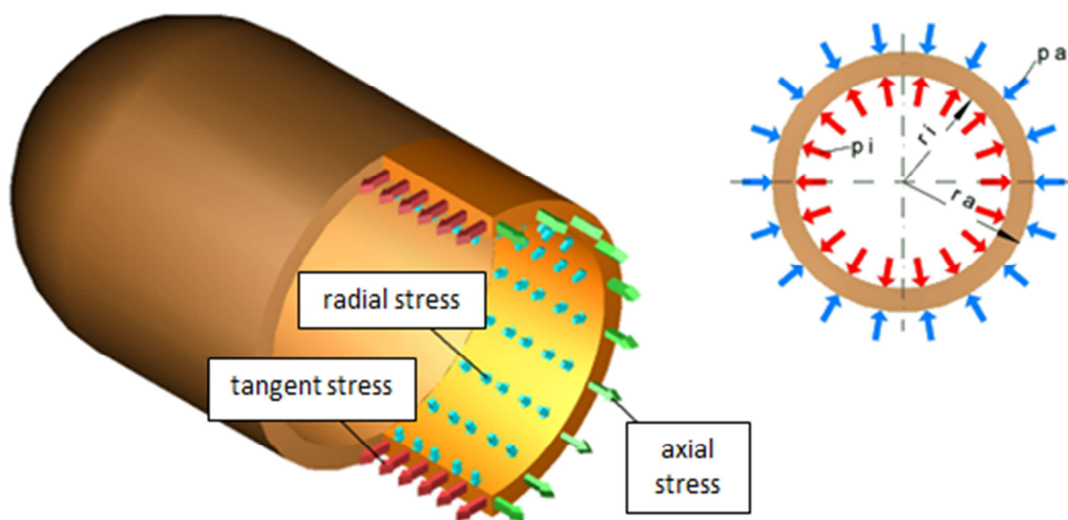


Figure 26: Schematic of the Primary Load Scenario [33]

The load scenario can be simplified to an external pressure acting on a closed straight pipe. The input parameters are the OD and the wall thickness of the pressure chamber. Furthermore, the external pressure and the internal pressure can be adapted. The output is the von Mises equivalent stress which is also used for the evaluation of the FEM simulations.

The equations used to calculate the stresses are as follows:

For the axial stress Eq. 24 [34] is used:

$$\sigma_a = \frac{(p_i * r_i^2 - p_o * r_o^2)}{(r_o^2 - r_i^2)} \quad (\text{Eq. 24})$$

For the tangential stress Eq. 25 [34] is used:

$$\sigma_t = -p_o * \frac{r_i^2}{(r_o^2 - r_i^2)} * \left(1 + \frac{r_i^2}{r_o^2}\right) \quad (\text{Eq. 25})$$

For the radial stress Eq. 26 [34] is used:

$$\sigma_r = -p_o * \frac{r_o^2}{(r_o^2 - r_i^2)} * \left(1 - \frac{r_i^2}{r_o^2}\right) \quad (\text{Eq. 26})$$

The stresses are then combined with the yield criterion to derive the resulting stress, the von Mises equivalent stress, see Eq. 27 [35,36].

$$\sigma_v = \sqrt{(\sigma_t^2 + \sigma_r^2 + \sigma_a^2 - \sigma_t \sigma_r \sigma_a - \sigma_r \sigma_a)}, \quad (\text{Eq. 27})$$

where  $\sigma_v$  is the von Mises equivalent stress (N/mm<sup>2</sup>),  $\sigma_r$  is the radial stress (N/mm<sup>2</sup>),  $\sigma_a$  is the axial stress (N/mm<sup>2</sup>),  $\sigma_t$  is the tangential stress (N/mm<sup>2</sup>),  $r_i$  is the inner radius of the pipe (mm),  $r_o$  is the outer radius of the pipe (mm),  $p_i$  is the internal pressure acting on the pipe (MPa) and  $p_o$  is the external pressure acting on the pipe (MPa).

### 7.1.2 FEM Simulation Set Up

To evaluate the stresses of each concept in detail, a mesh based on the 3D model was generated. The used simulation software is scenario sensitive:

- Elfini-Solver
- CATIA-SIMULIA (Abaqus or ANSYS)

The load conditions for the simulation are also based on the assumption that the pressure chamber has to withstand the pressure difference. Therefore, a pressure of 600 bar is applied to the outer surface of the pressure chamber. The simulation model boundary conditions and loads are kept constant for all concepts to get comparable results. Also the material properties are kept constant for one simulation loop. The material properties, as well as the load scenarios, are changed in loops. This means that with one set up all models are checked, and the results are reviewed and compared. Then the next loop begins with

modified parameters. Figure 27 shows a screenshot of a material database in CATIA from one selected material.

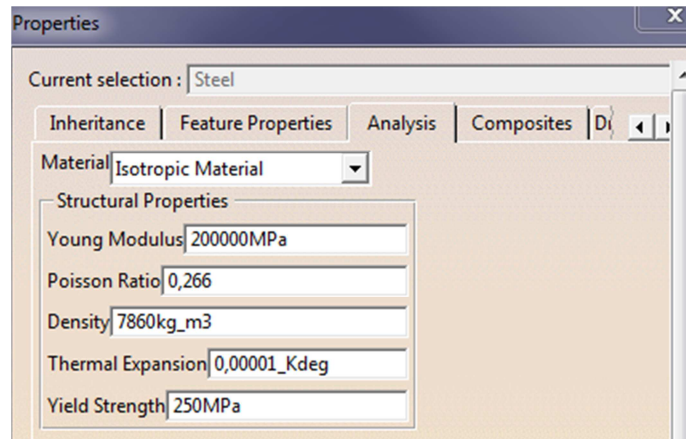


Figure 27:Input Material Properties

## Mesh

Since the models differ in the geometry and dimension, the cell size, the cell shape and the number of cells are adapted. An example of such a mesh is displayed in Figure 28. The parameters according to the mesh are presented in Figure 29.

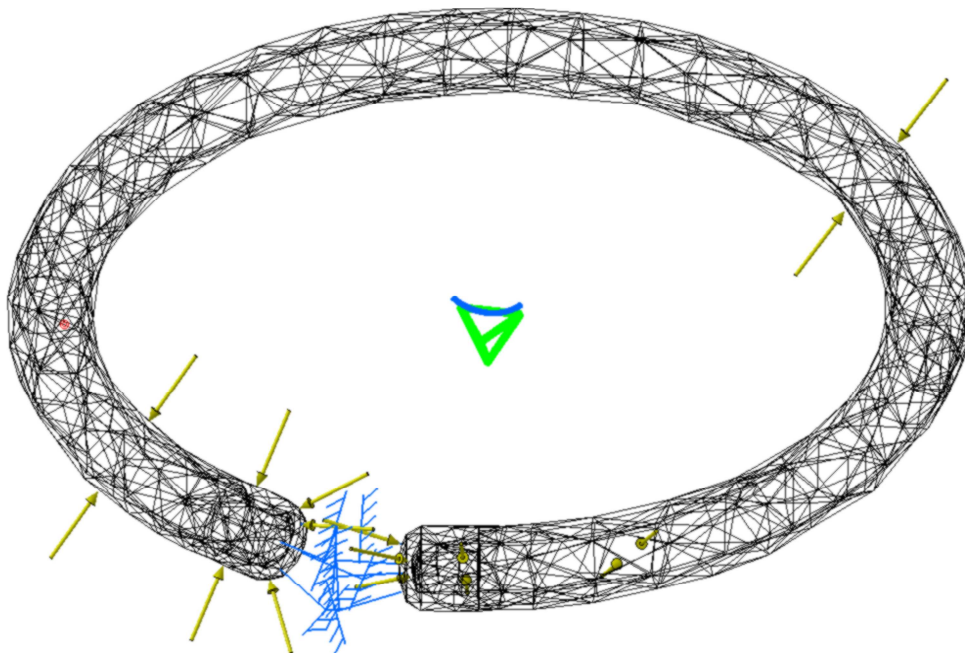


Figure 28: Mesh Ring Pipe



**MESH:**

Entity	Size
Nodes	931
Elements	2757

**ELEMENT TYPE:**

Connectivity	Statistics
TE4	2757 ( 100.00% )

**ELEMENT QUALITY:**

Criterion	Good	Poor	Bad	Worst	Average
Stretch	865 ( 31.37% )	1892 ( 68.63% )	0 ( 0.00% )	0.087	0.280
Aspect Ratio	1397 ( 50.67% )	871 ( 31.59% )	489 ( 17.74% )	15.299	5.885

Figure 29: Mesh Report - Bad Quality

By having a closer look at the mesh report, see Figure 29, it can be seen that the selected size and number of the cells is not correctly representing the model [37]. The amount of poor and bad elements is quite large. High quality is defined by having no bad elements and only a few percentage of poor elements [37]. Further the parameter statistics should range near 100%. The mesh quality check is strongly dependent on the size of the mesh, thus the mentioned values are only countable for this particular case. In such a case the mesh was improved using smaller cell size to achieve a better result. An example of how a good mesh looks like can be seen in Figure 30.

**MESH:**

Entity	Size
Nodes	28439
Elements	105035

**ELEMENT TYPE:**

Connectivity	Statistics
TE4	105035 ( 100.00% )

**ELEMENT QUALITY:**

Criterion	Good	Poor	Bad	Worst	Average
Stretch	105035 ( 100.00% )	0 ( 0.00% )	0 ( 0.00% )	0.356	0.636
Aspect Ratio	105035 ( 100.00% )	0 ( 0.00% )	0 ( 0.00% )	3.846	1.854

Figure 30: Mesh Report – Good Quality

### Model set up

Figure 31 displays the restrains, denoted as yellow points and the load conditions, shown as red arrows, of one concept. The figure represents a cross-section through the pressure chamber. The pressure is acting on the red surface, whereas the yellow points indicate the contact points with the inner tubing. In the model setup now the restrains are set on the contact surface. They are allowed to move radial and axial around the inner tubing. The load is placed on the outer surface of the model.

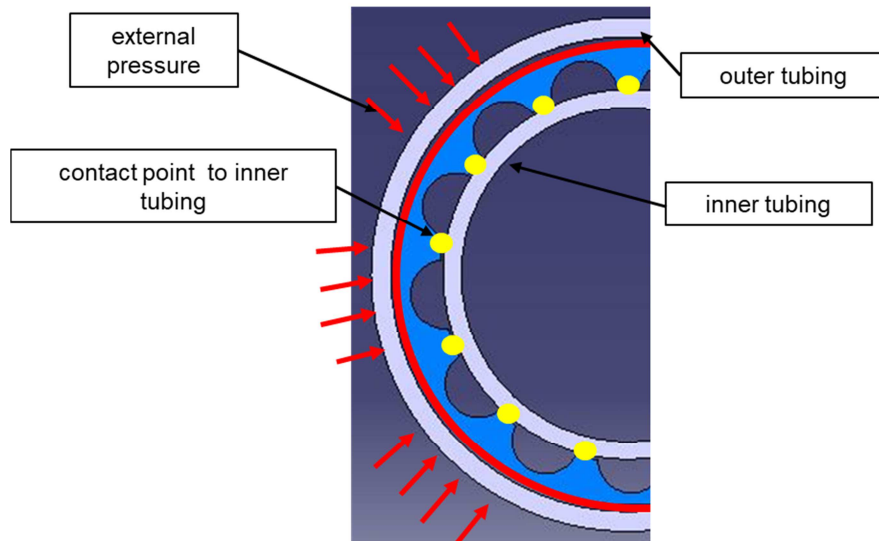


Figure 31: Schematic Model Set Up

An example of a model set up is displayed in Figure 32, for a basic load scenario as mentioned before, see chapter 7.1.1. The yellow arrows represent a constant outer pressure of 60 MPa. The pressure is acting on the outer surface of the tool. The blue lines indicate the fixing points. In this case the blue lines represent the contact points of the tool to the inner tubing, see Figure 31. The fixing points, lines or surfaces are dependent on the concept, thus they vary for each concept.

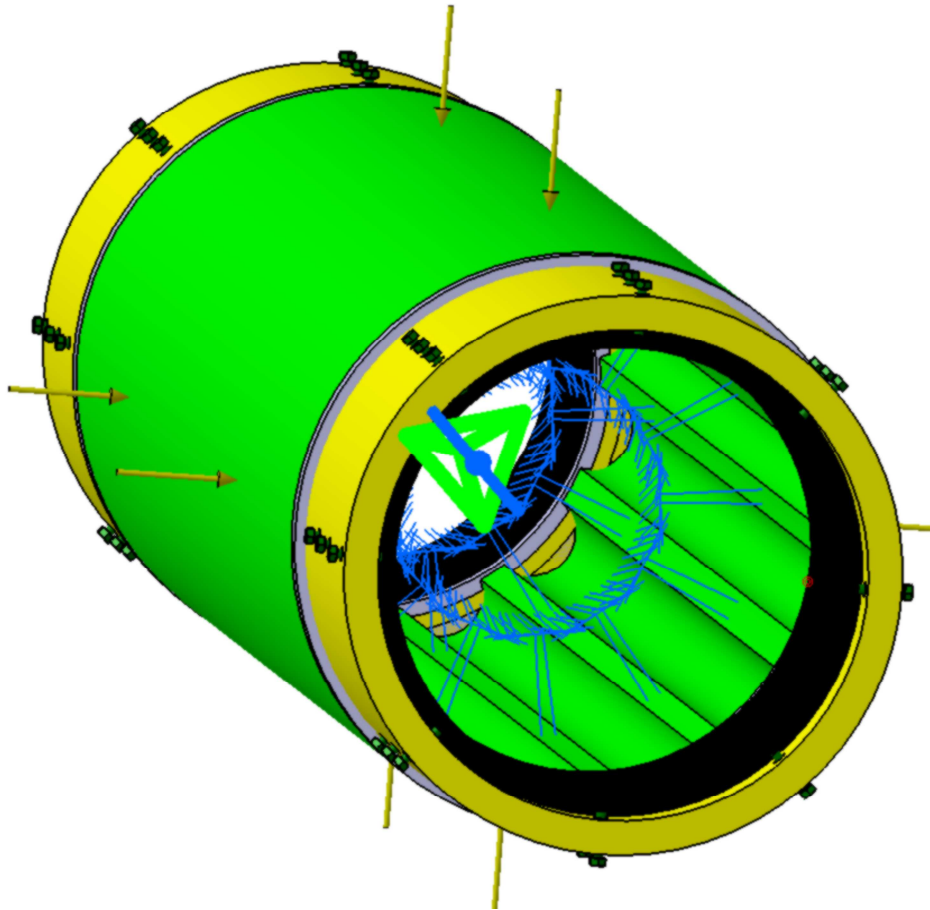


Figure 32: Screenshot of Model Set Up

### Evaluation of simulation results

To proof the reliability of the results the residual error is checked after every simulation. The global error should be beneath 10 % global and in stress critical zones beneath 5 % [38]. An example of such a check is presented in Table 10.

Table 11: Residual Error

Components	Applied Forces	Reactions	Residual	Relative Magnitude Error
Fx (N)	-1.6421e-009	-8.0381e-009	-9.6802e-009	3.0626e-013
Fy (N)	5.4700e-008	2.1937e-009	5.6893e-008	1.8000e-012
Fz (N)	4.7173e+002	-4.7173e+002	-1.5098e-010	4.7766e-015
Mx (Nxm)	5.3870e+000	-5.3870e+000	1.5218e-009	9.6291e-014
My (Nxm)	-2.1784e+001	2.1784e+001	1.1984e-009	7.5828e-014
Mz (Nxm)	-3.6380e-012	1.1913e-009	1.1877e-009	7.5150e-014

The residual error is minimal and therefore the simulation is reliable. Further to proof the simulation result, a detailed look on the deformation is necessary. If the result is credible, the

results are then compared to the manual calculation to see if the values are in the same range. An example of a deformation where the simulation is not credible can be seen in Figure 33.

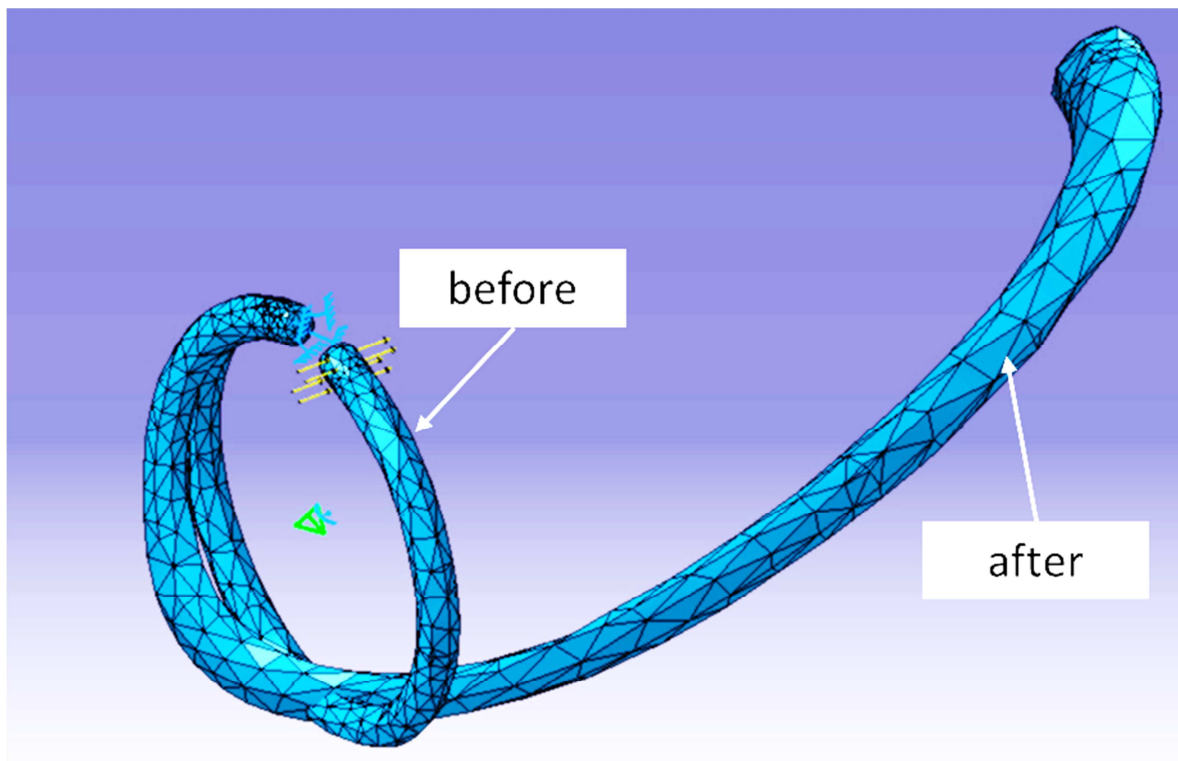


Figure 33: Deformation Simulation

In this scenario, the model shows a behaviour which is not realistic. The simulation is started with a circular model and after applying a constant external pressure the deformation shows a completely different geometry. By applying only overpressure on the pipe, the deformation could never look like this. By having a closer look into the mesh it turned out that the cell size was too large for the load scenario.

## Results

One important result of the simulations, for the evaluation of the concepts, is the von Mises stress. This stress was calculated for all concepts and compared to the manual calculation. As an example of the simulation results a screenshot is displayed in Figure 34. The colours indicate the magnitude of stress. The maximum value is then taken to rate the concept and compare it to other scenarios or concepts.

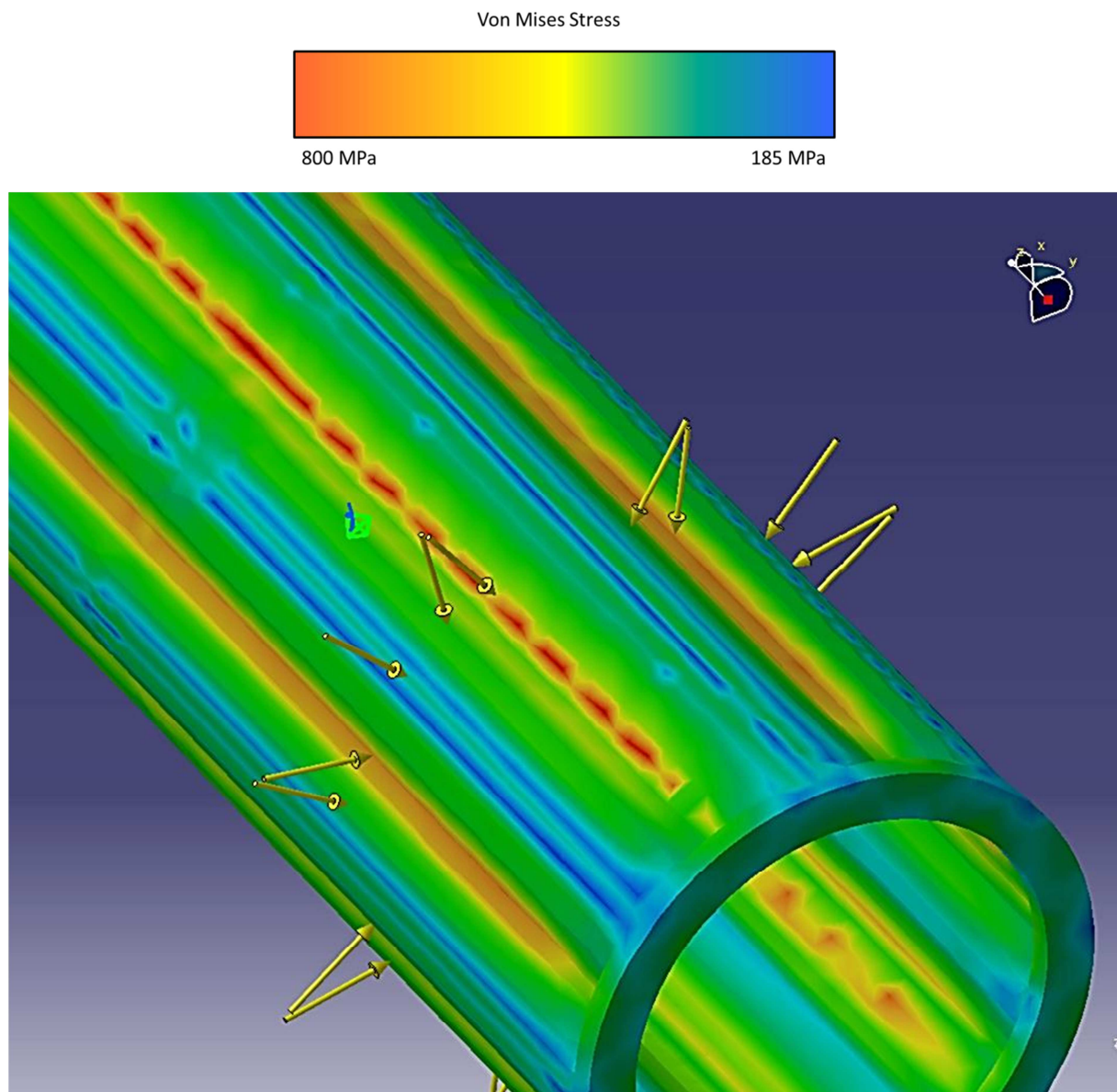


Figure 34: Screenshot of Stress Check

Further Figure 35 demonstrates the deformation, which is also an important output of a simulation. The deformation also was checked for all simulation cases to evaluate the concepts. The figure displays deformation of the pipe. To get a representative result, the deformation shown in the figure is over-scaled.



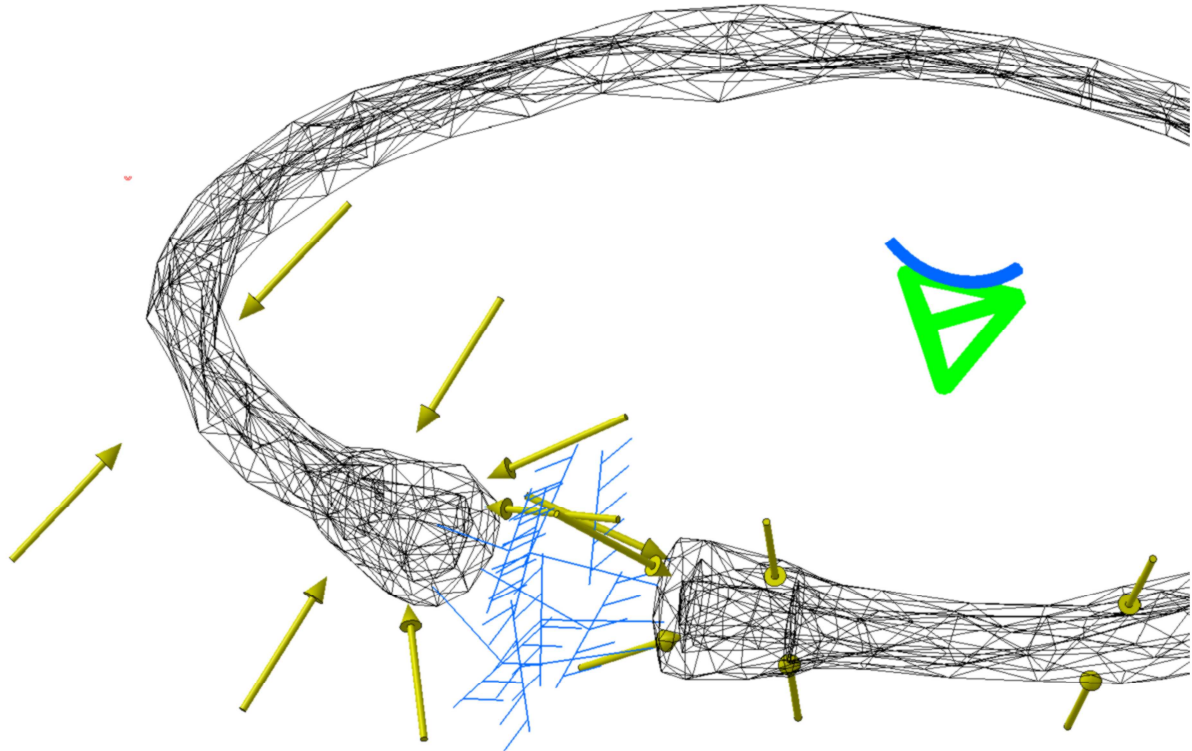


Figure 35: Output Simulation Result - Stress Check CATIA

On the end points of the pipe the deformation is zero, see Figure 35. The reason for this is that the fixing points in this case are set misleadingly to these points, thus no deformation is possible, and the calculated stresses are not reliable. This figure shows that it is very important to check each simulation result carefully to avoid wrong outcomes.

## 7.2 Material Selection

Due to the very high load conditions and the need to keep the wall thickness small, it was necessary to generate a material database to get a good overview of possible materials. The materials are selected according to the availability, costs, weldability, corrosion resistance and many more. The database was established in Microsoft Excel as well as in CATIA for the FEM simulation for evaluating the quality of the calculation.

The material range starts from standard pipe material up to special steel grades for the oil and gas industry and ends up with the hydraulic industry. Hydraulic pipes deal with small diameters and high pressures and have therefore analogous operation ranges. A list of all used materials is given in Table 12. This list is based on the material datasheets provided by the manufacturer and can be found in appendix D, Figure 84.

Table 12: Material and Yield Strength

Material	Yield Strength (20°C)	Source
1.4301	190 N/mm <sup>2</sup>	Deutsche Edelstahlwerke [39]
1.4462	450 N/mm <sup>2</sup>	Deutsche Edelstahlwerke [39]
1.5415	280 N/mm <sup>2</sup>	ThyssenKrupp AG [40]
1.7335	290 N/mm <sup>2</sup>	ThyssenKrupp AG [40]
3RE60	480 N/mm <sup>2</sup>	Sandvik [41]
700MLH	700 N/mm <sup>2</sup>	SSAB [42]
P235GH	235 N/mm <sup>2</sup>	ThyssenKrupp AG [40]
P265GH	265 N/mm <sup>2</sup>	ThyssenKrupp AG; Salzgitter Gruppe [40,43]
SAF 2205	895 N/mm <sup>2</sup>	Sandvik [41]
SAF 2304	450 N/mm <sup>2</sup>	Sandvik [41]
SAF 2507	550 N/mm <sup>2</sup>	Sandvik [41]
SAF 2707	700 N/mm <sup>2</sup>	Sandvik [41]
SAF 3207	770 N/mm <sup>2</sup>	Sandvik [41]
SANMAC® 2205	450 N/mm <sup>2</sup>	Sandvik [41]
Strenx 960	960 N/mm <sup>2</sup>	SSAB [42]
XABO; 1.8983	960 N/mm <sup>2</sup>	ThyssenKrupp AG [40]

To simplify the concept phase and to decrease the calculation time, the generated Microsoft Excel sheet automatically displays the stress for the selected diameter, wall thickness and pressure loads (external and internal pressure) in a plot. Figure 85, see appendix D, represents such a plot, whereas Figure 37 depicts a detail of Figure 85. The reduction of yield strength as a function of temperature can be seen also in Figure 85. A maximum temperature of 170°C was considered in the material selection. Thus, for all checked materials the yield strength up to 200°C is included. The SF of 1.5 is directly implemented in the equations. Therefore, it was possible to decide which material will withstand the load conditions and which material will tend to fail.

The input for the calculation is selected over a drop-down menu in the Microsoft Excel sheet, see Figure 36. To make it more user friendly, the parameters of the pipe are selected with respect to the standard definitions, like the standard diameter DN or the wall thickness schedule as XS, 10, 30. A screenshot of such a set up is shown in Figure 36, where “ $p_o$ ” is the external pressure, “ $p_i$ ” is the internal pressure, “DN” is the standard diameter and “#” represents the schedule of the wall thickness.

po	200 bar			
pi	200 bar		OD	26.7 mm
DN	20 mm		ID	18.88 mm
#	XS		t	3.91
rx	innen	position of stress calculation		
rx	9.44 mm			

Figure 36: Screenshot of Manual Stress Calculation

The program selects then in a separate database automatically the OD and ID of the pipe of interest and calculates the stress. A view examples of the source database are shown in the appendix E. Dependent on the load scenario the burst or collapse load, shown as a red line in Figure 37, is displayed in the chart. As mentioned before, this value includes the safety factor of 1.5.

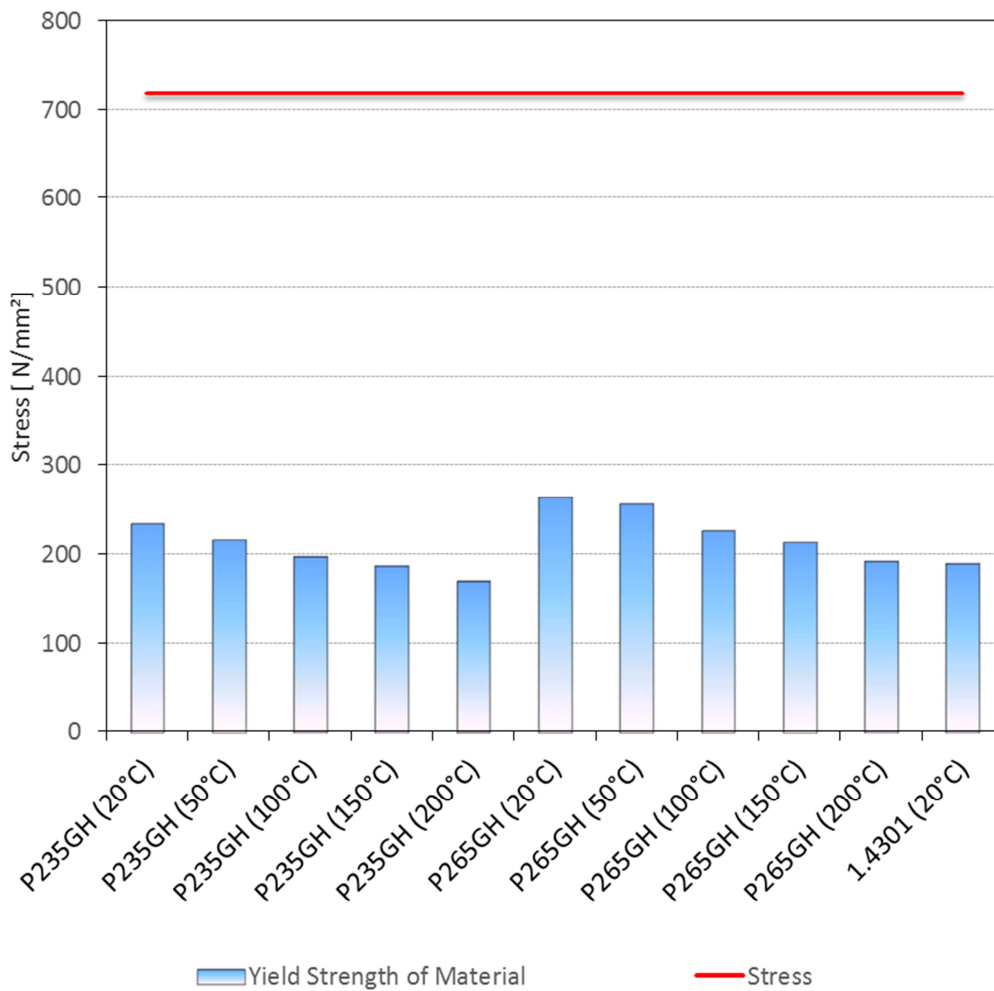


Figure 37: Detail of Figure 85



For instance, the collapse stress is displayed by the red line in the material database and it is possible to see in a quick way if the pipe can withstand this load. In Figure 37 the calculated collapse stress exceeds the yield strength of the available material.

To evaluate the concept and to see the opportunities of it, the program was applied for many different scenarios such as differing dimensions and materials of the pressure chamber. Figure 38 illustrates the relation between the pipe dimension, the material grade, and the volume of the pressure chamber. The “min” curve describes the volume of the pressure chamber which can be reached by using the lowest material grades. The “max” curve represents the maximum possible volume for the pressure chamber by using better material qualities. Thus, the operating range of the concept is between the two curves. It should be mentioned that the “min” curve does not automatically relate to a low material grade and a high pressure difference. This combination would result always in a high wall thickness and consequently in small volumes. The curves are based on reasonable combinations from the used material and the acting pressure difference linked to the disposability of the pipes. Therefore, the plot gives a good overview of the possible volumes of the concept and the corresponding material qualities and dimensions of the pressure chamber.

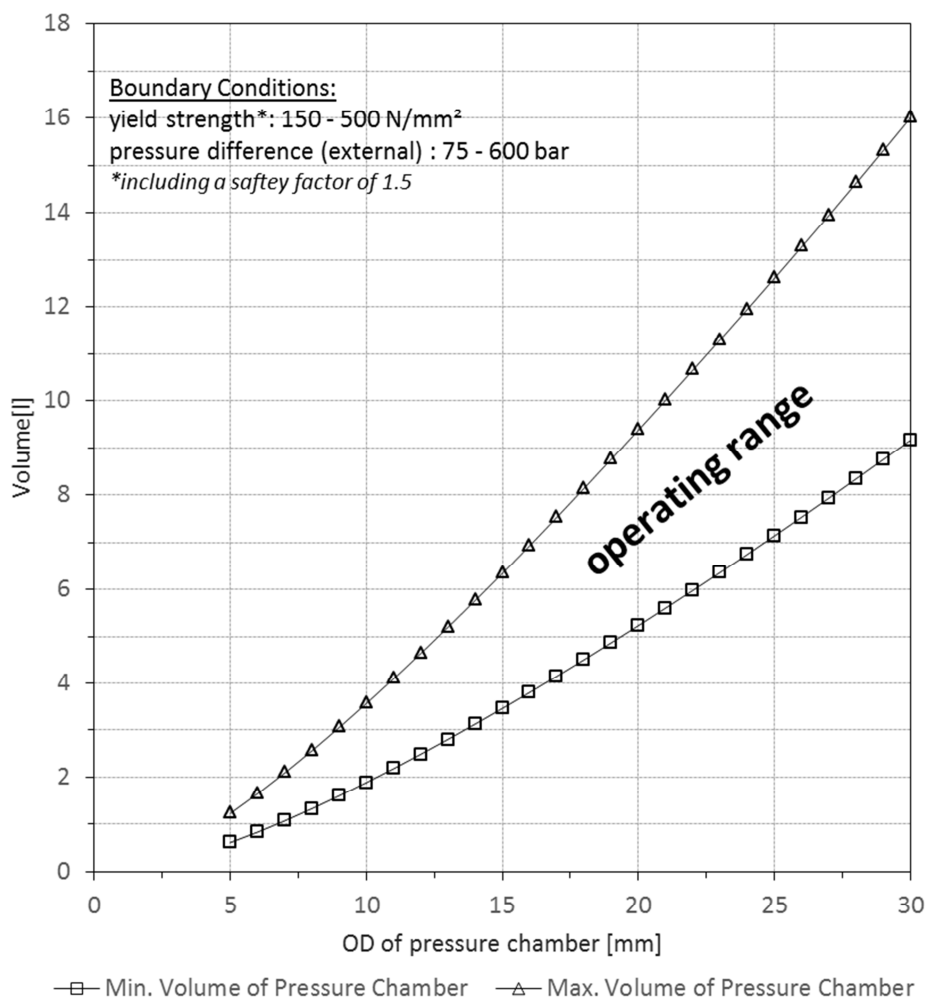


Figure 38: Dependency of Material Selection on the Pressure Chamber Volume

The chart highlights the possible operating volumes depending on the standard diameter of the pressure chamber and the design of the concept. The available volume of the pressure chamber is primarily defined by the design of the pressure chamber, which varies with the concepts and within a concept by the pressure load and the material strength. The length of the pressure chamber is predefined to 1m. The plot displays the operating range and the boundaries due to material strength.

Combining many plots from different concepts, like Figure 38, and overlaying those results in a plot represented in Figure 39.

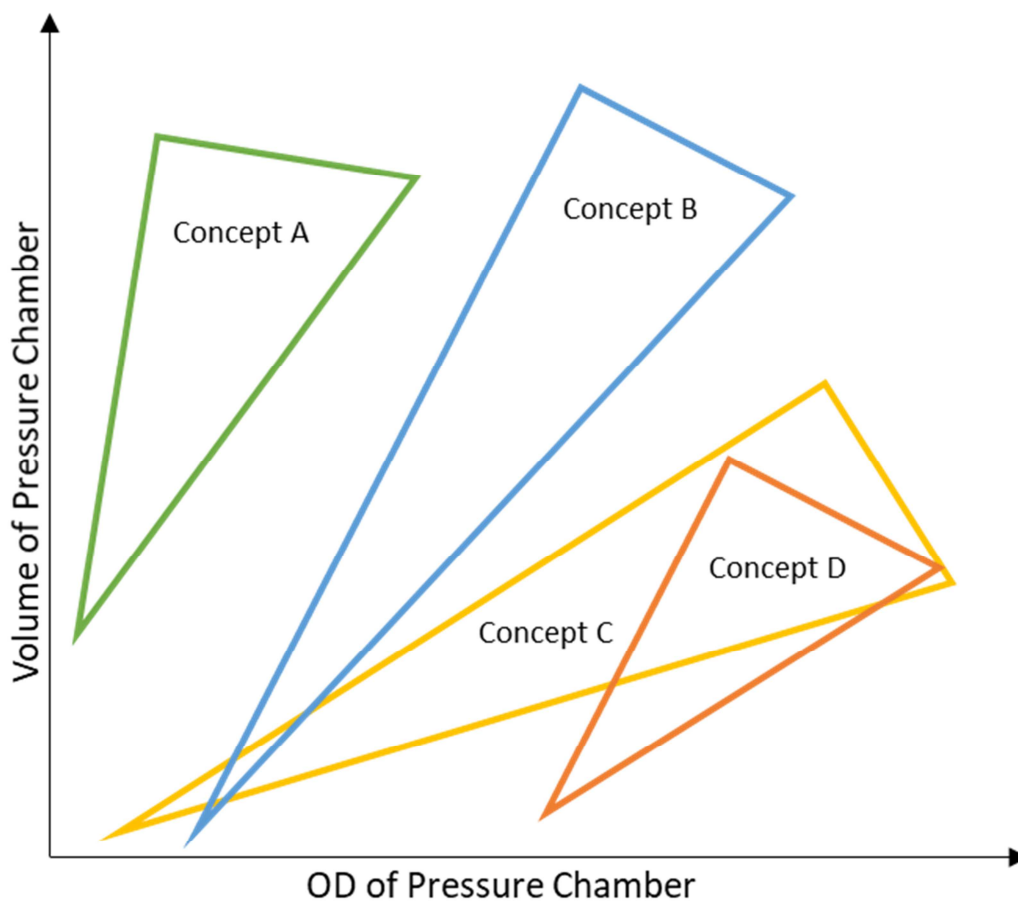


Figure 39: Volume Pressure Chamber – Concepts

These kinds of plots display which concept is the best by knowing the required volume and the available space in the annulus. The available space in the annulus corresponds mainly to the possible OD of the pressure chamber. The operating range can be easily compared against other concepts and thus it allows a good evaluation of the concepts against each other. For instance: concept D requires a larger annulus than concept A; concept C is more flexible in the diameter size of the pipe but the volume capacity is limited; concept B needs for the same amount of volume capacity much more space in the annulus than concept A.

### 7.3 Wall Thickness

In chapter 5 the strong influence of the wall thickness on the volume of the pressure chamber is described. To get a better understanding of the relationship between differential pressure, geometry and wall thickness and how they are related to the possible expansion volume, detailed analysis was required. The calculations to estimate the wall thickness are done in Microsoft Excel. Therefore, a script, based on Eq. 28, was written, see appendix E.

$$t = - \left[ \left( \frac{OD}{2} \right)^2 - \sqrt{ \left( 2 p_o \left( \frac{OD}{2} \right)^2 \frac{1}{\sigma} \right) - \left( \frac{OD}{2} \right)^2 } \right], \quad (\text{Eq. 28})$$

where  $t$  is the wall thickness of the pipe (mm),  $OD$  is the outer diameter of the pipe (mm),  $p_o$  is the pressure load at the outside of the pipe and  $\sigma$  is the yield strength of the material (MPa) including a safety factor of 1.5.

Figure 40 and Figure 41 schematically show the importance of the wall thickness. Further, the difference between the maximum constructed space, see Figure 40 and the constructed space in cases the tool uses the full cross-section, shown in Figure 41, is also presented.

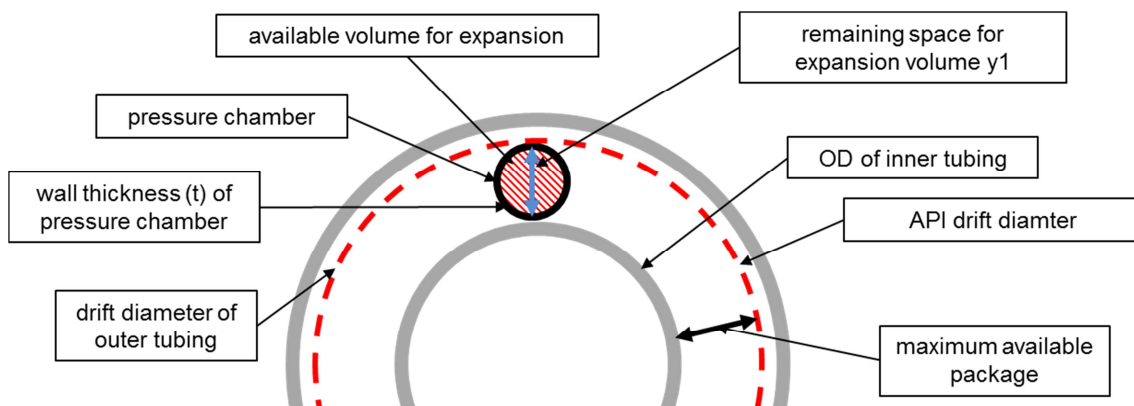


Figure 40: Schematic if the Tool Occupies not the Full Cross-Section of the Annulus

$Y_1$ , see Figure 40, represents the remaining space for the expansion volume if the tool does not fill the whole cross-section of the annulus and  $y_2$ , see Figure 41, represents the space when the tool fills the whole cross-section.

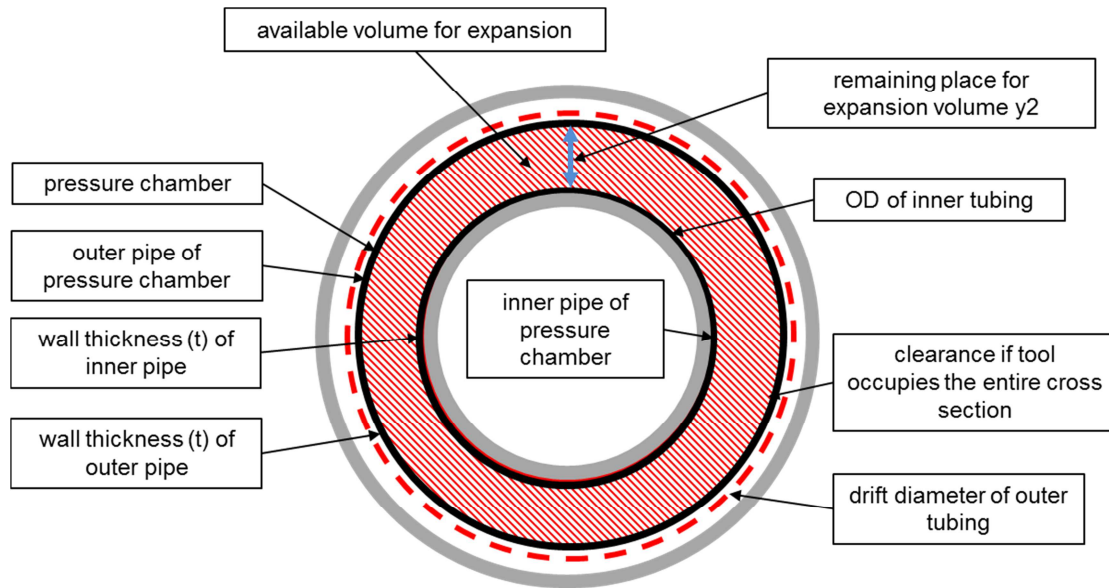


Figure 41: Schematic if the Tool Occupies the Full Cross-Section of the Annulus

Figure 42 displays the wall thickness of the pipe in relation to the selected material grade and the OD of the pipe. The red arrows mark the remaining space for the inner volume of the pressure chamber. The available space on each side of the annulus is the total space of the constructed space divided by two. The dotted lines represent the maximum available constructed space in the annulus depending on the scenarios, see Figure 40 and Figure 41.

The plot shows clearly that the required wall thickness of the corresponding diameters above 3 in (approximately 75 mm) occupy nearly the complete available constructed space in the annulus. Therefore, the space left for the inner volume of the pressure chamber reduces to zero. Only a high material grade gives some opportunities to use larger diameters. To overcome this problem, it is necessary for the design process to develop concepts with a small wall thickness and large inner volume.

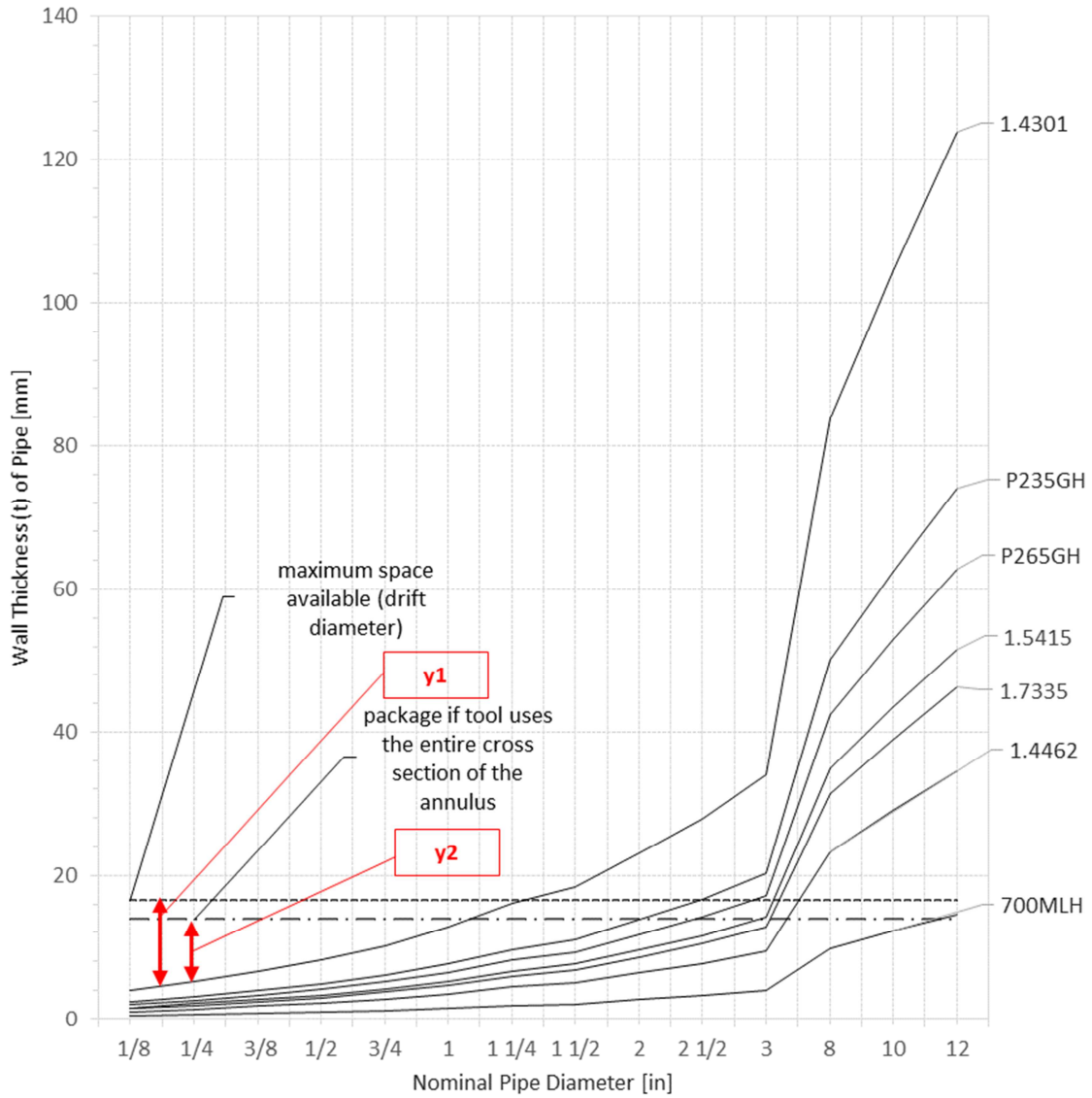


Figure 42: Wall Thickness in Depending on the Material Selection

Figure 43 is a detailed view of Figure 42. The area of interest, up to a nominal pipe diameter of 3 in), is analyzed in detail. The plot displays that diameters above 1/2 in occupy more than one-third of the available constructed space in the annulus. Therefore, from this point, the space left for the inner volume of the pressure chamber reduces with increasing pipe diameter. Consequently, for the design, it is necessary to start with concepts which use small pipes. Further, y1 and y2 represent again the remaining space for the inner volume of the pressure chamber.

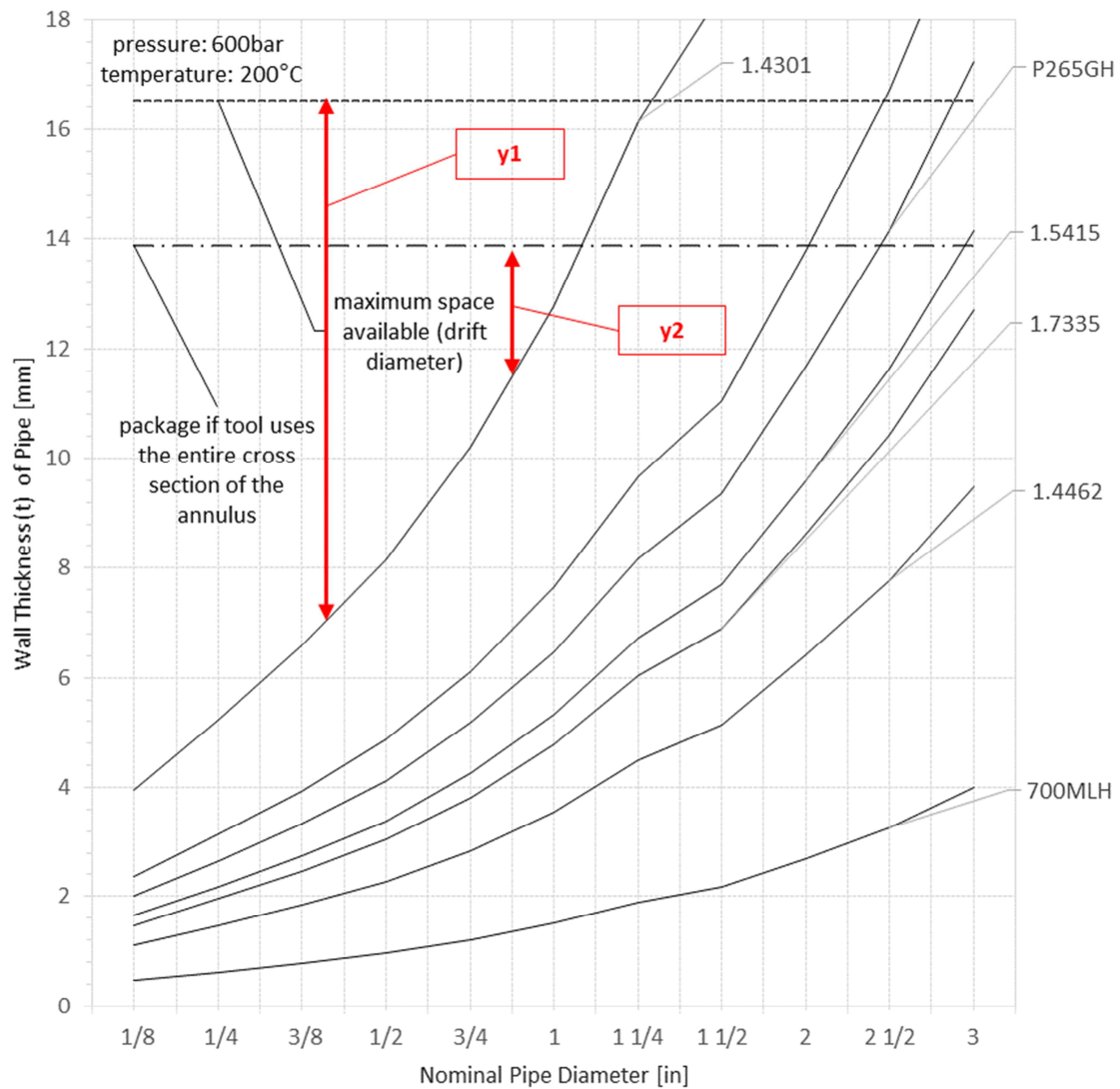


Figure 43: Detail - Wall Thickness in Depending on the Material Selection

## 7.4 Feasibility Study

Another big challenge was the proof of feasibility of the concepts. Since the thesis deals only with the first estimation of possible concepts, the main task was to develop many different concepts and proof their fundamental feasibility. All concepts are checked against available literature to proof their principle feasibility. As a consequence, an accurate proof is not possible and must be done after the selection of the most promising concept.

All concepts are checked on fulfilling the following requirements:

- minimum bend radius for pipes
- weldability of the pressure chamber
- demouldability of the tool
- clearance and tolerances for holes and threads
- minimum wall thickness for threads

## 8 Concept Description

This chapter describes the favourable concepts, which are proven to be the most suitable in the course of development. The principle design of the APRS is based on a pressure chamber in the middle with two fixing parts on each end.

The pressure chamber is the central part of the system. To prevent the tool from moving and therefore to fix the system to the inner casing, a fixing part is mounted on each side of the pressure chamber.

The concepts are designed for the usage at the assumed positions A, B1/B2 related to the parameters given as boundary conditions. However, such a concept can also be used, with small adaptations, in any other well. Other wells have different designs and boundary conditions and therefore require a change of the diameter or wall thickness of the tool and the fixing part.

### 8.1 Concepts for Fixation of the Pressure Chamber

Most concepts use either the Small Fix or the Big Fix system. Therefore, they are mentioned and explained at the beginning of this chapter. Table 13 links the fixing system to the concepts:

Table 13: Fixing Systems – Link to Concepts

Concept Name	Fixing System
A – Small Pipe	-
B - Big Pipe	-
C – Single Pipe	Big Fix
D - Ring Pipe	Small Fix
E – Half Pipe	Big Fix
F – Cross Pipe	Small Fix
G - Membran Pipe	Small Fix
I - Rip Pipe	Big Fix

Concept A and B are using a separate fixing system, which is described in the concept itself.

### 8.1.1 Fixing Concept “Small Fix”

This element consists of a steel body, manufactured as a cast or turning part, with screws for fastening. The main idea behind this element is to protect the pressure chamber from damage during installation and to prevent axial movement of it. The design minimizes the friction during run in hole. Furthermore the design of the fixing part permits enough clearance for performing the cement job.

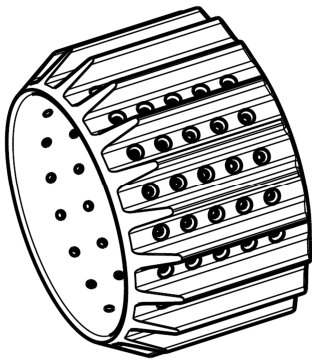


Figure 44: 3D - Small Fix

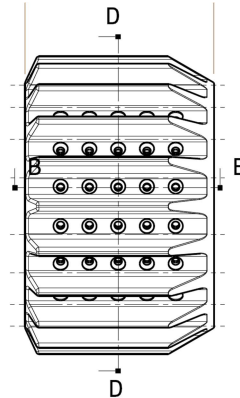


Figure 45: Side View - Small Fix

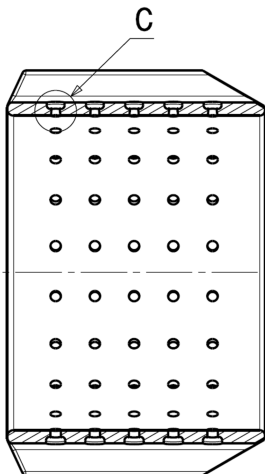


Figure 46: Section Cut B – Small Fix

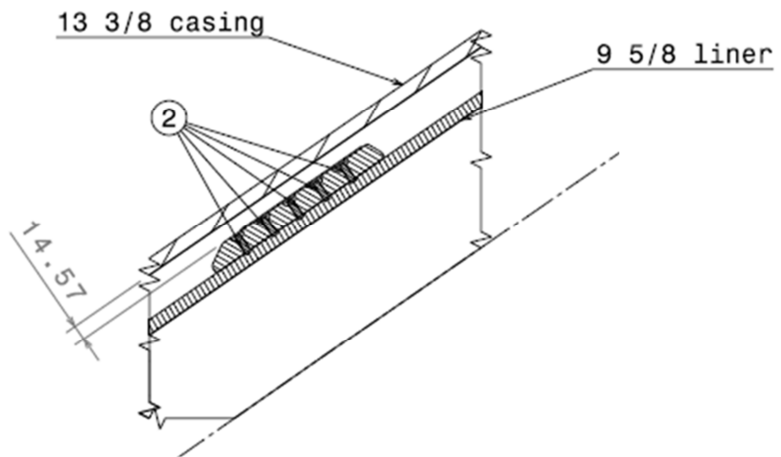


Figure 47: Fixing Concept - Small Fix

Figure 44 shows the 3D-model of the part with the holes for the screws and the ribs to minimize the friction and further to protect the pressure chamber. Figure 46 is the section cut B of Figure 45. The section cut displays the concept of the screws, denoted as item 2, to fix



the tool to the casing. Figure 47 represents the part in the well. The idea is linked to the principle of a stop collar used by a centralizer which can be seen in Figure 48. In Figure 49 the screws for fixing the stop collar can be seen. Since stop collars are widely used in the oil and gas industry, the functionality is proven.



Figure 48: Centralizer and Stop Collar [44]



Figure 49: Stop Collar [45]

Figure 50 and Figure 51 show an updated version of the Small Fix concept which was developed after the first design loops. The number of ribs is reduced to increase the remaining space for cementing. The new design decreases also the production costs.

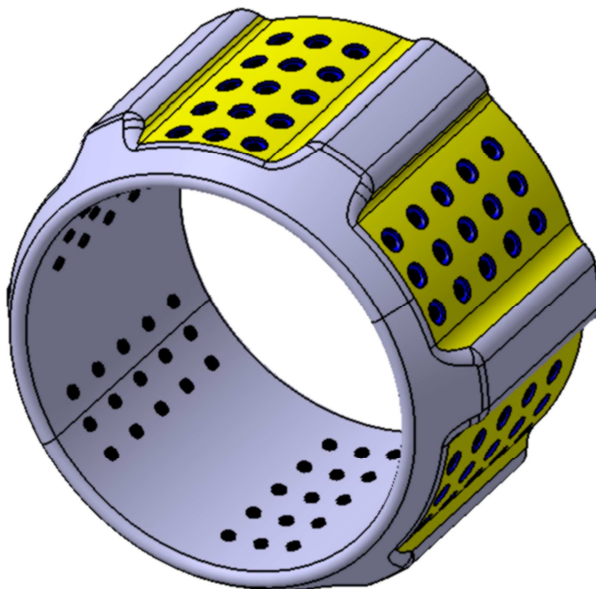


Figure 50: 3D-Model of Small Fix - Improved

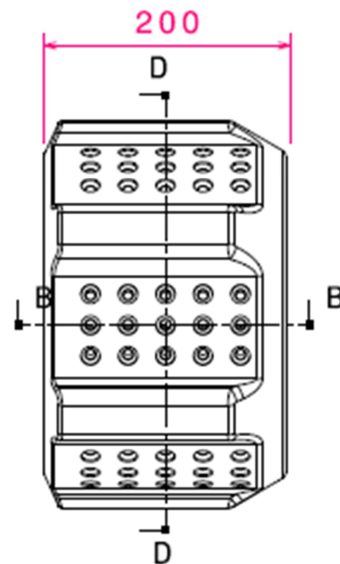


Figure 51: Manufacturing Drawing of Small Fix - Improved

### 8.1.2 Fixing Concept “Big Fix”

Figure 52 shows the 3D – model of the part. This fixing system additionally fulfills a sealing function between the pressure chamber and the inner tubing.

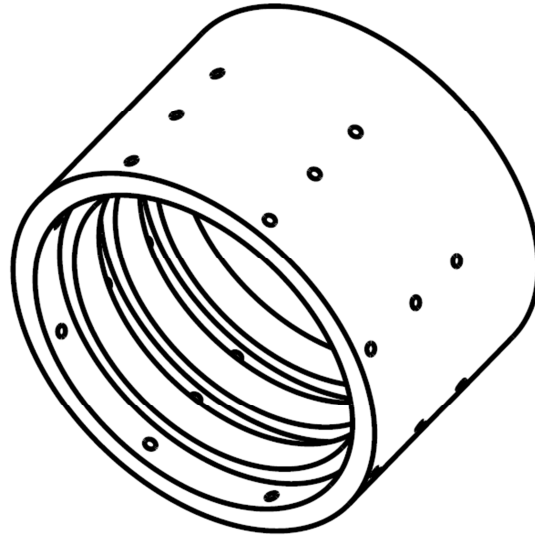


Figure 52: 3D View - Big Fix

Figure 53 shows a section cut of the fixing system. The seals create a barrier between the inner tubing and the pressure chamber and therefore generate the volume for the allowable fluid expansion. The Big Fix is then welded to the pressure chamber to form a unit. The manufacturing process could be either casted or mechanically processed, like the Small Fix system. The seals must withstand high differential pressure and high temperatures. To take this into account, the number of seals per part is increased to three, although already one could resist the pressure difference. The other two act as a safety barrier in case that the first seal fails.

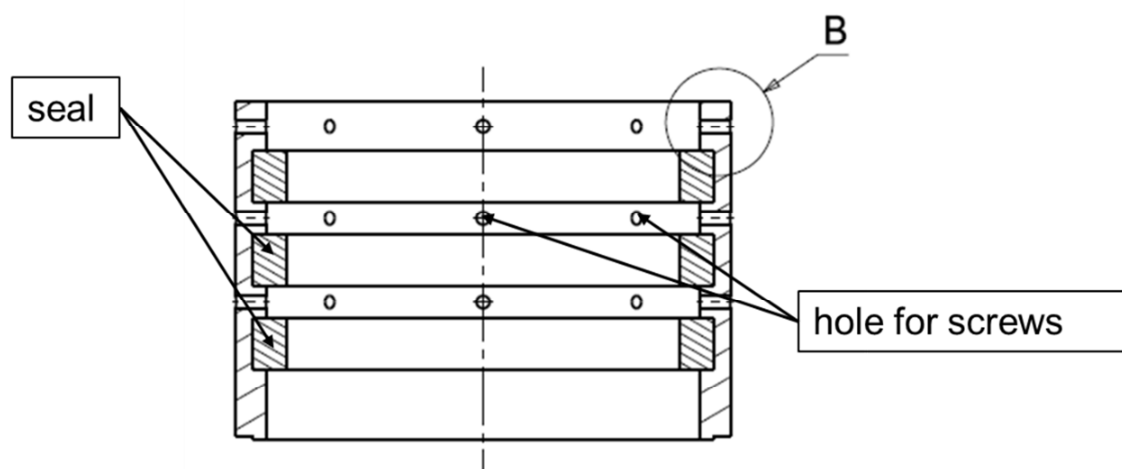


Figure 53: Section Cut - Big Fix

## 8.2 Concept A – “Small Pipe”

The concept displayed in Figure 54 uses standard ANSI or DIN pipes for the pressure chamber, see item 2. The pipes are placed in the annular space around the 9 5/8 in liner in axial direction, and the endpoints of each pipe are sealed with burst discs. The burst disc is screwed into the connection pipe, which is welded to the main pipe of the pressure chamber. The connection pipe consists of an end-cap, which is also a standard part and a small cylinder for mounting the burst disc. The sum of the inner volume of the pipes represents the available volume for the tool. Figure 54 also illustrates the fixing system, see item 1. The single pipes are fixed with two separate mounting parts, represented as item 1, together and around the 9 5/8 in liner. The mounting part also acts as a protector of the tool during installation and supports the cementation process.

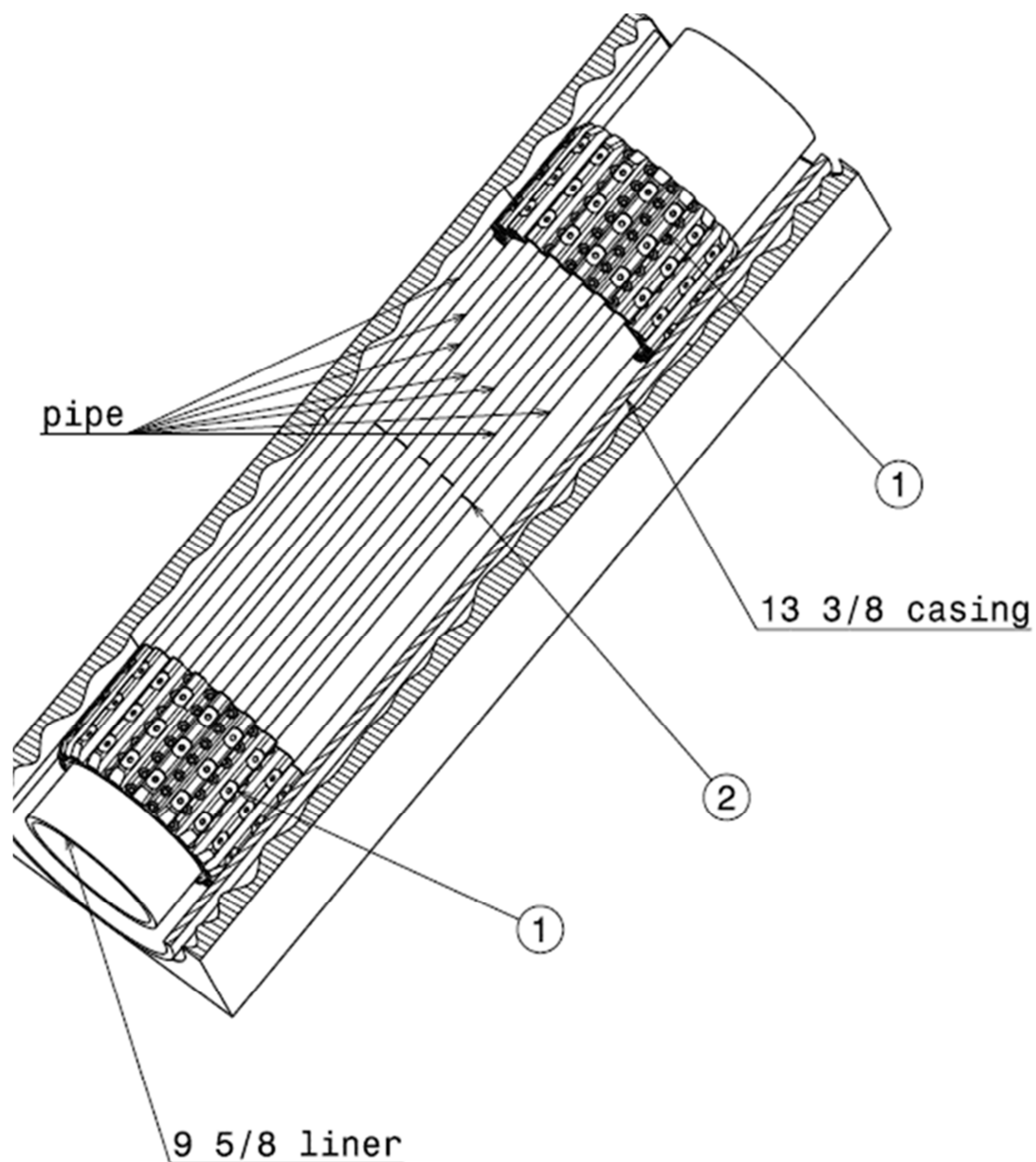


Figure 54: 3D View - Small Pipe

The design of the pressure chamber is simple, thus the manufacturing is not complex. The pressure chamber is based standard parts, and is therefore the pipes are available in many sizes and materials. The dimension of the OD of the pressure chamber is related to the high pressure difference and consequently a small design is desirable. The wall thickness is around 2.5 to 4 mm, depending on the OD of the pipe. The only disadvantage is that the pressure chamber consists of many individual parts. For position A the tool is consists of up to 15 separate pipes, and for position B1 and B2 the number must be increased, to achieve the necessary expansion volume of the pressure chamber. Further, each pipe is 1000 mm long, to equalize the fluid expansion. The production of the individual parts is not complicated. However, due to the many separate parts the assembly at the workshop is a disadvantage. Due to that, this system has a significant disadvantage in handling quality, which can result in many unknown errors during the assembly process. Further, mounting and assembling at the well site could become very complicated and time-consuming.

The flexibility and adaptability of this concept can be rated as good. The burst discs are easily changeable at the well site, and therefore the operating pressure can be adjusted prompt. The only disadvantage, in terms of flexibility, of the concept is that the mounting part is related to the casing diameter. Consequently, if the casing diameter changes, a new fixing part has to be produced. Furthermore, it makes sense to adjust the diameter of the pressure chamber pipes if the available area in the annulus increases.

By having a closer look, the fact that the system consists of many single parts which are not welded together might become a potential risk. In the worst case, it would be possible that the integrity of the tool is lost and the whole casing string gets stuck.

Summarizing, this concept is not sufficient, but the idea of fixing the burst disc is kept in mind for the following designs. An overview of the important parameters of this concept is shown in Table 14. The pipe specifications are as follows: the pressure chamber consists out of a DN20 pipe with an OD of 26.7 mm and a wall thickness of 2.41 mm. The cross-section represents the area which is available for the cementing job in the annulus after installing the tool.

Table 14: Important Parameters – Small Pipe

Volume of Pressure Chamber [l]	Stress [N/mm <sup>2</sup> ]	Remaining Cross-Section [mm <sup>2</sup> ]
5.95	548.01	6571.87

### 8.3 Concept B – “Big Pipe”

This concept is entirely different from concept A. Instead of using many small pipes to achieve a high expansion volume, concept B uses one big pipe with a large diameter.

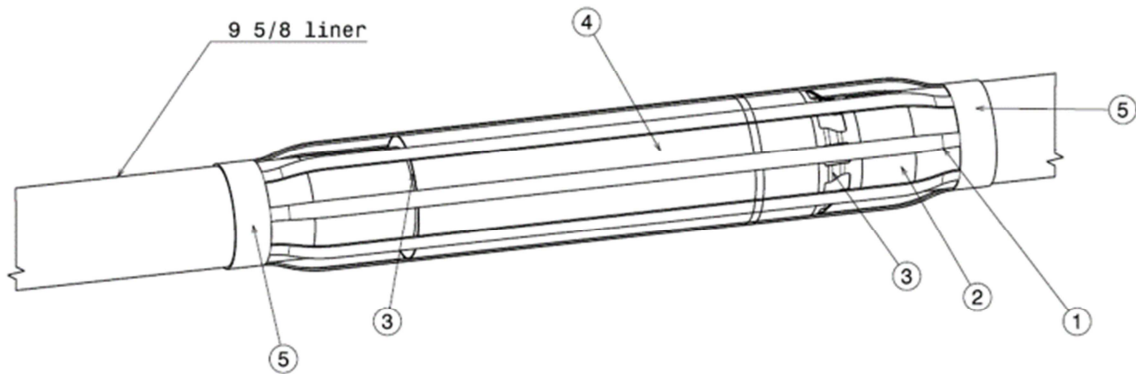


Figure 55: 3D View - Big Pipe

The concept is based, as shown in Figure 55, on two pipes, see item 4 and item 2, surrounding concentric the inner casing or liner. The burst discs are located on the connector, see item 3, which is welded to the outer pipe, represented as item 4 and the inner pipe, displayed as item 2. A section cut can be seen in Figure 56.

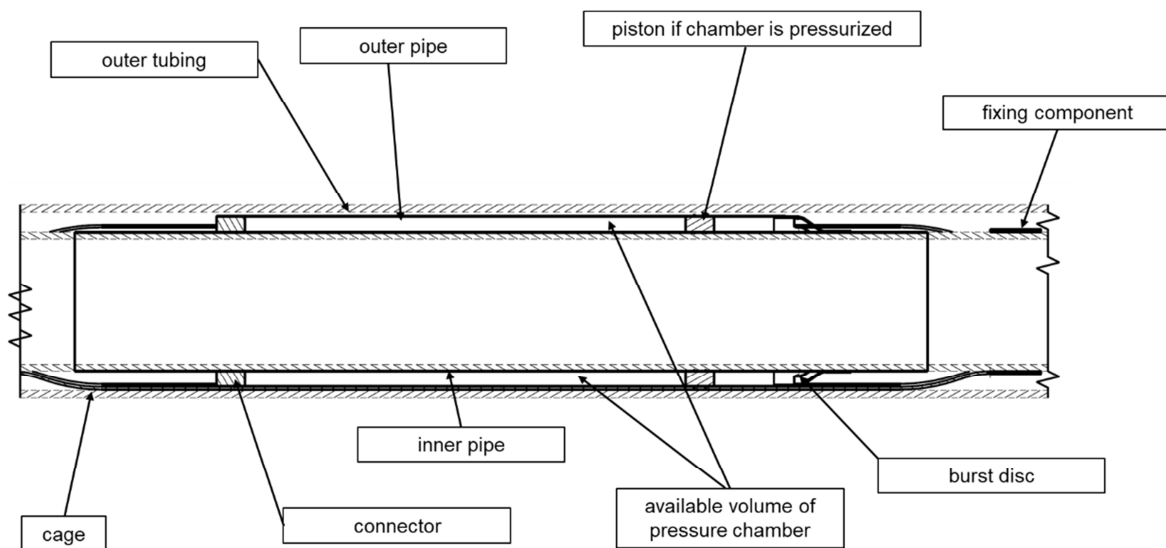


Figure 56: Section Cut - Big Pipe

The main idea behind this concept is to maximize the volume of the pressure chamber by using the complete cross-section of the annulus. The ID and OD of each pipe must be mechanically processed to achieve the required diameter. The volume, which is generated between these two pipes, represents the available volume of the pressure chamber. The ends of the pipes are welded with two separate parts together, see item 3, for sealing the pressure chamber. The fixing component, represented as item 5, fixes on each side the pressure chamber to the inner pipe. Summarized the tool consists out of two large diameter pipes, two separate connectors, see item 3, and two fixing parts. Additionally, a cage, shown

as item 1, can surround the two pipes to protect the tool against damage during installation. According to the small clearance in the annulus, the possible wall thickness of each pipe is limited, hence limiting the possible pressure differences and thus the necessary boundary conditions are not able to be reached in this case. According to Figure 42, a corresponding diameter of nearly 10 in, results in a wall thickness of about 40 mm by using an average material grade. These values must be considered twice: once for the outer pipe and once for the inner pipe.

The summarized wall thickness is then 80 mm compared to the available free space in the annulus of:

- Position A:
  - max distance (x): 27.76 mm (full cross-section)
  - max distance (x): 33.26 mm (partial cross-section)
- Position B1:
  - max distance (x): 55.13 mm (full cross-section)
  - max distance (x): 61.13 mm (partial cross-section)
- Position B2:
  - max distance (x): 46.01 mm (full cross-section)
  - max distance (x): 40.01 mm (partial cross-section)

Thus, the annulus is too small for the required wall thickness.

To overcome this problem, we could think about pressurizing the tool before installing it to reduce the differential pressure acting on the pressure chamber. Hence, a reduction in wall thickness would be possible. But another problem remains: the concentricity between the two pipes must be perfect and this would be very hard to be achieved.

Due to the relatively small wall thickness, compared to the OD and the length of the pipe, the whole pressure chamber is not robust enough. Another possibility would be to balance the pressure in the chamber with the annular pressure during installation continuously. A piston in the pressure chamber, which balances the pressure between the expansion volume and the annulus, would equalize the system. Unfortunately, the loss in expansion volume would be approximately 95%, and the tool would not be efficient. Further, the sealing system in the pressure chamber would become very complex and would pose a big design challenge.

The missing flexibility is also a disadvantage: in order to adapt the tool to another diameter, the whole system must be modified.

Due to these disadvantages, the possible risks and problems with this concept would be substantial. The main problem of this concept is the stiffness and strength of the system. Due to the large diameter pipes, the material strength must be high and the wall thickness of the pressure chamber must be large, to prevent the chamber from collapsing. Based on the calculations, the feasible pressure difference would be maximum 20 MPa. Supplementary, the large diameter combined with the proper wall thickness leads to an unstable system. This results in a functional and tolerance problem of the tool, which ends up in difficulties during assembling.

An overview of the important parameters of this concept is shown in Table 15. The pipe specifications are as follows: the pressure chamber consists out of a pipe with an OD of 300 mm and a wall thickness of 12.71 mm. The tool design is not able to withstand an external pressure of 600 bar, because the required wall thickness would be larger than the available space. Thus, the stress is calculated according to an external pressure of 300 bar.

Table 15: Important Parameters – Big Pipe

Volume of Pressure Chamber [l]	Stress [N/mm <sup>2</sup> ]	Remaining Cross-Section [mm <sup>2</sup> ]
2	3234.04	5351.96

## 8.4 Concept C – “Single Pipe”

A pipe shaped geometry, see item 2 in Figure 57, is fixed to the inner liner within a certain distance by two parts, represented as item 1. The parts, also act as fixing elements for the tool, for details see chapter 8.1.2.

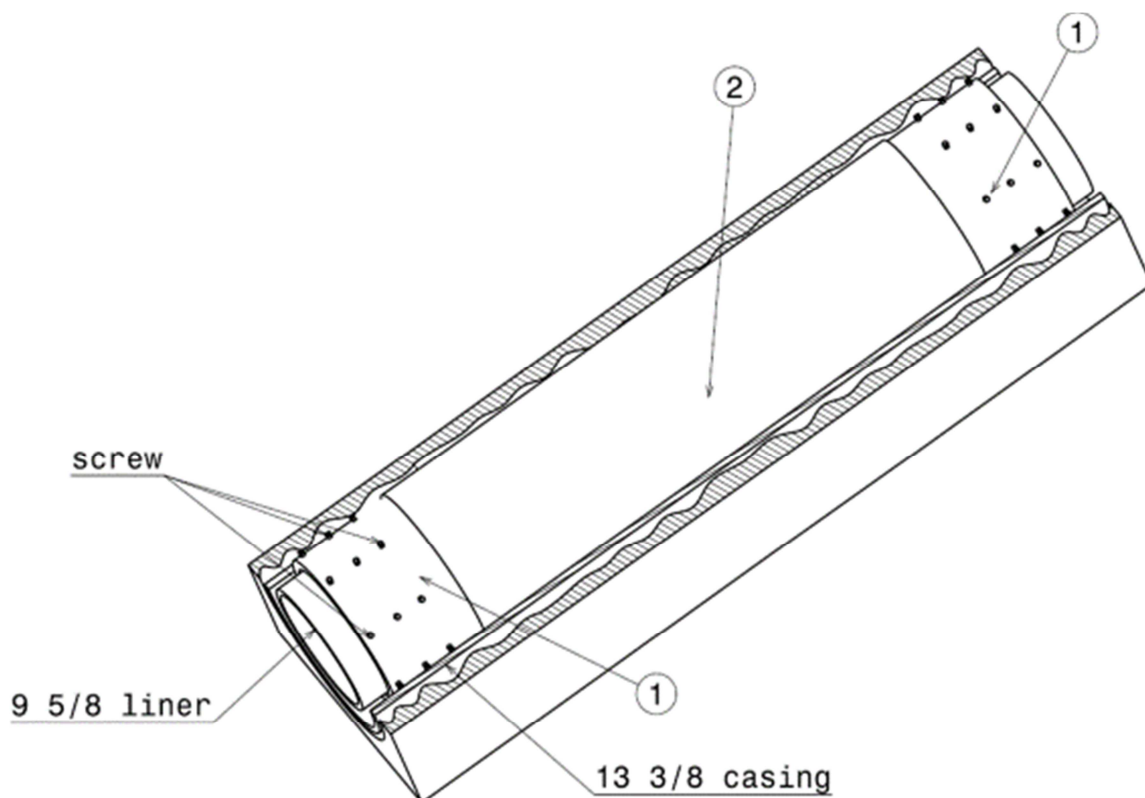


Figure 57: 3D View - Single Pipe

The pipe is manufactured out of a standard pipe, ANSI or DIN, with additional mechanical processes to achieve the necessary dimension. The concept is shown in Figure 58 and is based on the previously mentioned big pipe. The improvement is that instead of a second pipe the outer surface of the inner tubing is used, to generate the expansion volume for the pressure chamber. Thus, the sum of the wall thicknesses of the new pressure chamber is decreased to twice the wall thickness of the inner pipe. Therefore the wall thickness of the

pressure chamber, see item 2, can be increased, allowing high pressure differences. The Big Fix system connects the pressure chamber with the inner tubing, as described in chapter 8.1.2.

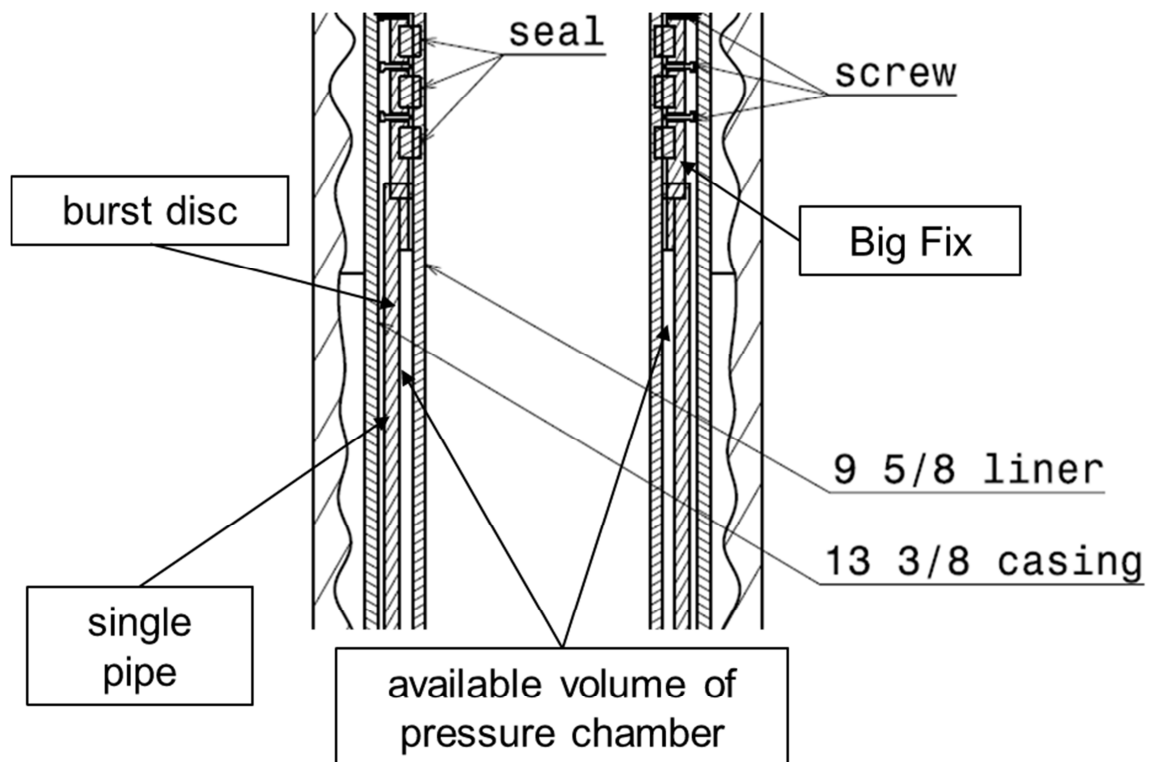


Figure 58: Section Cut - Single Pipe

The expansion volume for APB is generated by connecting and sealing the pressure chamber with the 9 5/8 in liner. Alternatively, the tool could be casted as one part by combining the pressure chamber and the Big Fix system. The advantages of one part would be that the amount of components can be decreased and the weld between the Big Fix and the pressure chamber can be avoided.

Using this tool at different locations includes a change in the dimensioning of the Big Fix and the pressure chamber. Therefore, the flexibility and adaptability of this concept to different well designs are worse compared to the former mentioned concept "Small Pipe". The adaption of the operating pressure can be easily handled by changing the burst disc.

This concept is an improvement of the Big Pipe, but has still many disadvantages and is not able to remove the problems of the Big Pipe concept. The main disadvantage is the stiffness of the pressure chamber. Due to the large diameter of the pressure chamber and the relatively small wall thickness, the concentricity of the pressure chamber to the inner tubing is very important. Further, the wall thickness is still very large, and the remaining space for the fluid expansion is not satisfying.

By using again Figure 43, we can see that if we select a high material grade, still a wall thickness of 14 mm is necessary. Thus, the remaining space for the fluid expansion is very small.



An overview of the important parameters of this concept is shown in Table 16. The pipe specifications are as follows: the pressure chamber consists of a pipe with an OD of 300 mm and a wall thickness of 17.95 mm.

Table 16: Important Parameters – Single Pipe

Volume of Pressure Chamber [l]	Stress [N/mm <sup>2</sup> ]	Remaining Cross-Section [mm <sup>2</sup> ]
7.8	800	5351.96

#### 8.4.1 Concept E – “Half Pipe”

The concept is a further development of the Single Pipe with a differently shaped geometry of the pressure chamber, see Figure 59. The aim of the concept is to improve the stress resistance of the pipe by developing a more stable pressure chamber. The idea is to decrease the outer diameter of the pressure chamber and further to reduce the wall thickness. When the diameter of the pressure chamber is reduced the wall thickness can be reduced too. Hence, the remaining space for fluid expansion increases, see Figure 42. The new design allows a reduction of the necessary wall thickness.

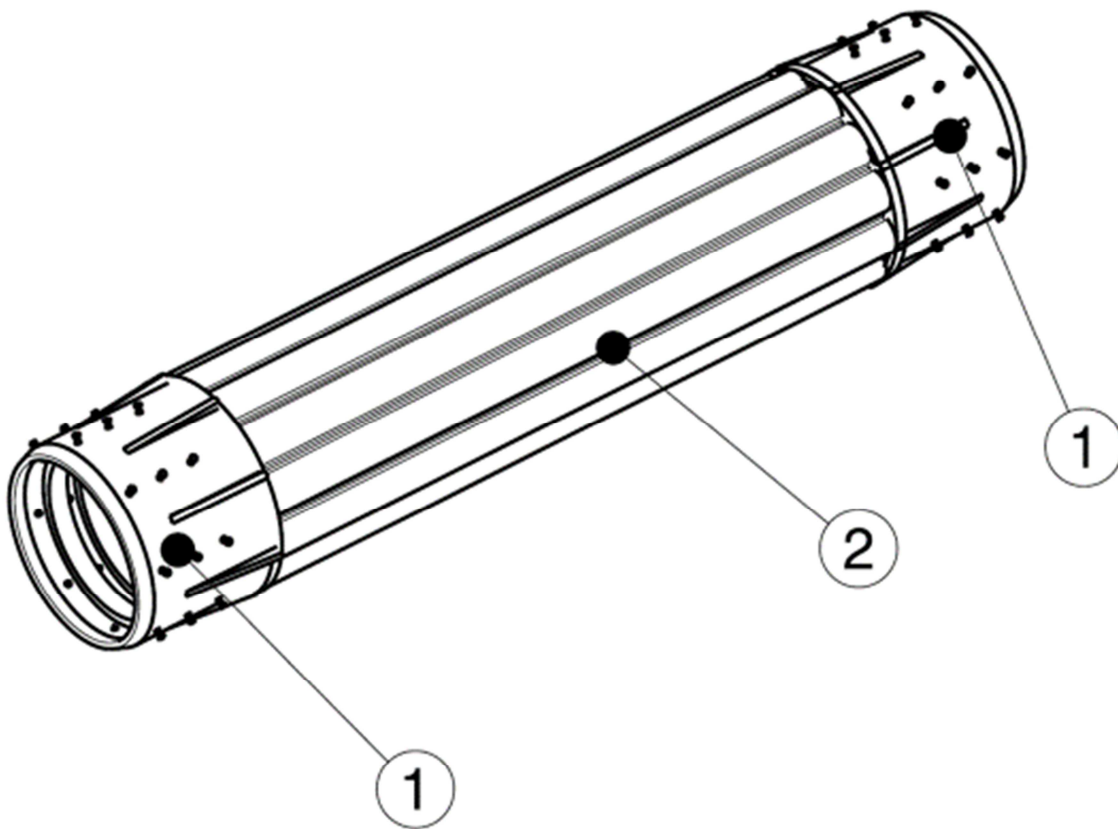


Figure 59: 3D View - Half Pipe

Figure 60 represents the next concept. The concept consists of a casted pressure chamber with the shape of many small half pipes which are merged along the boundary of the inner liner. The Big Fix closes the internal volume of the half pipes and generates the available volume for the pressure chamber. Alternatively, the tool could also be casted in one part. This means, that the fixing element is included in the pressure chamber.

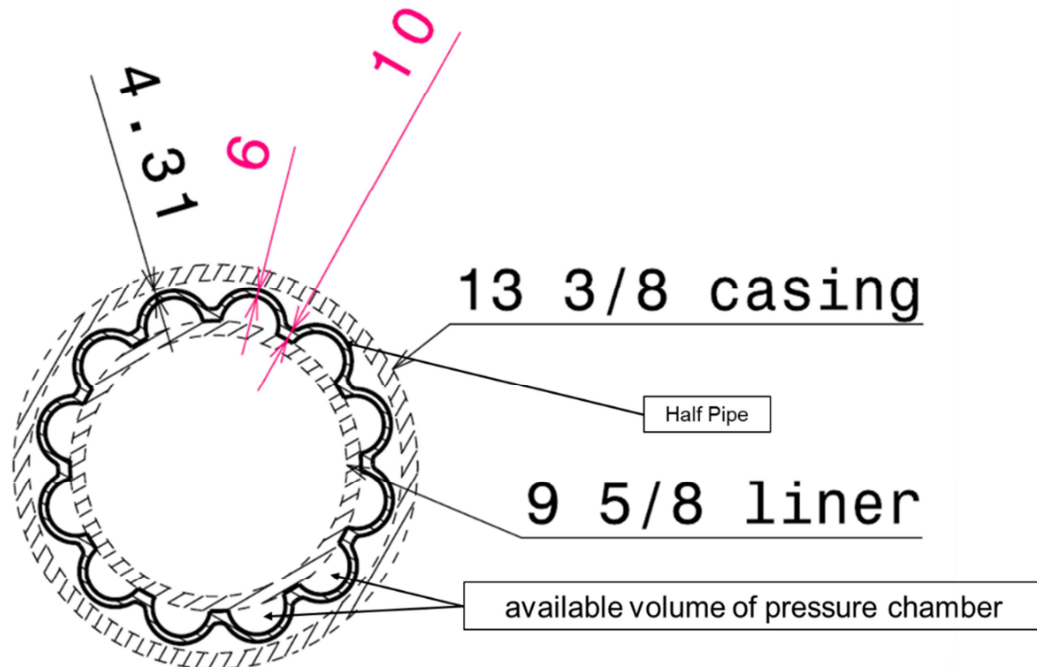


Figure 60: Cross-Section Cut - Half Pipe

The design of the system is relatively simple. Due to the shape of the design, the tool is stiff and stable without further improvement. Affected by the geometry, the available space for the cement job increases and reduces problems during installation. The contact area between the tool and the outer casing is reduced to a few single contact points, compared to the single pipe where the entire surface can contact the outer casing. Thus, also the friction during installation decreases as well.

An overview of the important parameters of this concept is shown in Table 17. The pipe specifications are as follows: the pressure chamber consists of a pipe with an OD of 305 mm and a wall thickness of 4 mm.

Table 17: Important Parameters – Half Pipe

Volume of Pressure Chamber [l]	Stress [N/mm <sup>2</sup> ]	Remaining Cross-Section [mm <sup>2</sup> ]
13.84	491.68	3119.78

### 8.4.2 Concept I – “Rip Pipe”

Figure 61 represents the 3D view of the Rip Pipe model. The Rip Pipe is also an improvement of the Single Pipe concept with a different geometry of the pressure chamber, denoted as item 2.

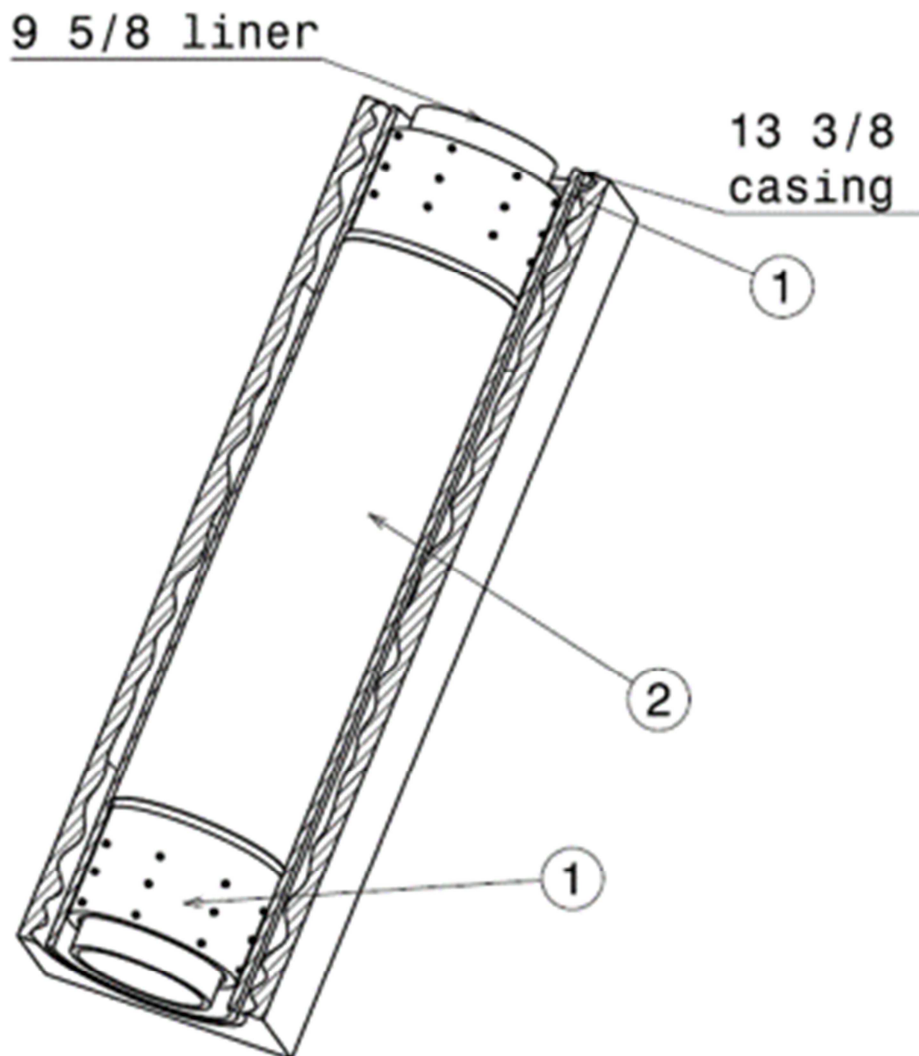


Figure 61: 3D View - Rip Pipe

This concept is based on the idea of using the inner tubing as a stabilizing element for the pressure chamber, similar to concept E. Figure 31 illustrates the schematic of the load path and Figure 32 represents the simulation model of the FEM calculation. Thus, an additional load path for the pressure forces is generated. Rips on the inner side of the pressure chamber transport the load of the external pressure to the inner tubing as shown in Figure 62. Hence, the wall thickness can be reduced, and the volume increases. The rips inside the pipe increase the strength of the tool and reduce therefore concentricity problem. This fact is a big disadvantage of the Single Pipe concept. The Big Fix, see item 1, on each side closes the inner volume of the tool and generates the expansion volume.

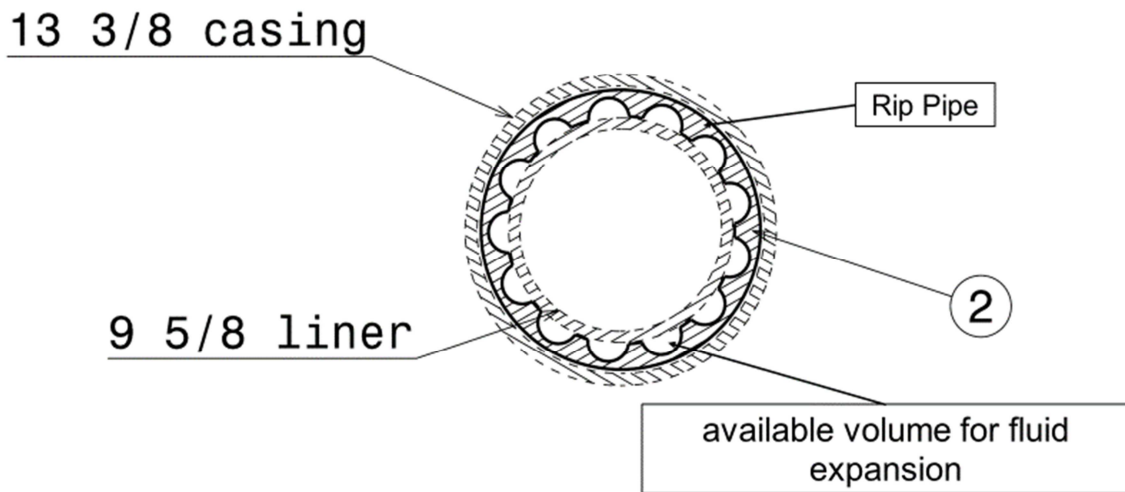


Figure 62: Cross-Section Cut - Rip Pipe

An overview of the important parameters of this concept is shown in Table 18. The pipe specifications are as follows: the pressure chamber consists of a pipe with an OD of 305 mm and a wall thickness of 5 mm.

Table 18: Important Parameters – Rip Pipe

Volume of Pressure Chamber [l]	Stress [N/mm <sup>2</sup> ]	Remaining Cross-Section [mm <sup>2</sup> ]
14	294	2976.13

## 8.5 Concept D – “Ring Pipe”

This concept is a further development of the Small Pipe concept. To get rid of the disadvantages of the Small Pipe concept, a new design of the pressure chamber, see item 2, and the fixing part, denoted as item, 1 was necessary. The main difference can be seen in the orientation of the pipe shown in Figure 63. Instead of an axial direction the pipe is bent around the inner liner, see Figure 64. Therefore, the shape of the pressure chamber looks like a ring.

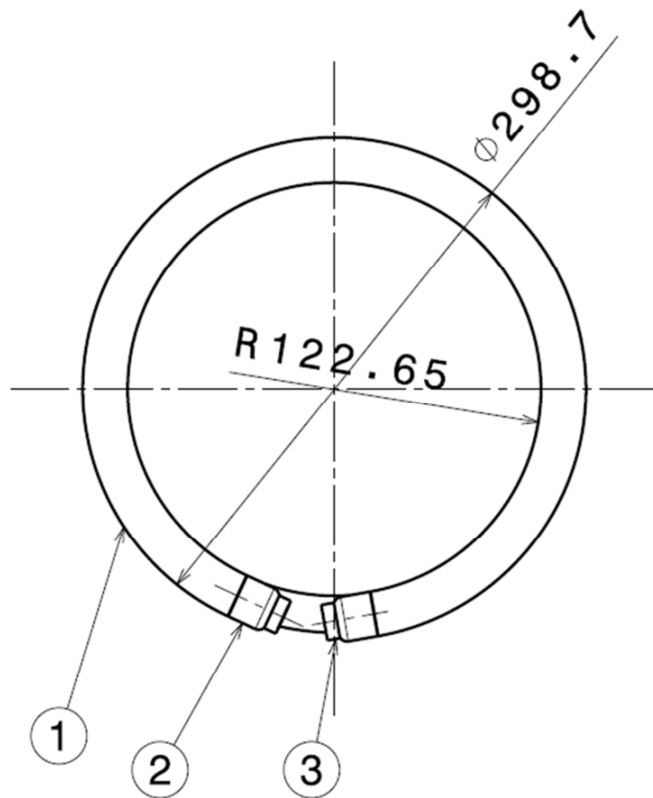


Figure 63: Ring Pipe - Single Part

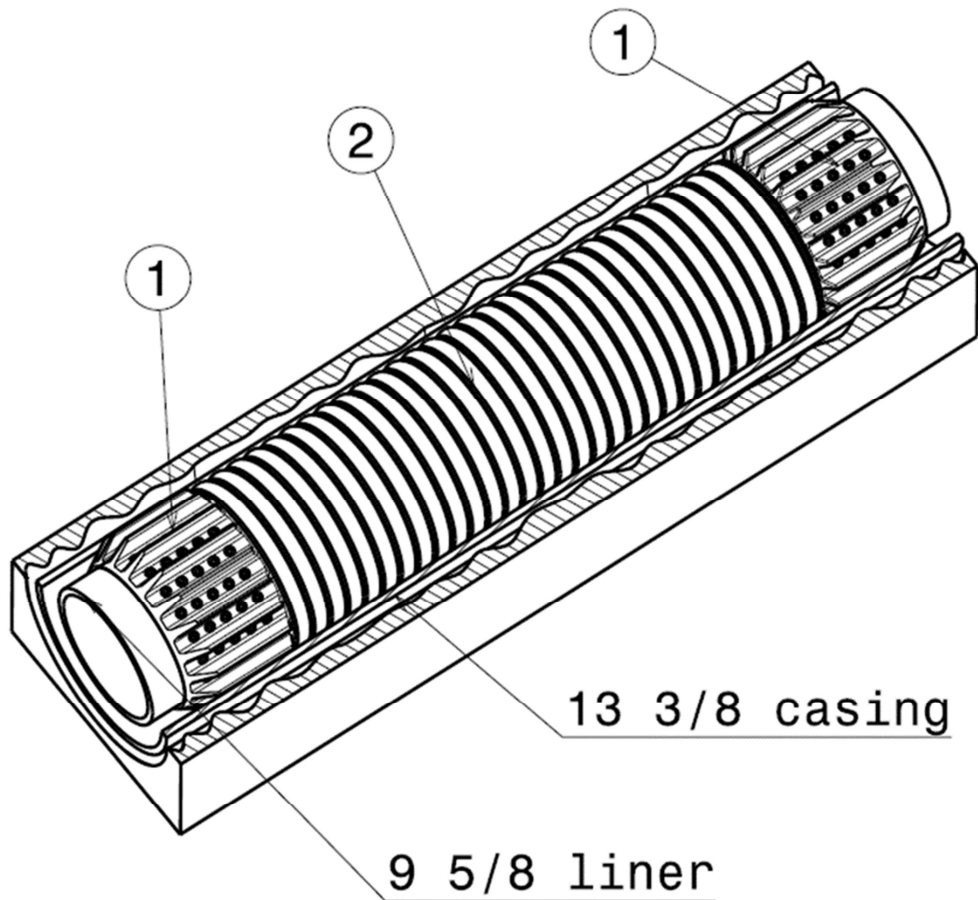


Figure 64: 3D View - Ring Pipe

The primary advantage of this shape is that the tool can only move in axial direction. Thus, a complicated fixing system can be avoided. As shown in Figure 65 the ring pipe is then overlain by the next ring pipe and welded together to form a unit element displayed in Figure 66.

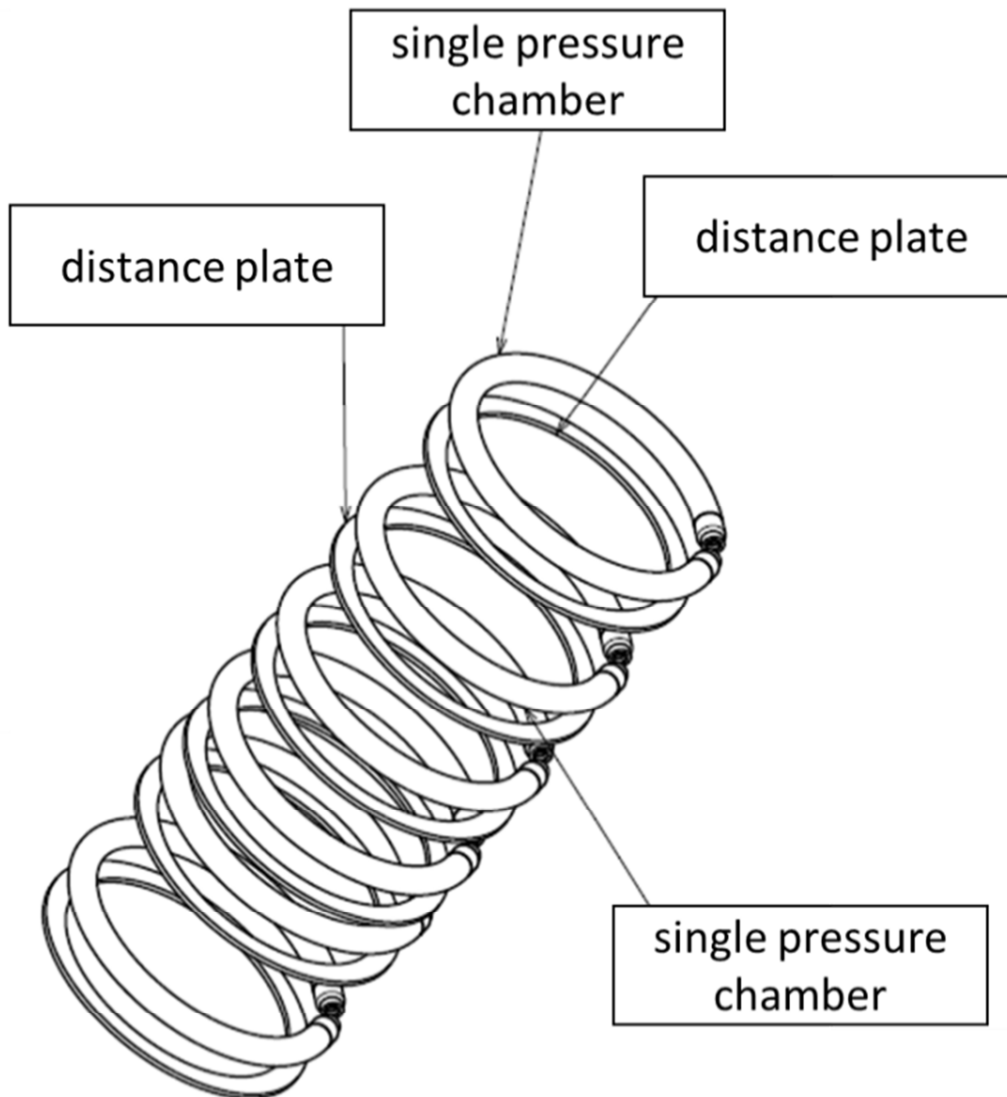


Figure 65: Assembly Ring Pipe

The sum of the volume of each pipe represents the available volume of the pressure chamber.

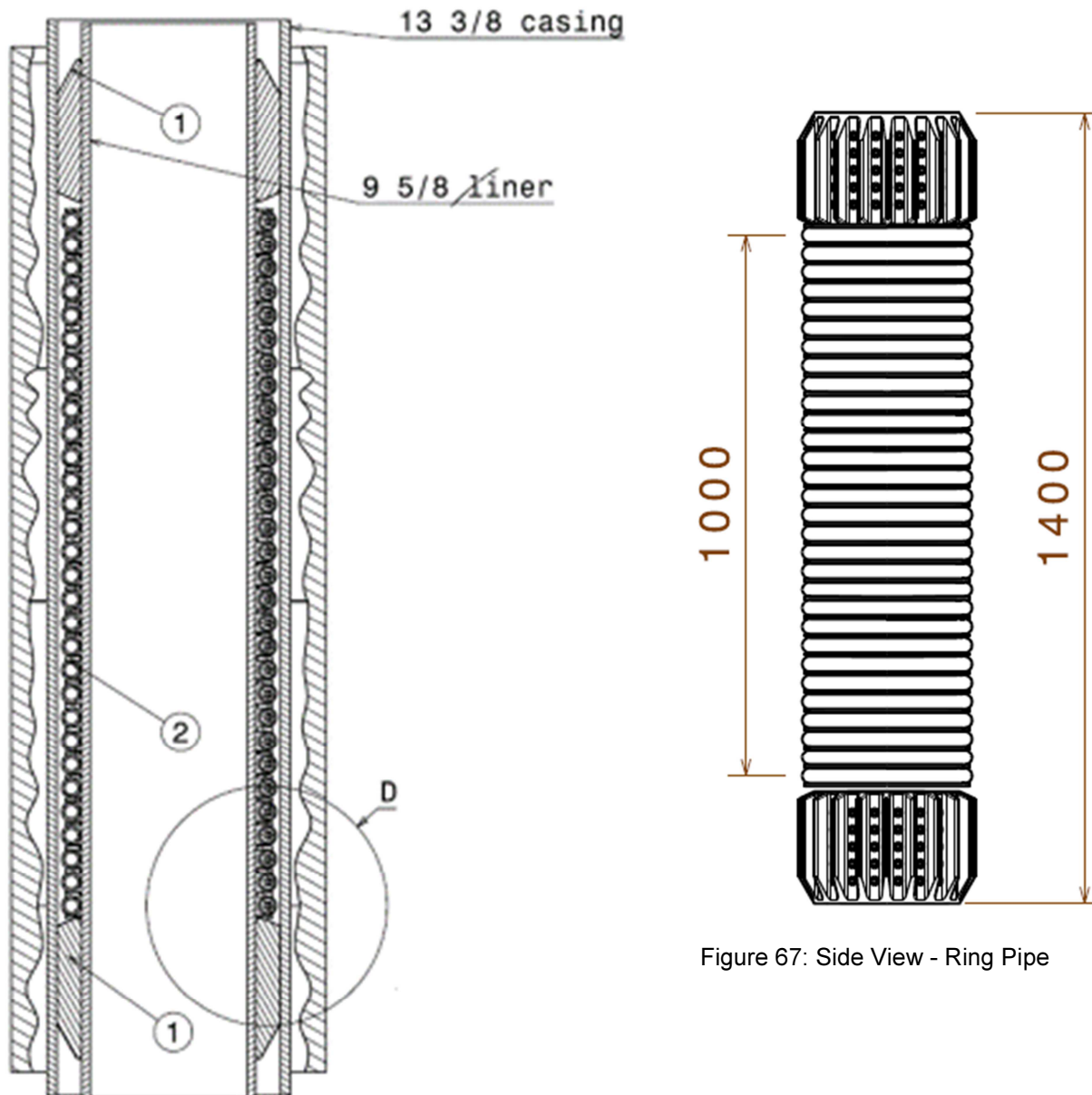


Figure 66: Section Cut - Ring Pipe

Figure 67 represents the assembled APRS. The burst discs are located on each end of the pipe, see Figure 63. Therefore, the tool can be used for different operating pressures within one tool, by using different burst discs. Thus, the tool can work stepwise and can avoid a vast pressure drop when the burst disc enables the fluid to enter the chamber. A disadvantage in production is that, the tool requires a high number of burst discs. In Figure 66 two fixing parts, denoted as item 1, are shown. Alternatively, the pipes are not welded together and will be fixed together by the fixing parts. To adjust the tool to another diameter the whole system must be redesigned. But the advantage is that only the bent radius and the length of the individual tubes of the pressure chamber must be redesigned and not the entire chamber.

The manufacturing process of one pressure chamber is simple, but the large amount of single components results in a time consuming manufacturing process. For the desired tool



length of 1000mm, it is necessary to manufacture and assemble up to 37 pipes. Also, the number of burst discs is high, because each pipe needs at least one. But this can be also seen as an advantage, because if one burst disc fails to open, the tool has another 36 discs which are opened. Moreover, it would be possible to adjust the burst pressure of the tool stepwise. So, the first will open at XX bar and the next at XX bar + YY bar. Hence, a smoother pressure drop can be achieved.

An overview of the important parameters of this concept is shown in Table 19. The pipe specifications are as follows: the pressure chamber consists of a DN20 pipe with an OD of 26.7 mm and a wall thickness of 2.41 mm.

Table 19: Important Parameters – Ring Pipe

Volume of Pressure Chamber [l]	Stress [N/mm <sup>2</sup> ]	Remaining Cross-Section [mm <sup>2</sup> ]
11.9	548.01	6571.87

## 8.6 Concept F – “Cross Pipe”

Figure 68 represents the 3D model of the Cross Pipe concept. This concept is entirely different from all other concepts. The reason for developing this variation was based on the idea to see if a tool, mainly based on standard parts, can be designed. The pressure chamber is a combination of fittings, such as T-cross and bow, as shown in Figure 69 and Figure 70.

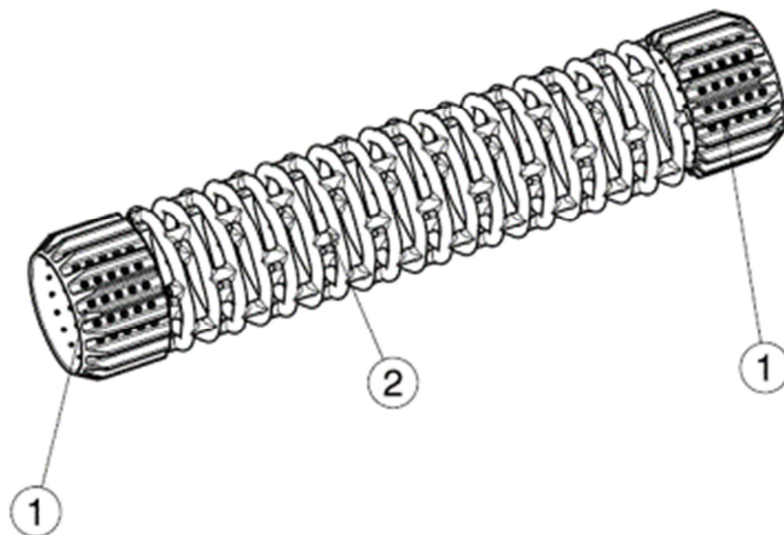


Figure 68: 3D View - Cross Pipe



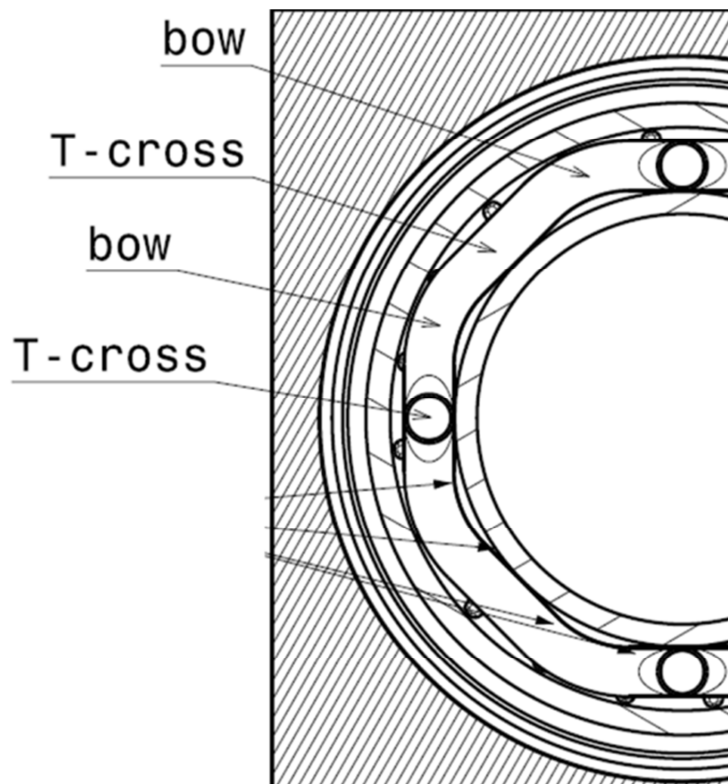


Figure 69: Cross-Section Cut - Cross Pipe

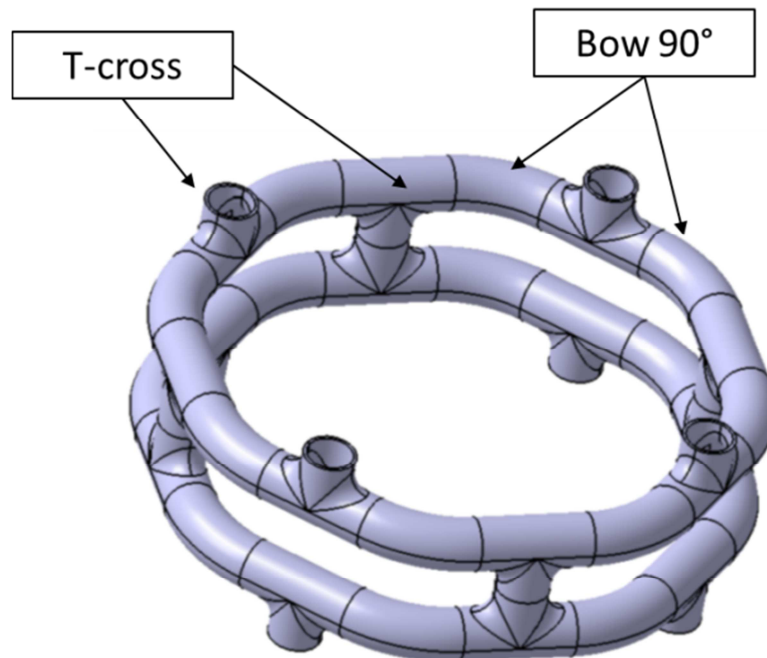


Figure 70: 3D – Screenshot Cross Pipe

The elements are welded together to one single pressure chamber. On each side, four burst discs seal the volume. The geometry of the pressure chamber allows only axial movement,

so the tool does not need any complicated fixing system and the Small Fix can be used, see Figure 71.

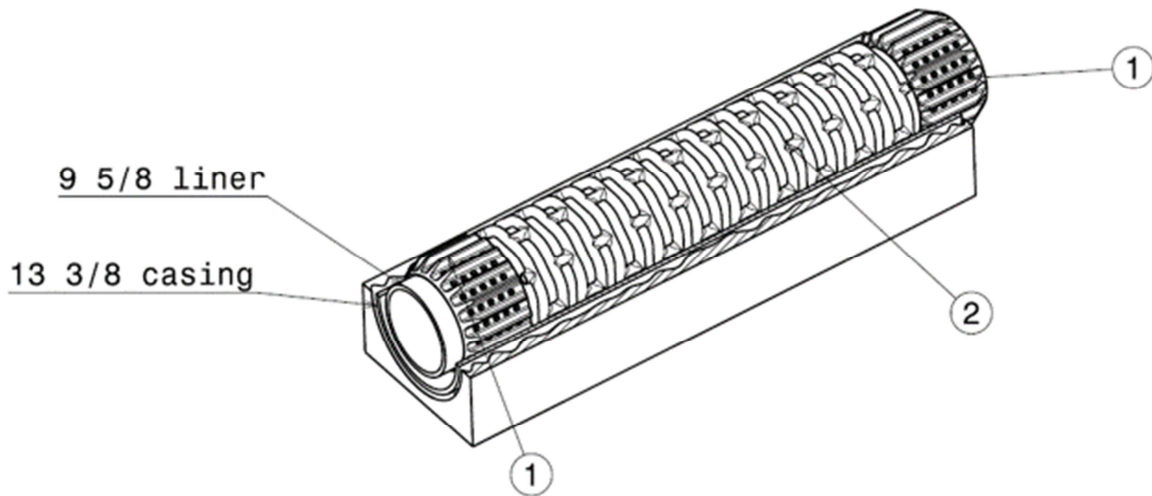


Figure 71: Section Cut - Cross Pipe

This concept is simple since only standard parts are used. The number of required parts is large and therefore the whole manufacturing process is not efficient, if many tools are demanded. But this concept is an alternative option to build and test in a simply way the functionality of the basic working principle of the APRS. Thus, this concept could be a prototype to check the functionality the concepts. Another big advantage is that no expensive manufacturing tools are necessary, and the tool could be produced at low costs and within a short period of time.

An overview of the important parameters of this concept is shown in Table 20. The pipe specifications are as follows: the pressure chamber consists of a DN20 pipe with an OD of 26.7 mm and a wall thickness of 2.41 mm.

Table 20: Important Parameters – Cross Pipe

Volume of Pressure Chamber [l]	Stress [N/mm <sup>2</sup> ]	Remaining Cross-Section [mm <sup>2</sup> ]
7.6	548.01	6571.87

## 8.7 Concept G – “Membrane Pipe”

Figure 72 displays the Membrane Pipe. This concept is an improvement of the concept Small Pipes and avoids a complicated fixing system of the pressure chamber. This is achieved by welding the pipes axially together to form a mono pressure chamber, denoted as item 2.

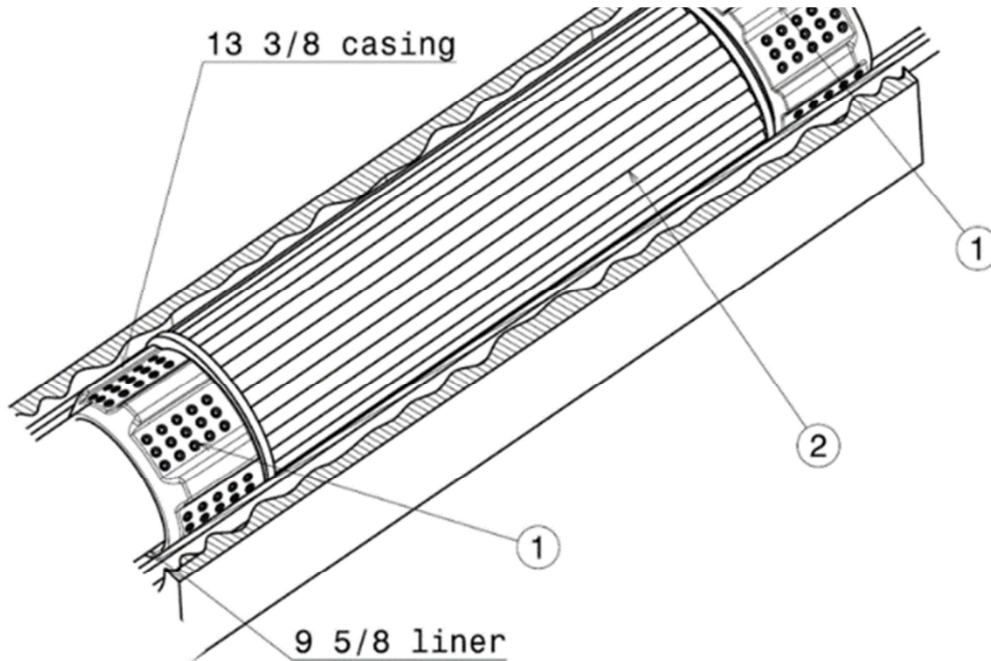


Figure 72: 3D View - Membrane Pipe

Hence, a complicated mounting system can be avoided, and the number of pipes per tool can be enlarged, see Figure 73 and Figure 74.

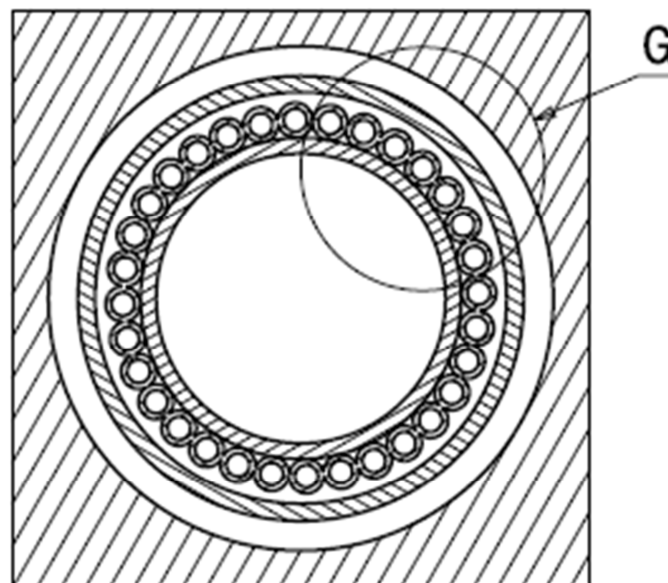


Figure 73: Cross-Section Cut - Membrane Pipe

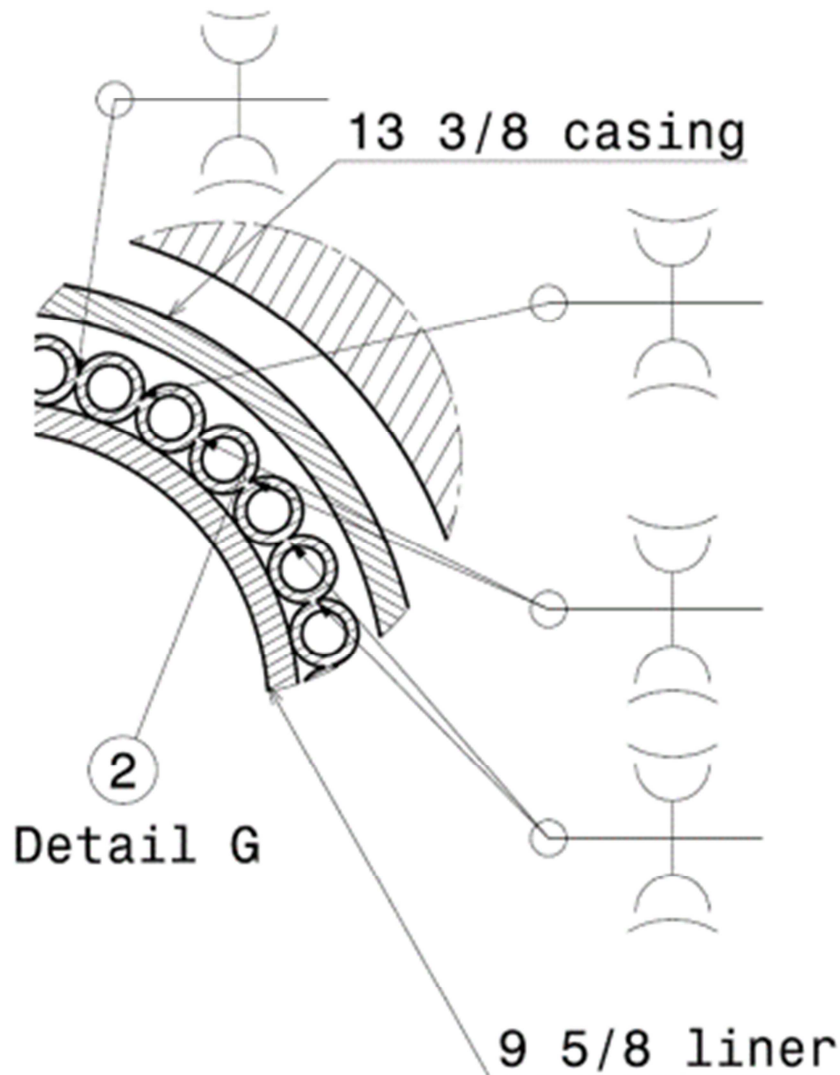


Figure 74: Detail G - Membrane Pipe

Thus, the available volume for fluid expansion can be increased. On each end, the pressure chamber is secured with the Small Fix, denoted as item 1 in Figure 72, to the inner casing which also prevents the tool from damage during installation. The idea is based on the process of pipe welding for large steam boilers, so-called membrane walls [46]. Figure 76 presents such a boiler during construction. As visible in the figure, nearly every shape and geometry can be manufactured. A detailed figure of the welding process is shown in Figure 75, where the distance between the pipes is user-specific. For the pressure chamber the arrangement of the pipes is presented in Figure 73.

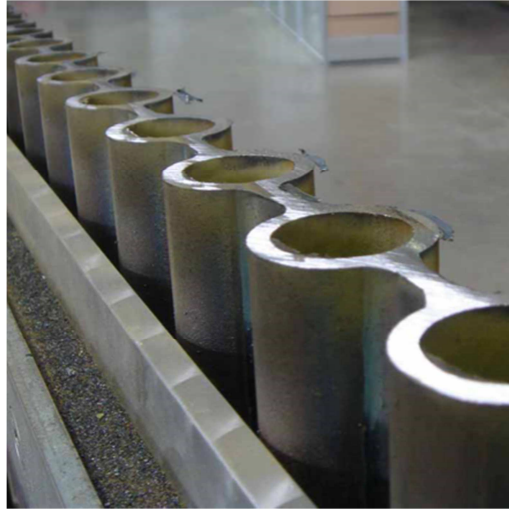


Figure 75: Detailed Picture of Membrane Wall [46]

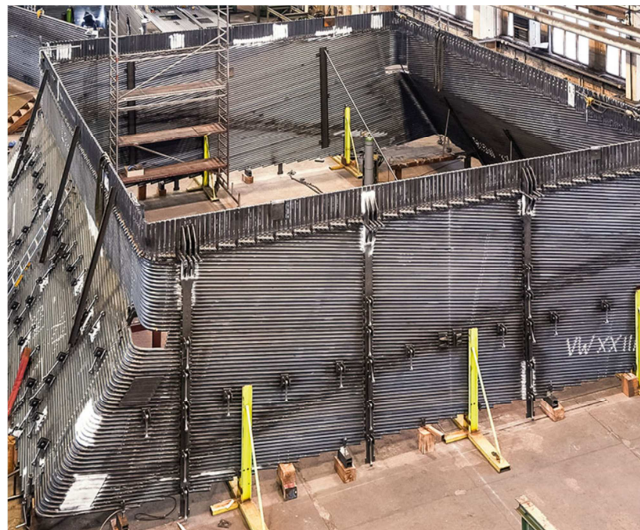


Figure 76: Steam Boiler – Foundation of Membrane Pipe [46]

To adapt the tool to another casing diameter, only the welding and assembling process must be changed. The usage of standard parts allows for a quick adaption if the requirements are changed. Supplementary, it is necessary to adapt the fixing part as well. The manufacturing process is simple but cost-intensive. Therefore, the concept would be only effective if a large amount of tools is necessary.

An overview of the important parameters of this concept is shown in Table 21. The pipe specifications are as follows: the pressure chamber consists of a DN15 pipe with an OD of 21.3 mm and a wall thickness of 1.65 mm.

Table 21: Important Parameters – Membrane Pipe

Volume of Pressure Chamber [l]	Stress [N/mm <sup>2</sup> ]	Remaining Cross-Section [mm <sup>2</sup> ]
9	629.69	11525.53

## 9 Concepts Overview

The overview includes a rating of all designed concepts mentioned in the previous chapter. The rating is based on parameters like volume and weight of the pressure chamber and their disadvantages and advantages. It is used to get an idea of which concept is suitable and which dimensions are necessary to meet the requirements. For instance: is the combination of a small wall thickness with high steel grades and high volumes better than low steel grades and low volumes with high wall thickness? Since the number of possible arrangements is large, an automated rating process was established. To decrease the amount of possibilities it was decided to keep the von Mises equivalent stress at a maximal value of 800 N/mm<sup>2</sup>, including a safety factor of 1.5. This means that whenever it was possible, the wall thickness was decreased until the 800 N/mm<sup>2</sup> were reached. Therefore, not all possible configurations were checked. Only a few from each concept were chosen to show the direction of the further way of design. Additionally, it was decided to stop the variations of the dimension of a concept as soon as the results degraded. According to the design criteria mentioned in chapter 7, the rating categories were defined.

To achieve a representative result, the categories were weighted against each other corresponding to their relevance. For instance, the functionality of the concept is more essential than the weight of the tool. Hence, the weighting of the category “functionality” was increased, and for the “weight of the tool”, it was decreased.

Further, the categories were defined in a way that they can be rated with high, medium and low. To process it in Microsoft Excel, corresponding values are used as shown in Table 22. This was done by numbers from one to three, whereas three means that the concept accomplishes the requirement and one that the concept failed. Therefore, the answer “high” can lead to a value of one or three, depending on the questions.

Table 22: Rating Example

Category	Description	Value
Costs	high	1
	medium	2
	low	3
Functionality	high	3
	medium	2
	low	1

The result of this rating process is shown in Table 23 and discussed in chapter 10. The detailed rating can be found in appendix F in the following tables: Table 29, Table 30, Table 31, Table 32 and Table 33.



Table 23: Overview Rating

concept name	length of pressure chamber [mm]	DN of main pipe	OD of main pipe	wall thickness of main pipe [mm]	material grade required	weight [kg]	costs						important parameters			flexibility		risks and problems		summary	
							feasibility						available area for cementjob [mm <sup>2</sup> ]	stress according to dp = 600bar [N/mm <sup>2</sup> ] SF=1.5	volume of pressure chamber [l]	flexibility of tool for different pressure regimes	addaptability of tool to different casing diameters	risks and problems during installation of tool	complexity of tool (failure occurance)		
small pipe	1000	25	33.4	2.77	high	62	medium	medium	low	low	high	medium	high	171	592	9	medium	low	high	high	1.70
	1000	25	33.4	4.55	medium	63	medium	medium	low	high	medium	medium	high	171	382	7	medium	high	high	high	1.90
	1000	20	26.7	2.41	high	52	medium	medium	low	low	high	medium	high	6572	548	6	medium	high	high	high	1.63
	1000	20	26.7	3.91	medium	63	medium	medium	low	low	high	medium	high	6572	360	4	medium	high	high	high	1.82
big pipe	1500	-	300	4.57	high	606	high	low	medium	high	medium	high	high	5352	3234	16	low	high	high	high	1.73
	1500	-	300	12.7	high	356	high	low	medium	high	high	high	high	5352	1194	2	low	high	high	high	1.33
single pipe	1000	-	300	17.95	high	377	high	low	medium	high	medium	medium	high	5352	800	8	low	high	high	medium	1.68
	1000	-	300	24.5	high	464	high	low	medium	high	high	high	high	5352	600	3	low	high	high	medium	1.60
ring pipe	1000	20	26.7	2.41	medium	121	medium	high	low	low	low	medium	low	6572	548	12	medium	high	low	low	2.35
	1000	20	26.7	3.91	medium	144	medium	high	low	low	low	medium	low	6572	360	9	medium	high	low	low	2.54
half pipe	1000	50	60.7	4	high	96	medium	low	medium	high	low	high	low	3120	711	16	low	high	high	medium	2.05
	1000	50	60.7	6	medium	113	medium	low	medium	high	low	high	low	3120	492	13	low	high	high	medium	2.08
cross pipe	1000	20	26.7	2.41	high	91	low	high	medium	high	low	high	low	6572	548	8	low	high	medium	low	2.27
	1000	20	26.7	3.91	medium	123	low	high	medium	high	low	high	low	6572	360	5	low	high	medium	low	2.12
membran pipe	1000	25	33.4	2.77	high	90	low	high	high	low	low	low	171	592	14	medium	high	medium	medium	medium	2.12
	1000	25	33.4	4.55	medium	119	medium	low	high	low	low	low	171	382	11	medium	high	medium	medium	medium	2.24
	1000	20	26.7	2.41	high	84	medium	low	high	low	low	low	6572	548	11	medium	high	medium	medium	medium	2.27
	1000	20	26.7	3.91	medium	106	medium	high	low	high	low	low	6572	360	8	medium	high	medium	medium	medium	2.46
	1000	15	21.3	1.65	high	74	high	low	high	low	low	low	11526	630	9	medium	high	medium	medium	medium	2.27
	1000	15	21.3	3.73	low	101	low	high	high	low	low	low	11526	312	5	medium	high	medium	medium	medium	2.27
rip pipe	1000	305	-	8	low	136	medium	low	medium	medium	low	low	2976	246	12	low	high	high	medium	medium	2.16
	1000	305	-	5	low	120	low	medium	medium	medium	low	low	2976	294	14	low	high	high	medium	medium	2.16

## 10 Conclusion and Outlook

This chapter presents the results of the concept rating and further improvements for the discussed concepts. Figure 77 presents the concept name and the dimension of the used system with the corresponding rating result.

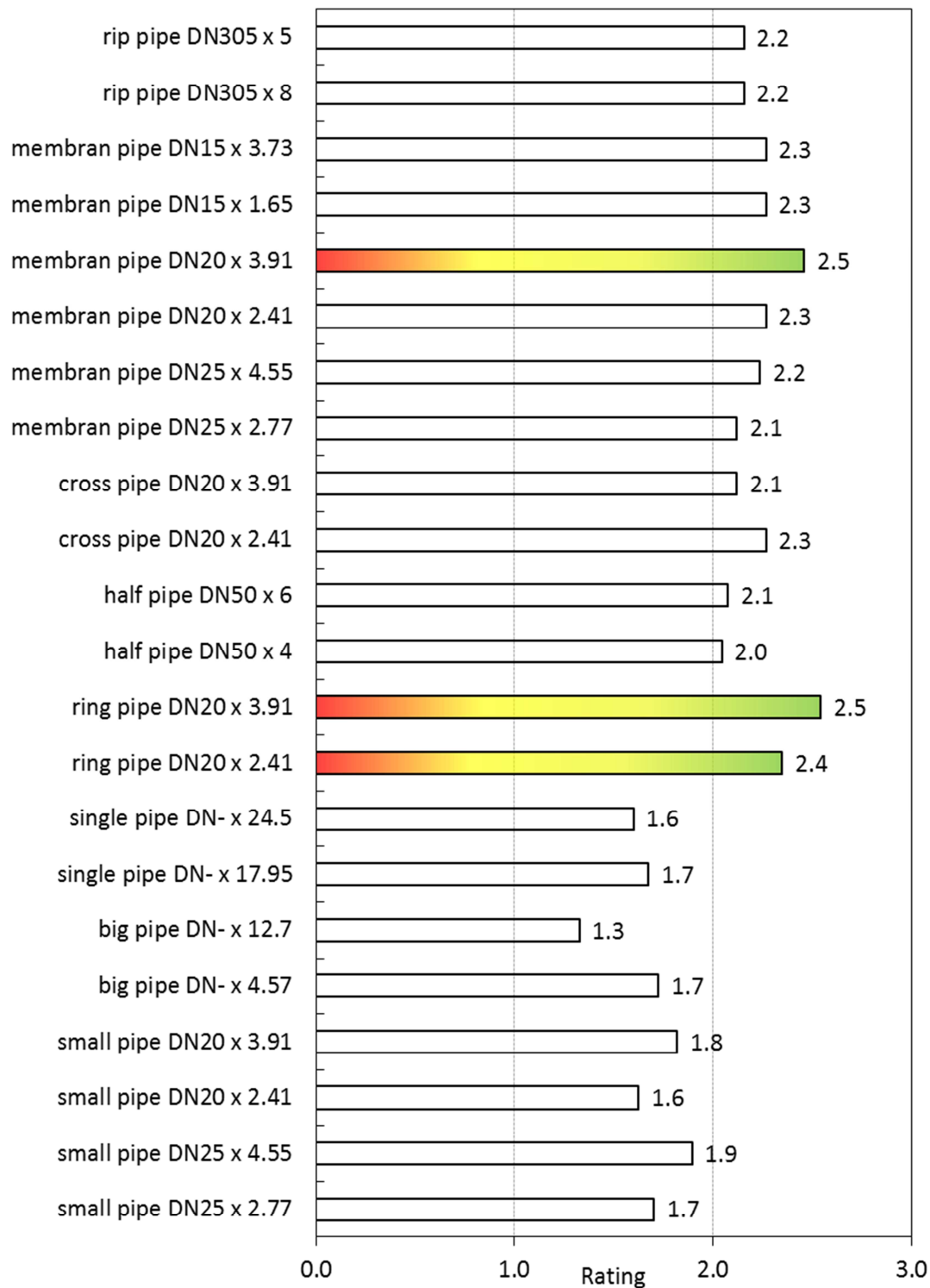


Figure 77: Results – Concept Rating



According to the last chapter and Figure 77, the following two concepts are in a close range to satisfy the requirements:

- Membrane Pipe (chapter 8.7 concept G)
- Ring Pipe (chapter 8.5 concept D)

Figure 78 shows the 3D-model of the installed APRS related to the concept Ring Pipe.

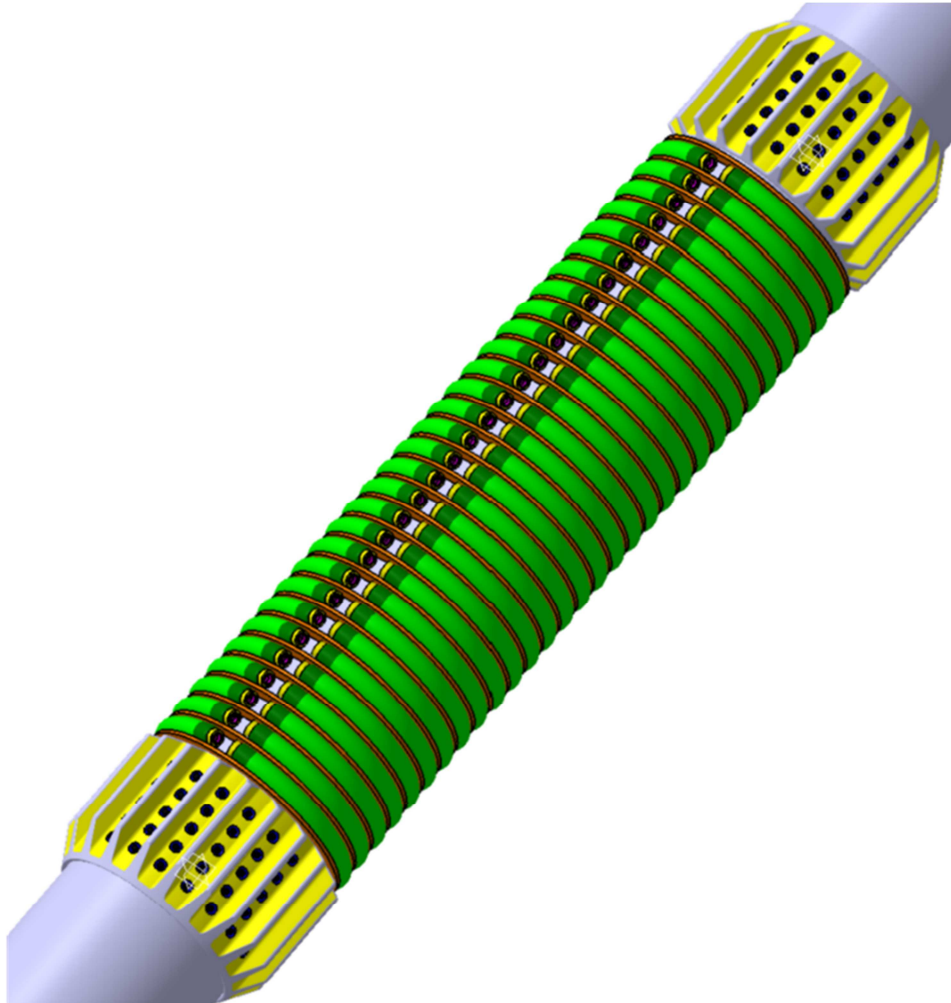


Figure 78: 3D Model Wellbore – Ring Pipe

Both ideas have similar advantages: the low material grade of the pressure chamber and the stiffness of the tool. The application spectrum for the APRS ranges from great depths and high temperatures with correspondingly low compensation volume to shallow depths of use with comparatively high compensation volumes. The simple and robust design of the pressure chamber allows for high working pressures and high temperature ranges. The adjustment of the working pressure on site is quick and easy. One principle of mounting the burst disc, denoted as item 4, to the pressure chamber, see item 1, is shown in detail in Figure 79 related to Figure 80 and Figure 81 for concept D – “Ring Pipe”.

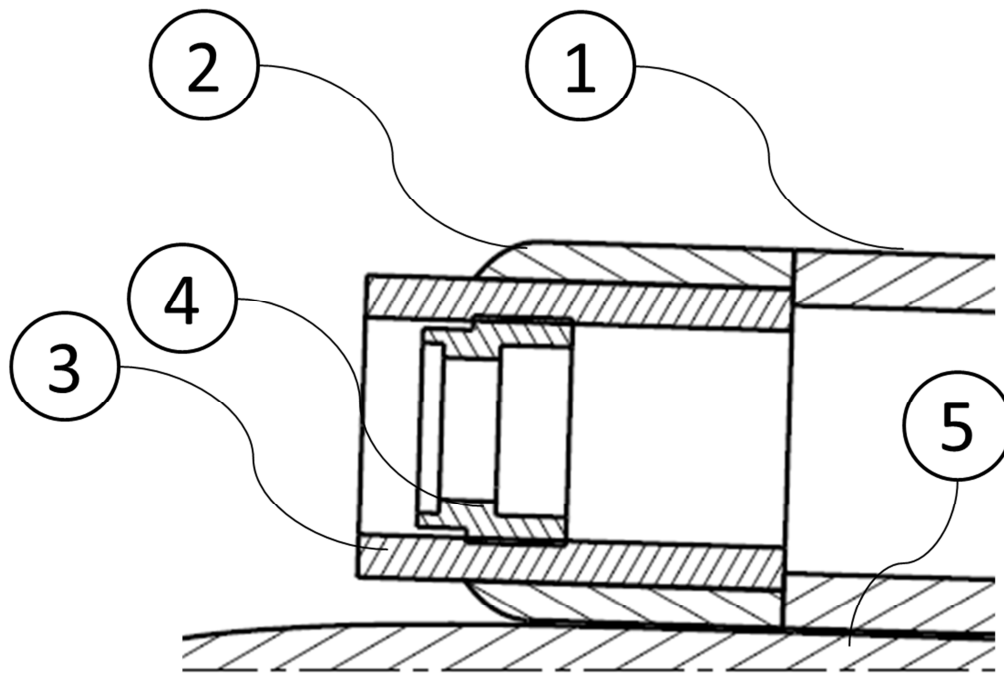


Figure 79: Detail View – Burst Disc Fixation

The principle of mounting the burst disc, see item 4, is for both concepts the same. A hole is drilled into the end cap, denoted as item 2. The diameter of the hole is dependent on the OD of the small pipe, shown as item 3. In this hole a small piece of a straight pipe, see item 3, is welded. Item 3 includes an internal thread to screw the burst disc, denoted as item 4. Dependent on the required diameter, it could be necessary to process the pipe mechanically before the tapped hole is manufactured. After welding the endcap, see item 2, and the small pipe, see item 3, together, the assembly is welded to the main pipe of the pressure chamber, denoted as item 1. This system has the big advantage that it uses standard fittings and pipes. Hence every dimension of the pressure chambers and endcaps is available. Further, if the dimensioning of the burst disc needs to be changed, only the inner diameter of the small pipe of the screw must be changed.

Figure 80 represents a detail of the assembled or mounted pressure chamber including the burst disc downhole. In this case the APRS is fixed a 9 5/8 in liner.

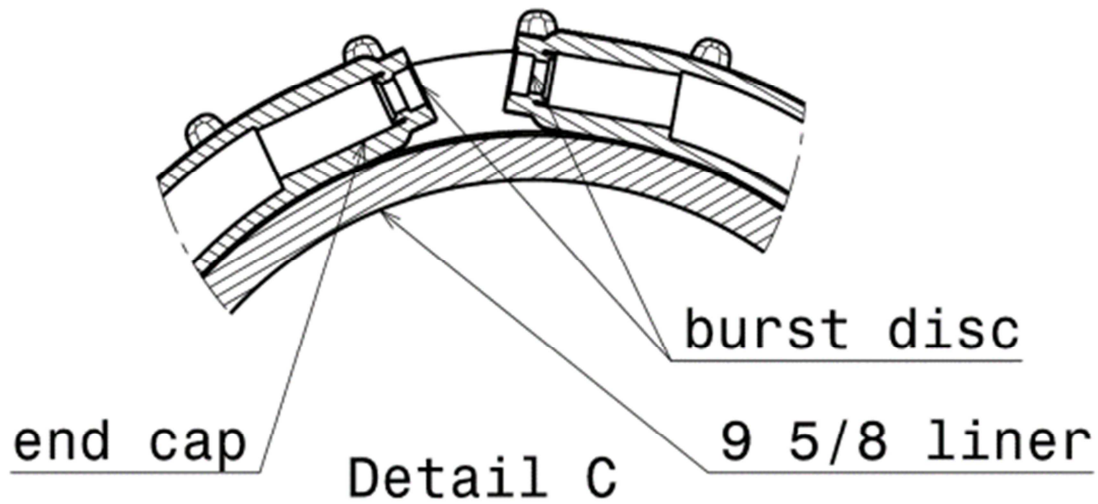


Figure 80: Detail C - Ring Pipe

Figure 81 shows again the required components for one pressure chamber, the numbers are linked to Figure 79.

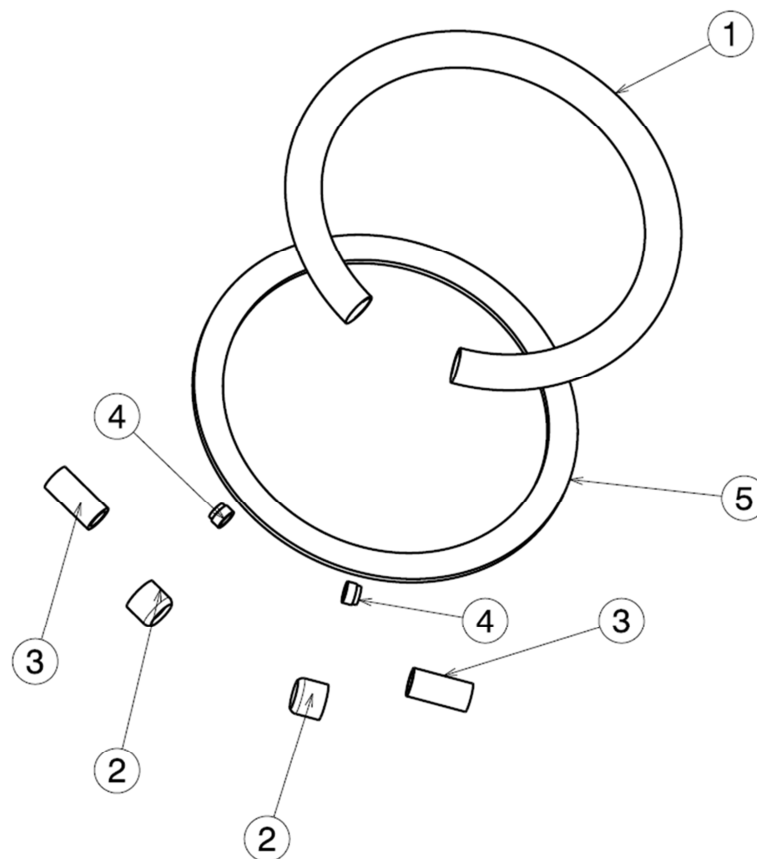


Figure 81: Assembly Ring Pipe

Item 5, see Figure 81, represents a distance plate used to weld the pressure chamber easily to the next pressure chamber. The distance plate is not essential, it is designed to simplify the welding process and can be also neglected.

The design of the fixing part also supports the usage at great depths. The fixing part, denoted as item 1 in Figure 82, is used to bring the APRS to the desired depth with little friction and without damage. The diameter of the Small Fix, shown as item 1 in Figure 82, is larger than the diameter of the pressure chamber, denoted as item 2 in Figure 82. Thus, the Small Fix acts as a protector of the pressure chamber. In addition, the comparatively narrow design of the Small Fix and the pressure chamber also supports the cementation process.

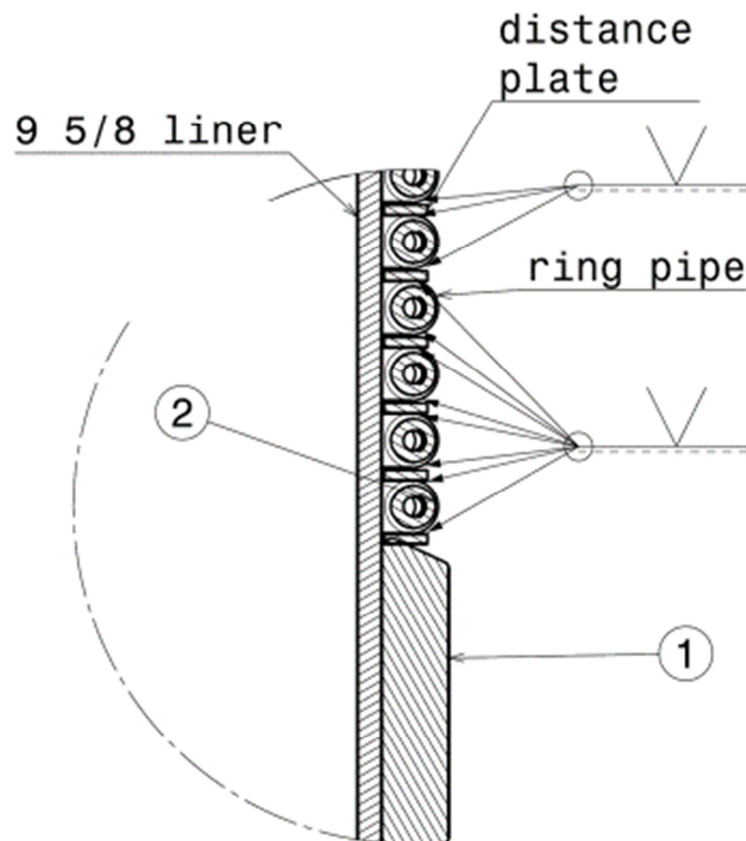


Figure 82: Detail D - Ring Pipe

The shape of the pressure chamber enables large compensation volumes while at the same time making the system robust. The adaptation of the system and the adjustment for different compensation volumes can be easily done by changing the number of used tools or the number of pipes used per tool. Due to the use of standardized pipes (according to: DIN, ISO, ASME) the essential elements of the pressure chamber, like wall thickness, diameter and material, can be adjusted quickly and easily.

The design and operation of the pressure chamber and the associated avoidance of moving components additionally ensures a cost-effective and less error-prone construction. Also, the minimized number of individual components leads to a reduced susceptibility to errors and at the same time reduces the assembly effort in the factory and at the place of use.

An open task is still the dimensioning of the pipe. According to Table 23, we can see that the concept was checked only for a few possible sizes. But the market has more to offer and therefore one of the next steps should be a detailed analysis of the best combination of

material grade, OD and wall thickness. Thus, it would probably also be a good point to increase the volume of the tool by decreasing the wall thickness and increasing the OD. But it must be mentioned that if the material grade is lowered, the manufacturing costs will drop. Accordingly, it would be possible that two tools with low material grade and high wall thickness and low OD might be much cheaper than using only one tool with a high material grade and lesser wall thickness.

Figure 83 represents the spectrum of realisable expansion volumes related to the material grade and therefore the wall thickness. In this case, the pressure chamber is based on a DN15 pipe with an OD of 21.3 mm. The stress mentioned on the plot is the necessary yield strength of the selected material, the safety factor of 1.5 is included in the calculation. This plot shows the design options which are possible and must be checked.

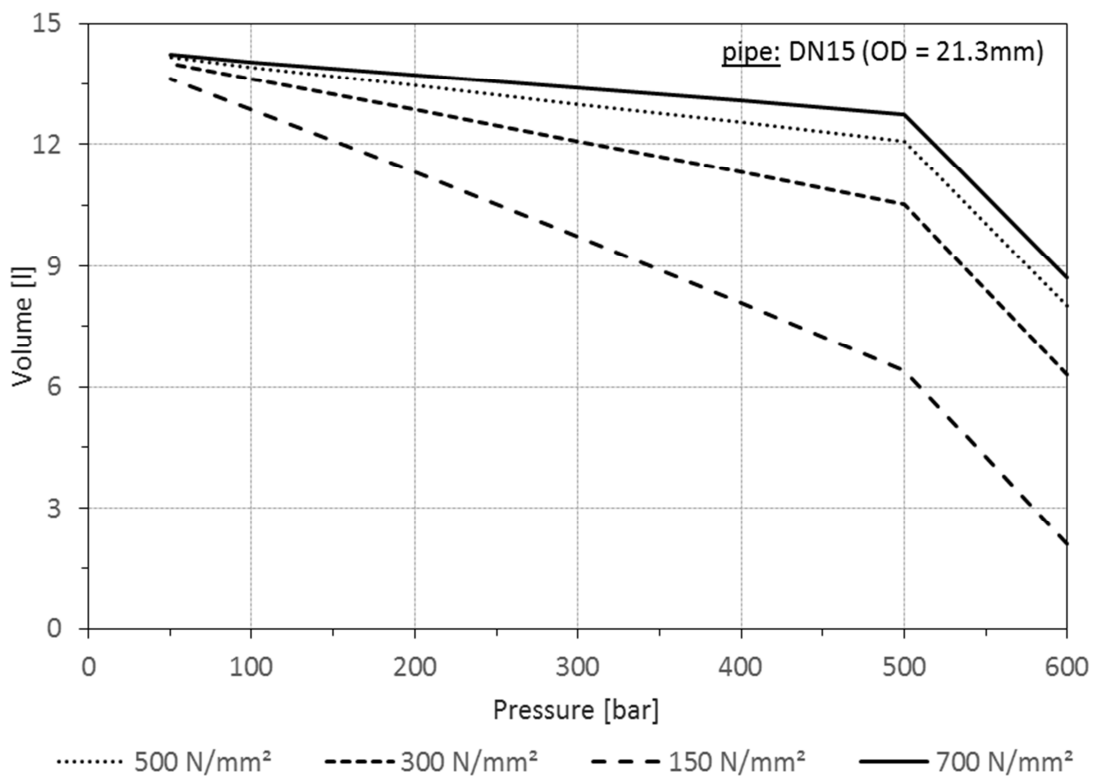


Figure 83: Expansion Volume Depending on the Material Selection

It should be mentioned that Table 23 only provides a possible direction based on the rating principle. The bases of the ratings are concept drawings, models and meshes with FEM-simulations to get an idea about the underlying problem of APB. But they are still conceptual studies and not final manufacturing drawings.

At this stage the concepts can be used for further development. The next steps would require a detailed construction of the concept, followed by FEM simulations to check if the concept can meet extra requirements. Requirements at this point means to define additional checks

and load scenarios to improve the functionality of the tool. This can include a stress check during installation as well as the proof of feasibility and economy in a detailed manner. In the concept phase, it seems to be the best choice to use the Ring Pipe concept, but also the Membrane Pipe is going in the right direction. Therefore, it would probably be useful to keep these concepts as a backup and try to improve them.

An essential point is the predefined pressure of 600 bar. The boundary conditions determine that the tool must withstand an outside pressure of 600 bar. This pressure is quite large and many wells would never touch this magnitude. Thus, it would be an opportunity to select the wall thickness and pipe diameter of the pressure chamber case sensitive. For instance it would be an option to design three pressure ratings: a low rating with 150 bar a medium level with 300 bar and high level with 600 bar, instead of only one with 600 bar. The fixing part will remain the same and only the pressure chamber is changed. It would be possible to choose for instance for a desired pressure of 300bar a completely different material and pipe dimension than for using it in a zone with only 150 bar external pressure.

This thesis shows that the relationship between available volume for the fluid expansion, the external pressure, the material of the pipe and the dimensions. Any change in one item affects the other intensely as seen in Figure 83. Hence, another option would still be to pressurize the chamber before installing it. Consequently, the differential pressure can be decreased. Thus, the wall thickness will decrease and the achievable volume within the pressure chamber can be increased.

## References

- [1] Deutsche Erdwärme, [https://www.foederal-erneuerbar.de/landesinfo/kategorie/erdwaerme/auswahl/414-installierte\\_thermis/bundesland/BY/sicht/diagramm/#goto\\_414](https://www.foederal-erneuerbar.de/landesinfo/kategorie/erdwaerme/auswahl/414-installierte_thermis/bundesland/BY/sicht/diagramm/#goto_414), Accessed May 10, 2019.
- [2] S. Eyerer, C. Schifflechner, S. Hofbauer et al., 2017, *Potential der hydrothermalen Geothermie zur Stromerzeugung in Deutschland*.
- [3] D. Lentsch, K. Dorsch, N. Sonnleitner et al., 2015, "Prevention of Casing Failures in Ultra-Deep Geothermal Wells (Germany)," in *Proceedings World Geothermal Congress: Drilling and Completion Technology*.
- [4] B. ZHANG, Z. GUAN, Y. SHENG et al., 2016, "Impact of wellbore fluid properties on trapped annular pressure in deepwater wells," *Petroleum Exploration and Development*, vol. 43, no. 5, pp. 869–875.
- [5] B. ZHOU, J. YANG, Z. LIU et al., 2015, "Mechanism of pressure management by injecting nitrogen in casing annulus of deepwater wells," *Petroleum Exploration and Development*, vol. 42, no. 3, pp. 422–426.
- [6] F. Yin and D. Gao, 2014, "Improved Calculation of Multiple Annuli Pressure Buildup in Subsea HPHT Wells," in *IADC/SPE Asia Pacific Drilling Technology Conference: Driving Sustainable Growth Through Technology and Innovation, 25-27 August 2014, Bangkok Convention Centre at CentralWorld, Bangkok, Thailand*, SPE, Richardson, Texas doi: 10.2118/170553-MS.
- [7] N. Sonnleitner, 2013, *Cementing Techniques for Geothermal Well Application in the Molasse Basin and Development of Adapted Practices*, Diplomarbeit, Montanuniversität, Leoben.
- [8] I. Müller and W. H. Müller, 2009, *Fundamentals of thermodynamics and applications: With historical annotations and many citations from Avogadro to Zermelo*, Springer Berlin Heidelberg, Berlin, Heidelberg. 9783540746454 doi: 10.1007/978-3-540-74648-5.
- [9] P. A. Tipler and G. Mosca, 2008, *Physics for scientists and engineers: Standard*, W.H. Freeman, New York, NY. 9781429201339.
- [10] P. Oudeman and M. Kerem, 2013, "Transient Behavior of Annular Pressure Build-up in HP/HT Wells," in *Abu Dhabi International Conference and Exhibition*, Society of Petroleum Engineers doi: 10.2118/88735-MS.
- [11] G. Dong and P. Chen, 2017, "A review of the evaluation methods and control technologies for trapped annular pressure in deepwater oil and gas wells," *Journal of Natural Gas Science and Engineering*, vol. 37, pp. 85–105.

- [12] D. Lentsch, "Internal ERDWERK document,".
- [13] C.S. McVay and R.E. Sweatman, 2007, *Annular pressure relief collar*.
- [14] C. P. Leach and A. J. Adams, 2013, "A New Method for the Relief of Annular Heat-Up Pressures," in *SPE Production Operations Symposium*, Society of Petroleum Engineers doi: 10.2118/25497-MS.
- [15] X. Z. Han, B. K. Gao, H. Q. Zhang et al., 2013, "Compressible Fluids Mitigation Effect Research in Deepwater Oil and Gas Well," *Advanced Materials Research*, 734-737, pp. 1165–1170.
- [16] M. L. Payne, D. Pattillo, R. Miller et al., 2013, "Advanced Technology Solutions for Next Generation HPHT Wells," in *International Petroleum Technology Conference*, International Petroleum Technology Conference doi: 10.2523/IPTC-11463-MS.
- [17] D. W. Bradford, D. G. Fritchie, D. H. Gibson et al., 2013, "Marlin Failure Analysis and Redesign: Part 1 - Description of Failure," *SPE Drilling & Completion*, vol. 19, no. 02, pp. 104–111.
- [18] J. Azzola, D. Tselepidakis, P. D. Pattillo et al., 2013, "Application of Vacuum Insulated Tubing to Mitigate Annular Pressure Buildup," *SPE Drilling & Completion*, vol. 22, no. 01, pp. 46–51.
- [19] W. CHU, J. SHEN, Y. YANG et al., 2015, "Calculation of micro-annulus size in casing-cement sheath-formation system under continuous internal casing pressure change," *Petroleum Exploration and Development*, vol. 42, no. 3, pp. 414–421.
- [20] T. Baumann, J. Bartels, M. Lafogler et al., 2017, "Assessment of heat mining and hydrogeochemical reactions with data from a former geothermal injection well in the Malm Aquifer, Bavarian Molasse Basin, Germany," *Geothermics*, vol. 66, pp. 50–60.
- [21] D. Rettenmaier, E. Gaucher, T. Kohl et al., 2013, "LOGRO - Langzeitbetrieb und Optimierung eines Geothermiekraftwerks in einem gekluftetporösen Reservoir im Oberrheingraben osen Reservoir im Oberrheingraben," *Technical Report KIT Karlsruhe*.
- [22] S. Regenspurg, E. Feldbusch, J. Byrne et al., 2015, "Mineral precipitation during production of geothermal fluid from a Permian Rotliegend reservoir," *Geothermics*, vol. 54, pp. 122–135.
- [23] D.L. Parkhurst and C.A.J. Appelo, 2013, *Description of input and examples for PHREEQC version 3: A computer program for speciation, batch-reaction, one-dimensional transport, and inverse geochemical calculations*.



- [24] C.A.J. Appelo, 2015, "Principles, caveats and improvements in databases for calculating hydrogeochemical reactions in saline waters from 0 to 200°C and 1 to 1000atm," *Applied Geochemistry*, vol. 55, pp. 62–71.
- [25] W. D. McCain, J. P. Spivey, and C. P. Lenn, 2011, *Petroleum reservoir fluid property correlations*, PennWell, Tulsa Okla. 1-593-70187-X.
- [26] W. D. McCain, 2013, "Reservoir-Fluid Property Correlations-State of the Art (includes associated papers 23583 and 23594 )," *SPE Reservoir Engineering*, vol. 6, no. 02, pp. 266–272.
- [27] R. A. Fine and F. J. Millero, 1973, "Compressibility of water as a function of temperature and pressure," *The Journal of Chemical Physics*, vol. 59, no. 10, pp. 5529–5536.
- [28] Petrowiki, [https://petrowiki.org/Produced\\_water\\_formation\\_volume\\_factor](https://petrowiki.org/Produced_water_formation_volume_factor), Accessed May 10, 2019.
- [29] elfab, <https://www.elfab.com/de/oem-and-rupture-disc/oe2/>, Accessed May 10, 2019.
- [30] VAM, [http://www.vamservices.com/technical\\_information/connection\\_ds.aspx](http://www.vamservices.com/technical_information/connection_ds.aspx), Accessed May 10, 2019.
- [31] W. Stadlmayr, 2018, *Thermodynamik - nicht nur für Nerds: Grundlagen der Thermodynamik mit Übungen und Beispielen*, Springer Vieweg, Wiesbaden. 9783658232900 doi: 10.1007/978-3-658-23291-7.
- [32] J. Feßmann and H. Orth, 2002, *Angewandte Chemie und Umwelttechnik für Ingenieure: Handbuch für Studium und betriebliche Praxis*, ecomed Sicherheit, Landsberg/Lech. 360968352X.
- [33] Schweizer-FN, [https://www.schweizer-fn.de/rohr/festigkeit/festigkeit.php#vergleichsspannung\\_bieg](https://www.schweizer-fn.de/rohr/festigkeit/festigkeit.php#vergleichsspannung_bieg), Accessed May 10, 2019.
- [34] V. Läßle, 2008, *Lösungsbuch zur Einführung in die Festigkeitslehre: Aufgaben, ausführliche Lösungswege, Formelsammlung*. 9783834804525.
- [35] S. Schwaigerer, 1978, *Festigkeitsberechnung im Dampfkessel-, Behälter- und Rohrleitungsbau*, Springer, Berlin, Heidelberg. 9783540087458 doi: 10.1007/978-3-662-11735-4.
- [36] Engineers edge, [https://www.engineersedge.com/material\\_science/von\\_mises.html](https://www.engineersedge.com/material_science/von_mises.html), Accessed May 10, 2019.
- [37] catiadoc.free, "Analyzing Mesh Quality," [http://catiadoc.free.fr/online/fmsug\\_C2/fmsugut0604.htm](http://catiadoc.free.fr/online/fmsug_C2/fmsugut0604.htm), Accessed February 22, 2019.

- [38] W. Klepzig, "CATIA V5 – FEM-Simulation: Ergänztes Skript zum früheren CAD-Praktikum „Aufbaukurs CATIA-FEM“ an der Westsächsischen Hochschule Zwickau," Hochschule Zwickau, [https://wwwstud.fh-zwickau.de/wk/CATIA\\_FEM/CATIA-FEM-Skript\\_2016.pdf](https://wwwstud.fh-zwickau.de/wk/CATIA_FEM/CATIA-FEM-Skript_2016.pdf), Accessed February 22, 2019.
- [39] Deutsche Edelstahlwerke, <https://www.dew-stahl.com/produkte/>, Accessed May 10, 2019.
- [40] ThyssenKrupp AG, <https://www.thyssenkrupp-steel.com/en/products/products-overview.html>, Accessed May 10, 2019.
- [41] Sandvik, <https://www.materials.sandvik/en/materials-center/material-datasheets/>, Accessed May 10, 2019.
- [42] SSAB, <https://www.ssab.de/produkte/warenzeichen/strenx/strenx-product-overview>, Accessed May 10, 2019.
- [43] Salzgitter Gruppe, <http://www.salzgitter-mannesmann-stahlhandel.com/products/index.php>, Accessed May 10, 2019.
- [44] Casing Centralizer, <http://www.casingcentralizer.com/news/casing-centralizer-selection.html>, Accessed May 10, 2019.
- [45] Centek Group, <https://www.centekgroup.com/our-products/premium/stop-collars/stop-collars/>, Accessed May 10, 2019.
- [46] DWT GmbH, [https://www.engineersedge.com/material\\_science/von\\_mises.htm](https://www.engineersedge.com/material_science/von_mises.htm), Accessed May 10, 2019.
- [47] C.A.J. Appelo, D. L. Parkhurst, and V.E.A. Post, 2014, "Equations for calculating hydrogeochemical reactions of minerals and gases such as CO<sub>2</sub> at high pressures and temperatures," *Geochimica et Cosmochimica Acta*, vol. 125, pp. 49–67.
- [48] T. Hörbrand, 2017, *Comparison of Hydrogeochemical Model Approaches for Problems in Deep Geothermal Energy: Comparison of Hydrogeochemical Model Vergleich von hydrogeochemischen Modellansätzen für Fragestellungen der tiefen Geothermie*, Masterarbeit, Technischen Universität München, München.
- [49] G. S. Kell, 1975, "Density, thermal expansivity, and compressibility of liquid water from 0.deg. to 150.deg. Correlations and tables for atmospheric pressure and saturation reviewed and expressed on 1968 temperature scale," *Journal of Chemical & Engineering Data*, vol. 20, no. 1, pp. 97–105.
- [50] RFF, <https://www.rff.de/de/service/mediathek--downloads/>, Accessed May 10, 2019.

## List of Tables

Table 1: Boundary Conditions – Temperature and Pressure [12] .....	14
Table 2: Artificial System .....	16
Table 3: Fluid Compositions .....	16
Table 4: Coefficients for Equation of State [25].....	18
Table 5: Density of Water $\rho(p, T)$ .....	19
Table 6: Volume of Trapped Fluid .....	21
Table 7: Mean values for $\gamma$ and $\kappa$ .....	22
Table 8: Results of Expansion Volume Calculation.....	27
Table 9: Reduction of Expansion Volume due to an Allowed Pressure Increase ( $\Delta p$ ).....	35
Table 10: Compressed Volume in Pressure Chamber.....	38
Table 11: Residual Error.....	46
Table 12: Material and Yield Strength.....	50
Table 13: Fixing Systems – Link to Concepts .....	58
Table 14: Important Parameters – Small Pipe .....	63
Table 15: Important Parameters – Big Pipe .....	66
Table 16: Important Parameters – Single Pipe .....	68
Table 17: Important Parameters – Half Pipe.....	69
Table 18: Important Parameters – Rip Pipe.....	71
Table 19: Important Parameters – Ring Pipe.....	75
Table 20: Important Parameters – Cross Pipe.....	77
Table 21: Important Parameters – Membrane Pipe .....	80
Table 22: Rating Example .....	81
Table 23: Overview Rating .....	82
Table 24: Aqueous Solution Composition of the Production Well in Bruchsal (table compiled by: [48]; according to: [21]) .....	102
Table 25: Aqueous Solution Composition of the Well Groß Schönebeck (table compiled by: [48]; according to: [22]).....	103
Table 26: Aqueous Solution Composition of the Well Pullach [20].....	103
Table 27: Volume Properties of Ordinary Water at 1atm (table compiled by: [49]) .....	104
Table 28: Standard Pipe Dimensions [50].....	108

---

Table 29: Rating Concepts - Detail - Part 1 ..... 109

Table 30: Rating Concepts - Detail - Part 2 ..... 110

Table 31: Rating Concepts - Detail - Part 3 ..... 111

Table 32: Rating Concepts - Detail - Part 4 ..... 112

Table 33: Rating Concepts - Detail - Part 5 ..... 113

## List of Figures

Figure 1: Camera Inspection of the Casing Collapse [7].....	1
Figure 2: Picture from the Camera and Pulled Casing String [7].....	2
Figure 3: Cross-Section Annulus .....	3
Figure 4: APB without APRS .....	4
Figure 5: APB with APRS .....	4
Figure 6: Schematic of Installed Rupture Disc [11] .....	7
Figure 7: Rupture Disc at Well Side [12].....	7
Figure 8: Schematic of Installed Annular Pressure Relief Collar [11].....	8
Figure 9: Schematic of Installed Foam [11].....	9
Figure 10: Crushable Foam [16].....	9
Figure 11: Well Schematic [12].....	11
Figure 12: Installation Examples APRS .....	12
Figure 13: Clearance in Well .....	15
Figure 14: Volume Expansion Depending on the Composition of the Fluid.....	17
Figure 15: Cross Section of Annulus .....	20
Figure 16: Thermal Expansion Coefficient of Pure Water .....	23
Figure 17: $\gamma(T)$ - Trendcurve.....	24
Figure 18: Volume Expansion at Position B.....	28
Figure 19: Pressure Increase Related to the Initial Downhole Temperature .....	30
Figure 20: Function of APRS – Initial Stage.....	31
Figure 21: Function of APRS – Start of Production.....	32
Figure 22: Rupture or Burst disc [29].....	33
Figure 23: Volume Expansion at Constant Pressure .....	34
Figure 24: Reduction of Needed Volume due to the Additional Pressure Increase .....	36
Figure 25: Influence of the Differential Pressure and Wall Thickness .....	37
Figure 26: Schematic of the Primary Load Scenario [33].....	41
Figure 27: Input Material Properties .....	43
Figure 28: Mesh Ring Pipe .....	43
Figure 29: Mesh Report - Bad Quality .....	44
Figure 30: Mesh Report – Good Quality .....	44

Figure 31: Schematic Model Set Up .....	45
Figure 32: Screenshot of Model Set Up.....	46
Figure 33: Deformation Simulation .....	47
Figure 34: Screenshot of Stress Check .....	48
Figure 35: Output Simulation Result - Stress Check CATIA .....	49
Figure 36: Screenshot of Manual Stress Calculation .....	51
Figure 37: Detail of Figure 85 .....	51
Figure 38: Dependency of Material Selection on the Pressure Chamber Volume .....	52
Figure 39: Volume Pressure Chamber – Concepts.....	53
Figure 40: Schematic if the Tool Occupies not the Full Cross-Section of the Annulus .....	54
Figure 41: Schematic if the Tool Occupies the Full Cross-Section of the Annulus .....	55
Figure 42: Wall Thickness in Depending on the Material Selection.....	56
Figure 43: Detail - Wall Thickness in Depending on the Material Selection.....	57
Figure 44: 3D - Small Fix.....	59
Figure 45: Side View - Small Fix.....	59
Figure 46: Section Cut B – Small Fix .....	59
Figure 47: Fixing Concept - Small Fix.....	59
Figure 48: Centralizer and Stop Collar [44].....	60
Figure 49: Stop Collar [45].....	60
Figure 50: 3D-Model of Small Fix - Improved .....	60
Figure 51: Manufacturing Drawing of Small Fix - Improved .....	60
Figure 52: 3D View - Big Fix.....	61
Figure 53: Section Cut - Big Fix.....	61
Figure 54: 3D View - Small Pipe .....	62
Figure 55: 3D View - Big Pipe.....	64
Figure 56: Section Cut - Big Pipe .....	64
Figure 57: 3D View - Single Pipe .....	66
Figure 58: Section Cut - Single Pipe.....	67
Figure 59: 3D View - Half Pipe .....	68
Figure 60: Cross-Section Cut - Half Pipe.....	69
Figure 61: 3D View - Rip Pipe .....	70

---

Figure 62: Cross-Section Cut - Rip Pipe .....	71
Figure 63: Ring Pipe - Single Part .....	72
Figure 64: 3D View - Ring Pipe .....	72
Figure 65: Assembly Ring Pipe .....	73
Figure 66: Section Cut - Ring Pipe .....	74
Figure 67: Side View - Ring Pipe .....	74
Figure 68: 3D View - Cross Pipe .....	75
Figure 69: Cross-Section Cut - Cross Pipe .....	76
Figure 70: 3D – Screenshot Cross Pipe .....	76
Figure 71: Section Cut - Cross Pipe .....	77
Figure 72: 3D View - Membrane Pipe.....	78
Figure 73: Cross-Section Cut - Membrane Pipe .....	78
Figure 74: Detail G - Membrane Pipe .....	79
Figure 75: Detailed Picture of Membrane Wall [46].....	80
Figure 76: Steam Boiler – Foundation of Membrane Pipe [46].....	80
Figure 77: Results – Concept Rating .....	83
Figure 78: 3D Model Wellbore – Ring Pipe.....	84
Figure 79: Detail View – Burst Disc Fixation .....	85
Figure 80: Detail C - Ring Pipe .....	86
Figure 81: Assembly Ring Pipe .....	86
Figure 82: Detail D - Ring Pipe .....	87
Figure 83: Expansion Volume Depending on the Material Selection.....	88
Figure 84: Example of Material Datasheet Provided by the Manufacturer [40].....	106
Figure 85: Material Selection – Full Size .....	107

## Abbreviations

2D	two dimensional
3D	three dimensional
APB	annular pressure build up
APRS	annular pressure relief system
CAD	computer aided design
DN	nominal diameter
Eq	equation
FEM	finite element method
FVF	formation volume factor
HP	high pressure
HT	high temperature
ID	inner diameter
max	maximal
MD	measured depth
min	minimal
OD	outer diameter
SF	safety factor
STB	stock tank barrels
TAP	trapped annular pressure
TVD	total vertical depth



## Nomenclature

$a(T)$	temperature depended factor of $\rho_w(T, 70MPa)$ , $E_w(T)$ , $F_w(T)$
$c_w(T,p)$	compressibility of pure water ( $MPa^{-1}$ )
$d_{i,outer, csg}$	ID of the outer casing (mm)
$d_{o,inner, csg}$	OD of the inner casing/liner (mm)
$dT$	temperature change in the annuls ( $^{\circ}C$ )
$dV$	volume change due to temperature change ( $mm^3$ , $m^3$ )
$h$	height of the fluid column in the annuls (mm, m)
$l_{chamber}$	length of the pressure chamber (mm, m)
$m$	the mass of the fluid (kg)
$n$	number of moles of the gas (mol)
$p$	pressure (bar, Pa, MPa, psia)
$p_i$	external (outer) pressure acting on the pipe (MPa)
$p_o$	internal (inner) pressure acting on the pipe (MPa)
$\rho_o$	pressure load at the outside of the pipe (MPa)
$R$	ideal gas constant ( $J K^{-1} mol^{-1}$ )
$r_i$	inner radius of the pipe (mm, m)
$r_o$	outer radius of the pipe (mm, m)
$t$	wall thickness of the pipe or of the pressure chamber (mm, m)
$T$	temperature (K, $^{\circ}C$ or $^{\circ}F$ )
$T_f$	end temperature or finale temperature of the fluid ( $^{\circ}C$ )
$T_i$	initial temperature of the fluid ( $^{\circ}C$ )
$V$	volume ( $mm^3$ , $m^3$ )
$V_{ann}$	annular volume (initial volume of fluid $V_i$ ) ( $mm^3$ , $m^3$ )
$V_{chamber}$	available volume for fluid expansion within the pressure chamber ( $mm^3$ , $m^3$ )
$V_f$	final volume of fluid (after expansion) ( $mm^3$ , $m^3$ )
$V_i$	initial volume ( $mm^3$ , $m^3$ )
$\gamma$	thermal expansion coefficient ( $K^{-1}$ )
$\kappa$	isothermal compressibility of the annular liquid ( $Pa^{-1}$ )
$\rho(T,p)$	density of fluid dependent on pressure and temperature ( $kg/m^3$ )

---

$\rho_w(T, \rho)$	density of pure water, $\rho_w(T, 70MPa)$ a reference pressure of 70MPa (g/cm <sup>3</sup> )
$\sigma$	yield strength of the material (N/mm <sup>2</sup> )
$\sigma_a$	axial stress (N/mm <sup>2</sup> )
$\sigma_r$	radial stress (N/mm <sup>2</sup> )
$\sigma_t$	tangential stress (N/mm <sup>2</sup> )
$\sigma_v$	van Mises equivalent stress (N/mm <sup>2</sup> )
$\Delta p$	pressure change due to temperature change (MPa, bar)
$\Delta V_{ann}$	change in annular volume due to thermal expansion (mm <sup>3</sup> , m <sup>3</sup> )
$\Delta V_{leak}$	amount of fluid leaking off the annulus while temperature increase (mm <sup>3</sup> , m <sup>3</sup> )

## Appendices

### Appendix A

$$V_{p,T}^0 = C \left[ a_1 + \frac{a_2}{\psi + p} + \frac{a_3}{T - \sigma} + \frac{a_4}{(\psi + p)(T - \sigma)} - \omega Q + \left( \frac{1}{\epsilon} - 1 \right) \frac{\partial \omega}{\partial p} \right] \quad (\text{Eq. 29})$$

With C being a conversion factor of 41.84 bar cm<sup>3</sup> cal<sup>-1</sup>

$$V_{m(T,p,l)}^0 = C \left[ \frac{b_1 * 0.1 + b_2 * 100}{\psi + p} + \frac{b_3}{T - \sigma} + \frac{b_4 * 10^4}{(\psi + p)(T - \sigma)} - \omega Q + \left( \frac{1}{\epsilon} - 1 \right) \frac{\partial \omega}{\partial p} \right] + \frac{z^2}{2A_v * f(I^{0.5})} + \frac{i_1 + i_2}{T - \sigma} + i_3(T - \sigma) * I^{i4} \quad (\text{Eq. 30})$$

The first line corresponds to the Helgeson–Kirkham–Flowers formalism with neglection the  $\left( \frac{1}{\epsilon} - 1 \right) \frac{\partial \omega}{\partial p}$  terms in the software, while the second line is in addition to it introduced by [47].

Table 24: Aqueous Solution Composition of the Production Well in Bruchsal (table compiled by: [48]; according to: [21])

	sample date	BRS-1109 03.11.2009	BRS-1110 13.10.2011	BRS-0312 20.03.2012	BRS-0213 08.02.2013	BRS-0213-2 09.02.2013
pH		n.d.	5.18	5.14	4.78	5.18
conductivity	mS/cm	n.d.	125.0	149.5	157.1	125
T	°C	n.d.	42.6	29.1	20.2	42.6
cations						
Li <sup>+</sup>	mg/L	157	148	157	160	156
Na <sup>+</sup>	mg/L	35800	35500	39200	35700	35600
K <sup>+</sup>	mg/L	4100	3310	3310	3390	3790
Ca <sup>2+</sup>	mg/L	7820	7500	7580	7510	7590
Mg <sup>2+</sup>	mg/L	371	368	385	390	350
Sr <sup>2+</sup>	mg/L	383	354	366	372	347
Ba <sup>2+</sup>	mg/L	11.0	10.0	9.9	10.7	10.4
Fe <sup>2+</sup>	mg/L	50	52	53	50	52
anions						
Cl <sup>-</sup>	mg/L	73700	74110	75050	75120	76380
Br <sup>-</sup>	mg/L	326	302	318	320	316
SO <sub>4</sub> <sup>2-</sup>	mg/L	302	330	325	386	347
HCO <sub>3</sub> <sup>-</sup>	mg/L	342	375	317	312	336
CBE	%	0.25	-1.30	2.02	-1.65	-2.30

Table 25: Aqueous Solution Composition of the Well Groß Schönebeck (table compiled by: [48]; according to: [22])

	sample	PW 2013-1	PW 2013-2	PW 2013-3	PW2014-1	PW2014-2
pH		7.6	7.6	7.7	6.3	7.1
conductivity	mS/cm	n.d.	n.d.	n.d.	n.d.	n.d.
T	°C	n.d.	n.d.	n.d.	n.d.	n.d.
cations						
Li <sup>+</sup>	mg/L	219	203	215	237	212
Na <sup>+</sup>	mg/L	37700	38000	39600	40900	33600
K <sup>+</sup>	mg/L	3600	2620	3120	2960	2560
Ca <sup>2+</sup>	mg/L	54800	52900	53800	51200	45400
Mg <sup>2+</sup>	mg/L	395	344	382	364	233
Sr <sup>2+</sup>	mg/L	1540	1520	1570	1630	1290
Ba <sup>2+</sup>	mg/L	58.8	44.7	47	31.8	30
Mn <sup>2+</sup>	mg/L	215	167	148	222	131
Fe <sup>2+</sup>	mg/L	174	95.3	63.5	51.5	47.1
anions						
Cl <sup>-</sup>	mg/L	160000	142000	144000	155400	138300
SO <sub>4</sub> <sup>2-</sup>	mg/L	190	144	175	80.5	94.3
HCO <sub>3</sub> <sup>-</sup>	mg/L	n.d.	n.d.	n.d.	n.d.	n.d.
CBE	%	0.63	5.29	6.02	1.50	-0.35

Table 26: Aqueous Solution Composition of the Well Pullach [20]

Hydrochemical composition of wells Th1a and Th2.

	Th1a		Th2	
	2005	2006–2012		2004
		Mean	Std. dev.	
	(mmol/L)	(mmol/L)	(mmol/L)	(mmol/L)
pH	6.42	6.67	0.36	6.52
Na <sup>+</sup>	6.59	10.4	0.66	20.05
K <sup>+</sup>	1.16	0.83	0.06	2.48
Mg <sup>2+</sup>	3.17	0.21	0.022	1.83
Ca <sup>2+</sup>	16.56	1.10	0.11	6.94
Cl <sup>-</sup>	23.55	7.53	0.60	24.58
SO <sub>4</sub> <sup>2-</sup>	0.35	0.30	0.082	1.36
HCO <sub>3</sub> <sup>-</sup>	4.80	5.7	0.43	5.35

## Appendix B

Table 27: Volume Properties of Ordinary Water at 1atm (table compiled by: [49])

Table III. Volume Properties of Ordinary Water at 1 Atm<sup>a</sup>

$t, ^\circ\text{C},$ IPTS-68	$\rho, \text{kg m}^{-3},$ Equation 16	$10^4 \alpha, \text{K}^{-1},$ Equation 16	$10^4 \kappa_T/\text{bar}^{-1}$		$t, ^\circ\text{C},$ IPTS-68	$\rho, \text{kg m}^{-3},$ Equation 16	$10^4 \alpha, \text{K}^{-1},$ Equation 16	$10^4 \kappa_T/\text{bar}^{-1}$	
			Equation 20	Equation 21				Equation 20	Equa
-30	983.854	-1400.0	80.79		34	994.3715	337.48	44.4956	
-25	989.585	-955.9	70.94		35	994.0319	345.73	44.4404	
-20	993.547	-660.6	64.25		36	993.6842	353.86	44.3903	
-15	996.283	-450.3	59.44		37	993.3287	361.88	44.3452	
-10	998.117	-292.4	55.83		38	992.9653	369.79	44.3051	
-9	998.395	-265.3	55.22		39	992.5943	377.59	44.2697	
-8	998.647	-239.5	54.64		40	992.2158	385.30	44.2391	
-7	998.874	-214.8	54.08		41	991.8298	392.91	44.2131	
-6	999.077	-191.2	53.56		42	991.4364	400.43	44.1917	
-5	999.256	-168.6	53.06		43	991.0358	407.85	44.1747	
-4	999.414	-146.9	52.58		44	990.6280	415.19	44.1620	
-3	999.550	-126.0	52.12		45	990.2132	422.45	44.1536	
-2	999.666	-106.0	51.69		46	989.7914	429.63	44.1494	
-1	999.762	-86.7	51.28		47	989.3628	436.73	44.1494	
0	999.8395	-68.05	50.8850		48	988.9273	443.75	44.1533	
1	999.8985	-50.09	50.5091		49	988.4851	450.71	44.1613	
2	999.9399	-32.74	50.1505		50	988.0363	457.59	44.1732	
3	999.9642	-15.97	49.8081		51	987.5809	464.40	44.189	
4	999.9720	0.27	49.4812		52	987.1190	471.15	44.209	
5	999.9638	16.00	49.1692		53	986.6508	477.84	44.232	
6	999.9402	31.24	48.8712		54	986.1761	484.47	44.259	
7	999.9015	46.04	48.5868		55	985.6952	491.04	44.290	
8	999.8482	60.41	48.3152		56	985.2081	497.55	44.324	
9	999.7808	74.38	48.0560		57	984.7149	504.01	44.362	
10	999.6996	87.97	47.8086		58	984.2156	510.41	44.403	
11	999.6051	101.20	47.5726		59	983.7102	516.76	44.448	
12	999.4974	114.08	47.3474		60	983.1989	523.07	44.496	
13	999.3771	126.65	47.1327		61	982.6817	529.32	44.548	
14	999.2444	138.90	46.9280		62	982.1586	535.53	44.603	
15	999.0996	150.87	46.7331		63	981.6297	541.70	44.662	
16	998.9430	162.55	46.5475		64	981.0951	547.82	44.723	
17	998.7749	173.98	46.3708		65	980.5548	553.90	44.788	
18	998.5956	185.15	46.2029		66	980.0089	559.94	44.857	
19	998.4052	196.08	46.0433		67	979.4573	565.95	44.928	
20	998.2041	206.78	45.8918		68	978.9003	571.91	45.003	
21	997.9925	217.26	45.7482		69	978.3377	577.84	45.081	
22	997.7705	227.54	45.6122		70	977.7696	583.74	45.162	
23	997.5385	237.62	45.4835		71	977.1962	589.60	45.246	
24	997.2965	247.50	45.3619		72	976.6173	595.43	45.333	
25	997.0449	257.21	45.2472		73	976.0332	601.23	45.424	
26	996.7837	266.73	45.1392		74	975.4437	607.00	45.517	
27	996.5132	276.10	45.0378		75	974.8490	612.75	45.614	
28	996.2335	285.30	44.9427		76	974.2490	618.46	45.714	
29	995.9448	294.34	44.8537		77	973.6439	624.15	45.817	
30	995.6473	303.24	44.7707		78	973.0336	629.82	45.922	
31	995.3410	312.00	44.6935		79	972.4183	635.46	46.031	
32	995.0262	320.63	44.6221		80	971.7978	641.08	46.143	
33	994.7030	329.12	44.5561		81	971.1723	646.67	46.258	

## Appendix C

```
Function rho_water(T_C, p_MPa As Double)
'T_C is temp in grad celsius
'p_MPa is pressure in MPa
'rho_water is density in kg/m³

Dim a11, a21, a31, a41, a51, a12, a22, a32, a42, a52, a13, a23, a33, a43,
    a53 As Double
Dim rho_T70, Ew, Fw, cw, Iw_T70, Iw_T_p As Double

a11 = -0.127213
a21 = 0.645486
a31 = 1.03265
a41 = -0.070291
a51 = 0.639589

a12 = 4.221
a22 = -3.478
a32 = 6.221
a42 = 0.5182
a52 = -0.4405

a13 = -11.403
a23 = 29.932
a33 = 27.952
a43 = 0.20684
a53 = 0.3768

rho_T70 = (a11 * (T_C / 100) ^ 2 + a21 * (T_C / 100) + a31) / (a41 * (T_C
    / 100) ^ 2 + a51 * (T_C / 100) + 1)
Ew = (a12 * (T_C / 100) ^ 2 + a22 * (T_C / 100) + a32) / (a42 * (T_C /
    100) ^ 2 + a52 * (T_C / 100) + 1)
Fw = (a13 * (T_C / 100) ^ 2 + a23 * (T_C / 100) + a33) / (a43 * (T_C /
    100) ^ 2 + a53 * (T_C / 100) + 1)
cw = (1 / 70) * 1 / (Ew * (p_MPa / 70) + Fw)
Iw_T70 = Log(Ew + Fw) / Ew
Iw_T_p = Log(Ew * p_MPa / 70 + Fw) / Ew

rho_water = rho_T70 * Exp(Iw_T_p - Iw_T70) * 1000

End Function
```

## Appendix D

Mindestwerte der 0,2% Dehngrenze bei erhöhten Temperaturen													
Erzeugnis	Erzeugnisdicke mm		0,2% Dehngrenze bei der Temperatur °C										
	über	bis	50	100	150	200	250	300	350	400	450	500	
			N/mm <sup>2</sup> min.										
P		16	273	264	250	233	213	194	175	159	147	141	
		16	40	268	259	245	228	209	190	172	156	145	139
		40	60	258	250	236	220	202	183	165	150	139	134
		60	100	238	230	218	203	186	169	153	139	129	123
		100	150	218	211	200	186	171	155	140	127	118	113
		150	250	208	202	191	178	163	148	134	121	113	108
T <sub>s</sub>		60		243	237	224	205	173	159	156	150	146	

Anhaltangaben über das Langzeitverhalten bei hohen Temperaturen												
Temperatur °C	1% Zeitdehngrenze <sup>1)</sup> für				Zeitstandfestigkeit <sup>2)</sup> für							
	10 000 h		100 000 h		10 000 h		100 000 h		200 000 h		250 000 h	
	N/mm <sup>2</sup>		N/mm <sup>2</sup>		N/mm <sup>2</sup>		N/mm <sup>2</sup>		N/mm <sup>2</sup>		N/mm <sup>2</sup>	
	P	T <sub>s</sub>	P	T <sub>s</sub>	P	T <sub>s</sub>	P	T <sub>s</sub>	P	T <sub>s</sub>	P	T <sub>s</sub>
450	216		167		298	298	239	236	217	218		210
460	199		146		273	273	208	205	188	188		179
470	182		126		247	247	178	176	159	158		148
480	166		107		222	221	148	149	130	129		122
490	149		89		196	196	123	124	105	105		98
500	132		73		171	171	101	102	84	84		78
510	115		59		147	148	81	83	69	67		63
520	99		46		125	125	66	65	55	53		50
530	84		36		102	104	53	51	45	42		38
540						84		40		34		
550						64		32		25		

1) Die auf den Ausgangsquerschnitt bezogene Spannung, die nach 10 000 oder 100 000 h zu einer bleibenden Dehnung von 1% führt.  
 2) Die auf den Ausgangsquerschnitt bezogene Spannung, die nach 10 000, 100 000, 200 000 oder 250 000 h zum Bruch führt.

Seite 2 Werkstoffblatt TKME 1.5415 03/2006

Figure 84: Example of Material Datasheet Provided by the Manufacturer [40]



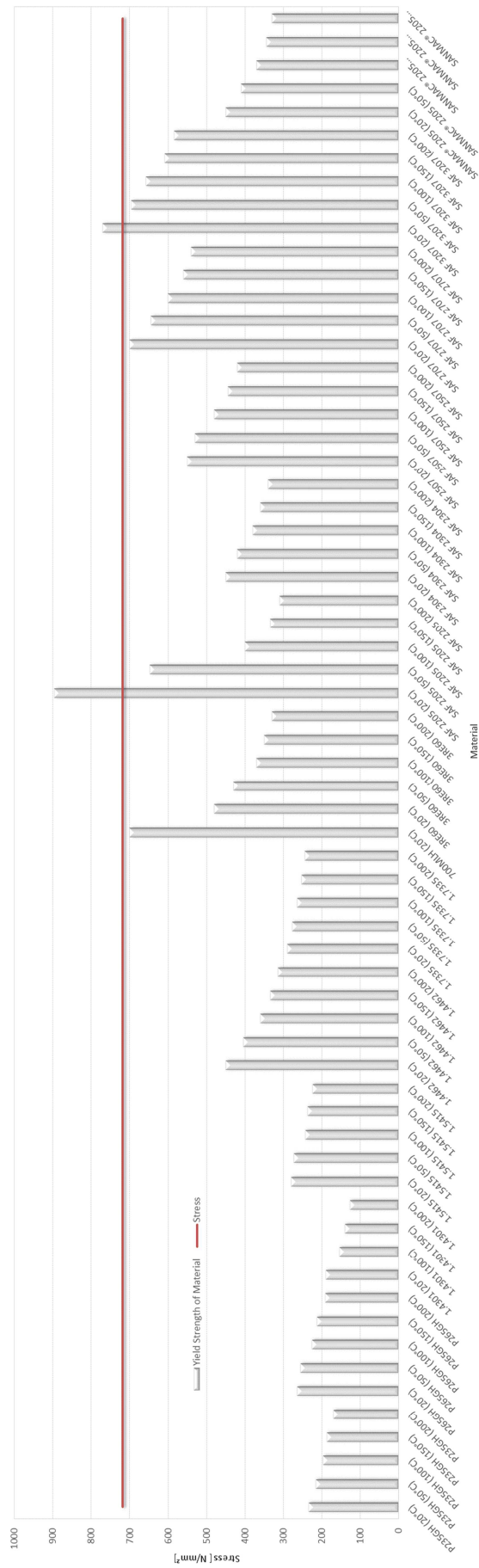


Figure 85: Material Selection – Full Size



# Appendix E

Table 28: Standard Pipe Dimensions [50]

NPS Zoll	Ø	DN	SCH 5S	SCH 10S	SCH 10	SCH 20	SCH 30	SCH 40S	STD	SCH 40	SCH 60	SCH 80S	Xs	SCH 80	SCH 100	SCH 120	SCH 140	SCH 160	XXs	
½"	10,3			1,24			1,45		1,73				2,41							
				0,27			0,32		0,37				0,47							
				0,28			0,32		0,37				0,48							
¾"	13,7			1,65			1,85		2,24				3,02							
				0,49			0,54		0,63				0,80							
				0,50			0,55		0,64				0,81							
¾"	17,2	10		1,65			1,85		2,31				3,20							
				0,63			0,70		0,85				1,10							
				0,64			0,71		0,86				1,12							
½"	21,3	15	1,65	2,11			2,41		2,77				3,73					4,78	7,47	
				0,80	1,00		1,13		1,27		1,62				1,95				2,56	
				0,81	1,02		1,14		1,27		1,65				1,98				2,59	
¾"	26,7	20	1,65	2,11			2,41		2,87				3,91					5,56	7,82	
				1,02	1,28		1,44		1,68		2,20				2,89				3,64	
				1,03	1,30		1,46		1,71		2,23				2,94				3,69	
1"	33,4	25	1,65	2,77			2,90		3,38				4,55					6,35	9,09	
				1,29	2,10		2,18		2,50		3,24				4,24				5,45	
				1,31	2,13		2,22		2,54		3,29				4,30				5,53	
1 ¼"	42,2	32	1,65	2,77			2,97		3,56				4,85					6,35	9,70	
				1,65	2,70		2,87		3,37		4,46				5,61				7,76	
				1,67	2,73		2,92		3,44		4,53				5,69				7,88	
1 ½"	48,3	40	1,65	2,77			3,18		3,68				5,08					7,14	10,16	
				1,90	3,10		3,54		4,05		5,41				7,24				9,55	
				1,92	3,15		3,59		4,11		5,49				7,35				9,69	
2"	60,3	50	1,65	2,77			3,18		3,91				5,54					8,74	11,07	
				2,39	3,93		4,48		5,44		7,49				11,12				13,45	
				2,42	3,99		4,55		5,52		7,60				11,29				13,66	
2 ½"	73,0	65	2,11	3,05			4,78		5,16				7,01					9,53	14,02	
				3,69	5,26		8,05		8,64		11,41				14,92				20,40	
				3,75	5,35		8,17		8,77		11,59				15,15				20,72	
3"	88,9	80	2,11	3,05			4,78		5,49				7,62					11,13	15,24	
				4,52	6,46		9,92		11,29		15,27				21,35				27,68	
				4,59	6,56		10,07		11,47		15,51				21,67				28,11	
3 ½"	101,6		2,11	3,05			4,78		5,74				8,08						16,15	
				5,18	7,41		11,41		13,57		18,63								34,03	
				5,26	7,53		11,57		13,78		18,92									34,56
4"	114,3	100	2,11	3,05			4,78		6,02				8,56					11,13	13,49	17,12
				5,84	8,37		12,91		16,08		22,32				28,32				33,54	41,03
				5,93	8,50		13,11		16,32		22,67				28,75				34,05	41,66
5"	141,3	125	2,77	3,40					6,55				9,53					12,70	15,88	19,05
				9,46	11,56				21,77		30,97				40,28				49,12	57,43
				9,61	11,74				22,10		31,44				40,90				49,87	58,32
6"	168,3	150	2,77	3,40					7,11				10,97					14,27	18,26	21,95
				11,31	13,82				28,26		42,56				54,20				67,55	79,21
				11,48	14,04				28,69		43,21				55,03				68,59	80,43
8"	219,1	200	2,77	3,76		6,35	7,04		8,18		10,31		12,70		15,09	18,26	20,62	23,01	22,23	
				14,78	19,97		33,31	36,81		42,54		53,08		64,64		75,91	90,43	100,91	111,26	107,91
				15,00	20,27		33,83	37,38		43,20		53,90		65,63		77,08	91,82	102,47	112,97	109,57
10"	273,0	250	3,40	4,19		6,35	7,80		9,27				12,70	15,09	18,26	21,44	25,40	28,58	25,40	
				22,61	27,78		41,76	51,02		60,30				81,54	95,99	114,73	133,03	155,12	172,30	155,12
				22,96	28,21		42,41	51,81		61,23				82,79	97,47	116,50	135,08	157,51	174,95	157,51
12"	323,8	300	3,96	4,57		6,35	8,38		9,53	10,31	14,27		12,70	17,48	21,44	25,40	28,58	33,32	25,40	
				31,24	35,98		49,72	65,19		73,90	79,72	108,94		97,45	132,06	159,89	186,94	208,10	238,72	186,94
				31,72	36,54		50,48	66,20		75,00	80,94	110,62		98,95	134,10	162,35	189,82	211,31	242,40	189,82

Zeile 1 schwarz    Wanddicke in mm  
 Zeile 2 blau     C-Stahl – Gewicht in kg  
 Zeile 3 rot        Edelstahl-rostfrei – Gewicht in kg

NPS    Nominal Pipe Size  
 DN     Diameter Nominal (NW = Nennweite)  
 Ø       Außendurchmesser  
 SCH    Schedule

Appendix F

Table 29: Rating Concepts - Detail - Part 1

concept name	costs										important parameters			flexibility		risks and problems		summary		
	feasibility										volume of pressure chamber [l]	stress according to a dp = 600bar [N/mm <sup>2</sup> ] SF=1.5	available area for cementjob [mm <sup>2</sup> ]	addaptability of tool to different casing diameters	risks and problems during installation of tool	complexity of tool (failure occurance)				
small pipe	input rating points	6296	6296	62	medium	2.5	1	1	1	1	1.5	high	9.14	592	171	medium	low	high	1.70	
	sum	2	3	0	2	2	3	3	3	3	1.5	1	15	10	5	1	3	10	5	X
	rating points	2	3	0	2	2	3	3	3	3	1.5	1	15	10	5	1	3	10	5	X
	sum	2	3	0	2	2	3	3	3	3	1.5	1	15	10	5	1	3	10	5	X
	input rating points	5368	5368	52	medium	2.5	1	1	1	1	1.5	high	5.95	548	6572	medium	high	high	1.63	
	sum	0	3	0	2	2	3	3	3	3	1.5	1	15	10	5	1	3	10	5	X
	rating points	0	3	0	2	2	3	3	3	3	1.5	1	15	10	5	1	3	10	5	X
	sum	0	3	0	2	2	3	3	3	3	1.5	1	15	10	5	1	3	10	5	X
	input rating points	5368	5368	63	medium	2.5	1	1	1	1	1.5	high	4.1	360	6572	medium	high	high	1.82	
	sum	0	2	0	2	2	3	3	3	3	1.5	1	15	10	5	1	3	10	5	X
rating points	0	2	0	2	2	3	3	3	3	1.5	1	15	10	5	1	3	10	5	X	
sum	0	2	0	2	2	3	3	3	3	1.5	1	15	10	5	1	3	10	5	X	
big pipe	input rating points	3770	3770	606	high	2.5	1	1	1	1.5	high	16	3234	5352	low	high	high	1.73		
	sum	0	2	0	2.5	1	1	1	1	1.5	1	15	10	5	1	3	10	5	X	
	rating points	0	2	0	2.5	1	1	1	1	1.5	1	15	10	5	1	3	10	5	X	
	sum	0	2	0	2.5	1	1	1	1	1.5	1	15	10	5	1	3	10	5	X	
	input rating points	3770	3770	356	high	2.5	1	1	1	1.5	high	2	1194	5352	low	high	high	1.33		
	sum	3	3	0	2.5	1	1	1	1	1.5	1	15	10	5	1	3	10	5	X	
	rating points	3	3	0	2.5	1	1	1	1	1.5	1	15	10	5	1	3	10	5	X	
	sum	3	3	0	2.5	1	1	1	1	1.5	1	15	10	5	1	3	10	5	X	
	input rating points	3770	3770	356	high	2.5	1	1	1	1.5	high	2	1194	5352	low	high	high	1.33		
	sum	0	2	0	2.5	1	1	1	1	1.5	1	15	10	5	1	3	10	5	X	

Table 30: Rating Concepts - Detail - Part 2

concept name	costs										important parameters			flexibility		risks and problems		summary
	feasibility										available area for cement job [mm <sup>2</sup> ]	stress according to dp = 600bar [N/mm <sup>2</sup> SF=1.5]	volume of pressure chamber [l]	addaptability of tool to different casing diameters	flexibility of tool for different pressure regimes	risks and problems during installation of tool	complexity of tool (failure occurancy)	
single pipe	input rating points	17.95	3770	high	low	high	medium	medium	medium	high	high	7.8	800	5352	low	high	medium	✖ 1.68
	rating points	0	2	2.5	1	1	1	1	1	1.5	1.5	15	10	5	1	10	5	
	points	3	3	1	1	2	2	2	2	1	1	2	1	3	1	1	2	
	sum	0	6	2.5	1	1	2	2	2	3.75	3.75	30	10	15	1	10	10	
ring pipe	input rating points	24.5	3770	high	low	high	medium	medium	high	high	high	2.5	600	5352	low	high	medium	✖ 1.60
	rating points	0	2	2.5	1	1	1	1	1	1.5	1.5	15	10	5	1	10	5	
	points	3	3	1	1	2	2	2	2	1	1	1	2	3	1	1	2	
	sum	0	6	2.5	1	1	2	2	2	1.5	1.5	15	20	15	1	10	10	
half pipe	input rating points	2.41	82158	medium	high	low	medium	low	medium	low	low	11.9	548	6572	medium	low	low	✔ 2.35
	rating points	0	2	2.5	1	1	1	1	1	1.5	1.5	15	10	5	1	10	5	
	points	1	1	3	3	3	2	2	2	3	3	2	2	3	2	3	3	
	sum	0	2	7.5	3	3	2	2	2	4.5	4.5	30	20	15	2	30	15	
half pipe	input rating points	3.91	82158	medium	high	low	medium	low	medium	low	low	8.9	360	6572	medium	low	low	✔ 2.54
	rating points	0	2	2.5	1	1	1	1	1	1.5	1.5	15	10	5	1	10	5	
	points	2	1	3	3	3	2	2	2	3	3	2	3	3	2	3	3	
	sum	0	2	7.5	3	3	2	2	2	4.5	4.5	30	30	15	2	30	15	
half pipe	input rating points	60.7	3770	medium	low	medium	high	high	high	low	low	15.6	711	3120	low	high	medium	✔ 2.05
	rating points	0	2	2.5	1	1	1	1	1	1.5	1.5	15	10	5	1	10	5	
	points	2	3	3	1	2	2.5	2.5	3	1	1	3	1	3	1	1.5	2	
	sum	0	6	7.5	1	2	2.5	3	3	1.5	1.5	45	10	15	1	15	10	
half pipe	input rating points	50	3770	medium	low	medium	high	high	high	low	low	13.5	492	3120	low	high	medium	✔ 2.08
	rating points	0	2	2.5	1	1	1	1	1	1.5	1.5	15	10	5	1	10	5	
	points	2	3	3	1	2	2.5	2.5	3	1	1	2	2	3	1	1.5	2	
	sum	0	6	7.5	1	2	2.5	3	3	1.5	1.5	30	20	15	1	15	10	

Table 31: Rating Concepts - Detail - Part 3

		summary		
risks and problems	complexity of tool (failure occurance)	low	5	
	risks and problems during installation of tool	medium	10	
flexibility	flexibility of tool for different pressure regimes	high	1	
	addaptability of tool to different casing diameters	low	1	
important parameters	available area for cementjob [mm²]	6572	5	
	stress according to dp = 600bar [N/mm²] SF=1.5	548	10	
	volume of pressure chamber [l]	7.6	15	
costs	feasability	montage of tool at wellside (fixing at wellside to casing or liner)	low	1.5
		complexity mounting of system components at workshop	high	1
		complexity of manufacturing pressure chamber	medium	1
		complexity of manufacturing mounting parts	low	1
		material and dimesion avaiability	high	1
		grade of tolerances required	low	2.5
		weight [kg]	91	0
		material grade required	high	3
		total length of welds [mm]	18454	2
wall thickness of main pipe [mm]	2.41	0		
OD of main pipe system [mm]	26.7			
DN of main pipe system	20			
tool length [mm]	1000			
		input rating points sum		
		input rating points sum		
concept name	cross pipe			

2.27

2

2.12

3

3

3

3

3

3

3

3

3

3

3

3

3

3

3

3

3

Table 32: Rating Concepts - Detail - Part 4

		summary		2.12		2.24		2.27		2.46		2.27		2.27	
risks and problems	complexity of tool (failure occurance)	medium	5	2	10	2	25	2	10	2	25	2	10	2	25
	risks and problems during installation of tool	medium	10	2.5	25	2.5	10	2.5	25	2.5	10	2.5	25	2.5	10
flexibility	flexibility of tool for different pressure regimes	high	1	3	3	3	3	3	3	3	3	3	3	3	3
	addaptability of tool to different casing diameters	medium	1	2	2	2	2	2	2	2	2	2	2	2	2
important parameters	available area for cementjob [mm <sup>2</sup> ]	171	5	1	5	1	5	1	5	1	5	1	5	1	5
	stress according to dp = 600bar [N/mm <sup>2</sup> ] SF=1.5	592	10	2	20	2	30	2	30	2	30	2	30	2	30
	volume of pressure chamber [l]	14	15	2	30	2	30	2	30	2	30	2	30	2	30
costs	feasibility	montage of tool at wellside (fixing at wellside to casing or liner)	low	1.5	3	4.5	1.5	3	4.5	1.5	3	4.5	1.5	3	4.5
		complexity mounting of system components at workshop	low	1	3	3	1	3	3	1	3	3	1	3	3
		complexity of manufacturing pressure chamber	high	1	1	1	1	1	1	1	1	1	1	1	1
		complexity of manufacturing mounting parts	low	1	3	3	1	3	3	1	3	3	1	3	3
		material and dimesion avaiability	high	1	3	3	1	3	3	1	3	3	1	3	3
		grade of tolerances required	low	2.5	3	7.5	2.5	3	7.5	2.5	3	7.5	2.5	3	7.5
		weight [kg]	90	0	3	0	3	0	3	0	3	0	3	0	3
		material grade required	high	3	1	3	3	6	3	6	3	6	3	6	3
		total length of welds [mm]	51770	2	1	2	2	2	2	2	2	2	2	2	2
		concept name	membran pipe												
	input rating points sum	2.77	33.4	25	1000	51770	90	high	low	low	high	low	low	high	low
	input rating points sum	4.55	33.4	25	1000	51770	119	medium	low	low	high	low	low	high	low
	input rating points sum	2.41	26.7	20	1000	63770	84	high	low	low	high	low	low	high	low
	input rating points sum	3.91	26.7	20	1000	63770	106	medium	low	low	high	low	low	high	low
	input rating points sum	1.65	21.3	15	1000	77770	74	high	low	low	high	low	low	high	low
	input rating points sum	3.73	21.3	15	1000	77770	101	low	low	low	high	low	low	high	low

